Contract No. NAS5-24316
(ERT Document No. P-2061-F)
Type III Final Report
for period September 1977 to March 1981
March 1981
Prepared for
NATIONAL AERONAUTICS & SPACE ADMINISTRATION
Goddard Space Flight Center
Greenbelt, Maryland 20771

The application of heat capacity mapping mission (HCMM) thermal data to snow hydrology

Prepared by
James C. Barnes, Principal Investigator
Clinton J. Bowley
Michael D. Smallwood
James H. Willand

ERT
ENVIRONMENTAL RESEARCH & TECHNOLOGY, INC.
ATLANTA · CHICAGO · CONCORD, MA · FORT COLLINS, CO
HOUSTON · LOS ANGELES · PITTSBURGH · WASHINGTON, DC

Contract No. NAS5-24316
(ERT Document No. P-2061-F)
Type III Final Report
for period September 1977 to March 1981
March 1981

Prepared for
NATIONAL AERONAUTICS & SPACE ADMINISTRATION
Goddard Space Flight Center
Greenbelt, Maryland 20771

The application of heat capacity mapping mission (HCMM) thermal data to snow hydrology

ENVIRONMENTAL RESEARCH & TECHNOLOGY, INC.
ATLANTA · CHICAGO · CONCORD, MA · FORT COLLINS, CO
HOUSTON · LOS ANGELES · PITTSBURGH · WASHINGTON, DC

TECHNICAL REPORT STANDARD TITLE PAGE

1. Report No.	2 Government Accession No.	3 Recipient's Catalog No

4. Title and Subtitle	5 Report Date
The Application of Heat Capacity Mapping Mission (HCMM) Thermal Data to Snow Hydrology	March 1981
	6. Performing Organization Code
7. Author(s) J.C. Barnes, C.J. Bowley, M.D. Smallwood and J.H. Willand	8. Performing Organization Report No P-2061-F
9. Performing Organization Name and Address Environmental Research & Technology, Inc. 696 Virginia Road Concord, MA 01742	10. Work Unit No.
	11. Contract or Grant No. NAS 5-24316
	13. Type of Report and Period Covered Type III Final Report Sept. 1977 - March 1981
12. Sponsoring Agency Name and Address National Aeronautics & Space Administration Goddard Space Flight Center Greenbelt, MD 20771	14. Sponsoring Agency Code

15. Supplementary Notes

16. Abstract An investigation was carried out to evaluate the application of HCMM thermal infrared (IR) data to snow hydrology and to assess whether these satellite observations can provide the hydrologist with additional information useful for predicting snowmelt runoff. HCMM data were analyzed for two study areas, the Salt Verde Watershed in central Arizona and the southern Sierra Nevada in California. The HCMM thermal measurements were compared to Landsat and NOAA VHRR satellite data, U-2 thermal data, and other correlative data.

The results of the investigation have shown that snow extent can be mapped as accurately from the daytime HCMM thermal imagery as from visible imagery. Comparison of the resolution of HCMM with that of other satellites suggests that the HCMM resolution may have the greatest utility for snow mapping. Analysis of the digital data indicates that with careful calibration, the HCMM thermal channel can provide snow surface temperature data useful for hydrologic purposes; the existing HCMM measurements were, however, found to be consistently 3 to 5°C lower than the values from correlative data. An approach to an automated analysis method was developed as part of the investigation.

17. Key Words (Selected by Author(s))	18. Distribution Statement
HCMM Thermal Data Snow Hydrology	Unlimited

19. Security Classif. (of this report)	20. Security Classif. (of this page)	21. No. of Pages	22. Price*
		101	

*For sale by the Clearinghouse for Federal Scientific and Technical Information, Springfield, Virginia 22151.

Figure 2. Technical Report Standard Title Page

FOREWORD

This investigation was performed by Environmental Research and Technology, Inc. (ERT) for the National Aeronautics and Space Administration, Goddard Space Flight Center (NASA/GSFC) under contract No. NAS5-24316. The author wishes to acknowledge the assistance provided throughout the contract period by Mr. Locke M. Stuart, HCMM Investigations Manager, and Mr. Frederick H. Gordon, Jr., the contract Technical Officer; their help particularly in providing the HCMM data needed for the investigation, is greatly appreciated. We also acknowledge the assistance provided by Dr. John C. Price, who was the HCMM Project Scientist during most of the duration of this contract. Snow survey data for the Arizona study area were provided by the Salt River Project office. The snow surface temperature data for the April, 1979 case in the Sierras study area were provided through the courtesy of Dr. Jeff Dozier, of the University of California at Santa Barbara.

ABSTRACT

An investigation was carried out to evaluate the application of HCMM thermal infrared (IR) data to snow hydrology and to assess whether these satellite observations can provide the hydrologist with additional information useful for predicting snowmelt runoff. HCMM data were analyzed for two study areas, the Salt Verde Watershed in central Arizona and the southern Sierra Nevada in California. For the Arizona study area, the data sample consisted of five daytime HCMM passes during the February to April, 1979 period; for the California study area, the data sample consisted of three cases with day/night data sets (late May, 1978; mid-July 1978; and early April, 1979). The HCMM thermal measurements were compared to Landsat and NOAA VHRR satellite data, U-2 thermal data, and other correlative data.

The results of the investigation have shown that snow extent can be mapped as accurately from the daytime HCMM thermal imagery as from visible imagery. Moreover, comparison of the resolution of HCMM with that of other satellites suggests that the HCMM resolution may have the greatest utility for snow mapping. Analysis of the digital data indicates that with careful calibration, the HCMM thermal channel can provide snow surface temperature data useful for hydrologic purposes; the existing HCMM measurements were, however, found to be consistently 3 to 5°C lower than the values from correlative data. The results of the study also indicate that for snow hydrology purposes, alone, it would be difficult to justify the production of day/night registered data sets. An approach to an automated analysis method was developed as part of the investigation.

TABLE OF CONTENTS

		Page
1.	INTRODUCTION	1
	1.1 Previous Studies of the Application of Satellite Data to Snow Hydrology	1
	1.2 Advantages of HCMM Over Previous Satellite Systems	3
	1.3 Objectives of Investigation	4
2.	CONSIDERATIONS IN THE INTERPRETATION OF SATELLITE THERMAL IR DATA	6
	2.1 Physical Parameters	6
	2.2 Satellite Sensor and Orbital Characteristics	8
	2.3 Sensor Calibration	8
	2.4 Comparisons Between Satellite Data and Temperatures Measured at Shelter Height	11
	2.5 The Field-of-View Problem	12
3.	DESCRIPTION OF STUDY AREA	13
	3.1 Sierra Nevada (California)	13
	3.2 Salt-Verde Watershed (Arizona)	17
4.	DATA SAMPLE	19
	4.1 HCMM Data	19
	4.2 Supporting Aircraft Data	20
	4.3 Surface Truth Information and Other Satellite Data	21
5.	DATA PROCESSING METHODS	23
	5.1 HCMM Imagery	23
	5.2 HCMM Digital Tape Data	23
	5.3 Atmospheric Correction	26
6.	DATA ANALYSIS FOR ARIZONA STUDY AREA	28
	6.1 Analysis of Imagery	28
	6.2 Analysis of Thermal Infrared Data Using Printouts	39
	6.3 Automated Contour Plotting	42
	6.4 Comparison of HCMM and U-2 Temperatures	44
	6.5 Correlation Between IR Temperatures and Other Data	47

		Page
7.	DATA ANALYSIS FOR SIERRAS STUDY AREA	53
	7.1 May 1978 Case	53
	7.2 July 1978 Case	68
	7.3 April 1979 Case	78
8.	DISCUSSIONS OF RESULTS	93
	8.1 Comparison Between HCMM and Other Satellite Imagery	93
	8.2 Calibration of HCMM Radiometer	94
	8.3 Automated Data Analysis Methods	95
	8.4 Usefulness of Day/Night Registered Data	95
	8.5 Use of HCMM Thermal Data to Assist in Snowmelt Runoff Prediction	96
9.	CONCLUSIONS	98
10.	REFERENCES	100

LIST OF ILLUSTRATIONS

Figure		Page
2-1	Spectral response curves for the HCMM HCMR	10
3-1	Map showing locations of four original study areas	14
3-2	Map showing southern Sierra Nevada study area	15
3-3	Map showing Arizona study area	18
5-1	Schematic diagram of data processing programs	25
6-1	HCMM visible image of 9 February 1979, Arizona study area	29
6-2	HCMM infrared image of 9 February 1979, Arizona study area	30
6-3	HCMM visible image of 15 February 1979, Arizona study area	31
6-4	HCMM infrared image of 15 February 1979, Arizona study area	32
6-5	HCMM visible image of 24 March 1979, Arizona study area	33
6-6	HCMM infrared image of 24 March 1979, Arizona study area	34
6-7	HCMM visible image of 4 April 1979, Arizona study area	35
6-8	HCMM infrared image of 4 April 1979, Arizona study area	36
6-9	HCMM visible image of 15 April 1979, Arizona study area	37
6-10	HCMM infrared image of 15 April 1979, Arizona study area	38
6-11	Diagram showing snow cover extent in Arizona study area as mapped from HCMM visible images of 24 March, 4 April and 15 April 1979	40
6-12	Example of a portion of alphanumeric IR data printout	43

Figure		Page
6-13	Examples of contour plotting program for Arizona study area	45
6-14	Comparison between HCMM and U-2 data, Arizona study area	46
6-15	Maps of Salt-Verde watershed showing snow depths for 15 February, 24 March, 4 April and 15 April 1979	49
6-16	Graph showing temperatures at Junipine for period 24 March - 15 April 1979	50
6-17	Graph showing temperatures at Happy Jack Ranger Station for period 24 March - 15 April 1979	51
6-18	Landsat-3 image (MSS-5) of 1 April 1979	52
7-1	HCMM visible and corresponding IR image for 30 May 1978, Sierras study area	55
7-2	HCMM visible and corresponding IR image for 31 May 1978, Sierras study area	56
7-3	HCMM nighttime IR image of 29 May and 30 May 1978, Sierras study area	58
7-4	Landsat-2 image (MSS-5) of 27 May 1978, viewing a portion of the southern Sierras	60
7-5	NOAA-5 daytime thermal IR images showing the Sierras snow cover on 30 May and 31 May 1978	61
7-6	Apparent snow cover boundary as mapped from HCMM day IR image and NOAA/VHRR IR image, 31 May	62
7-7	Examples of isotherm contour plots for 31 May night IR data	66
7-8	Temperature difference (ΔT) images, May case	69
7-9	HCMM visible image, daytime IR image, and nighttime IR image of 17 July 1978	71
7-10	Maps showing the Sierras snow line for 17 July mapped from HCMM visible and day IR images	72
7-11a	Landsat-2 image (MSS-5) of 20 July 1978	73
7-11b	Map showing snow line mapped from 20 July Landsat-2 image	74

Figure		Page
7-12	HCMM visible image of 5 April 1979, Sierras study area	79
7-13	Map showing extent of areas of varying snow cover reflectance mapped from 5 April HCMM visible image	80
7-14	HCMM day IR image of 5 April 1979, Sierras study area	82
7-15	HCMM nighttime IR image of 4 April 1979, Sierras study area	84
7-16	Graph showing examples of curves relating IR temperatures to gray-tone level	85
7-17	HCMM 36-hour temperature difference (ΔT) image for 5 April 1979	89
7-18	Apparent thermal inertia (ATI) image for the 36-hour data set of 4-5 April 1979	91

LIST OF TABLES

Table		Page
2-1	Heat Capacity Mapping Radiometer (HCMR) Summary Data Sheet	9
4-1	HCMM Data Sample for Primary Study Areas	19
4-2	Supporting Aircraft (U-2) Data	21
5-1	Alphanumeric Code Used in Print Program	24
5-2	Corrections for Atmospheric Attenuation	26
6-1	HCMM/U-2 Comparison for Arizona Study Area	47
7-1	Data Sample for Sierras Study Area	54
7-2	Summary of HCMM Thermal IR Temperatures for 29-31 May	64
7-3	Comparison of Surface Temperature Measurements for HCMM and U-2 HCMR Digital IR Data	77

1. INTRODUCTION

The Heat Capacity Mapping Mission (HCMM), launched in April 1978, was the first of a planned series of Applications Explorer Missions (AEM) that involved the placement of small spacecraft in special orbits to satisfy mission-unique data acquisition requirements. The sensor system on-board the HCMM was a two-channel radiometer called the Heat Capacity Mapping Radiometer (HCMR). One channel of the HCMR detected reflected solar radiation in the visible portion of the spectrum and the other detected radiation emitted by the Earth's surface and cloud tops in the thermal infrared spectral range. The primary purpose of the mission was to establish the feasibility of using a thermal infrared remote-sensor to measure the temperature of the Earth's surface twice within a 12-hour interval at the times of the daily temperature extremes. Another objectve was to apply the day/night temperature difference measurements to determine thermal inertia, the property of material to resist temperature changes as incident energy varies over a daily cycle. Data were collected by the HCMM until the spacecraft was taken out of operation at the end of September 1980.

Although the satellite was designed primarily for its geologic applications, investigations carried out under the HCMM project have demonstrated applications of the data to several other disciplines, as well. The purpose of the investigation reported herein was to evaluate the application of HCMM data to snow hydrology and to assess whether these satellite observations can provide the hydrologist with additional information useful for predicting snowmelt runoff. In particular, the intent of the study was to determine whether the HCMM thermal infrared (IR) data, and the derived day/night temperature difference measurements, can be related to snow conditions, such as melting versus non-melting snow.

1.1 Previous Studies of the Application of Satellite Data to Snow Hydrology

The first weather satellite of the United States space program, TIROS-1, was placed into orbit 20 years ago, on 1 April 1960. Even in the very first images returned by that satellite, it was possible to

detect areas where the Earth's surface was snow covered. In fact, snow and ice were about the only geophysical features, other than clouds, that could be mapped from these early, relatively poor resolution oblique images. Since then, as improved satellite systems have been developed, remote sensing from space has been used increasingly to map snow cover for hydrologic and other purposes.

Based on techniques developed initially in the mid and late 1960's, and updated in the 1970's when higher resolution data became available, satellites are now used on a routine basis to map percentage snow cover for several river basins in the western United States. Their proven interpretive techniques and high spatial resolution make visible-channel radiometers currently the most reliable sensors for mapping snow cover extent. Studies have also been carried out, however, using data from other portions of the spectrum, including near-infrared, thermal infrared, and microwave. Current methods for mapping snow cover and detecting certain snowpack properties from satellite remote sensing are described in the proceedings of two workshops held as part of the NASA Snow Applications Systems Verification and Transfer (ASVT) program (Rango, 1975; Rango and Peterson, 1980). Two handbooks describing satellite snow mapping techniques have also been prepared as part of the Snow ASVT program (Barnes and Bowley, 1974; Bowley et al., 1979); the latter handbook incorporates the results of the ASVT program with regard to the operational use of satellite snow mapping for runoff prediction. Another recent report (Wiesnet, 1979) describes applications of remote sensing to hydrology, in general, including snow and glaciers.

The only previous studies that have been conducted to determine specifically the application of satellite thermal IR data to snow hydrology are those reported by Barnes and Bowley (1972) and Barnes et al. (1974). The first of these two studies used data from the relatively poor resolution Scanning Radiometer (SR), whereas the second study used data from the improved Very High Resolution Radiometer (VHRR) flown on the NOAA series satellites.

The results of these studies indicated that in most instances snow could be delineated in the VHRR data because of its lower temperature as compared to the non-snow covered terrain. During the spring season, the thermal gradients associated with snow boundaries were considerably

better defined than during the winter; snow patterns were the least well-defined in winter nighttime thermal infrared data. In mountainous terrain, temperature differences due to variations in elevation often tended to obscure the temperature differences associated with snow cover. Absolute temperatures of the snow surface were also difficult to measure in mountainous terrain because the field-of-view of the radiometer, even at the improved VHRR resolution, usually included forest and bare rock features as well as snow. Nevertheless, the results of these earlier studies did indicate the potential of thermal IR measurements for mapping the snow surface temperature, as well as the extent of the snow.

1.2 Advantages of HCMM Over Previous Satellites Systems

As described in the previous section, studies related to snow hydrology had been carried out using thermal IR data from the operational NOAA system. Like the HCMR, the NOAA VHRR was also a two-channel radiometer, sensing in both the visible and IR bands. The HCMM, however, offered advantages over the NOAA system, which made these newer data attractive for use in extending the earlier research. The advantages of HCMM, both in terms of the HCMR sensor and certain orbital characteristics, were those listed below.

1) Improved spatial resolution. The HCMR had a spatial resolution of 500 meters in the visible and 600 meters in the thermal IR channel; the resolutions of the VHRR sensors was about 1 km in both channels.

2) Improved thermal resolution. The noise equivalent temperature difference (NEΔT) of the HCMR was 0.4°K, as compared to an NEΔT of about 1.2°K for the VHRR.

3) Improved sensor calibration. As part of the HCMM project, an external calibration of the HCMR was performed using ground-based measurements, making it possible to determine absolute temperatures more accurately than with the VHRR data; the procedures used in calibrating the satellite data and the in-flight performance of the sensor are described in a paper by Barnes and Price (1980).

4) Satellite overpass times to coincide with diurnal cycle. The HCMM orbit was such that the satellite passed over in the early morning and early afternoon (0230 and 1330 local time), with the afternoon pass being near the time of maximum daily heating.

5) Availability of day/night registered data. Through a careful pixel-by-pixel matching procedure, HCMM day/night registered data products were produced; the resulting temperature difference and thermal inertia products had not previously been available from the NOAA satellites.

1.3 Objectives of Investigation

The investigation to evaluate the application of HCMM data to snow hydrology had three overall objectives. These objectives were the following.

1) Determine the practical utility of HCMM thermal IR data for mapping snow cover distribution and determine the accuracy of the thermal IR temperature measurements. The specific tasks to be accomplished under this first overall objective were:

   a) map thermal patterns from the HCMM thermal IR data and compare the patterns with HCMM visible-channel imagery and other correlative snow data;

   b) determine the accuracy of HCMM thermal IR surface temperature measurements through comparison with aircraft thermal IR measurements and available surface-based data;

   c) determine the relative resolution utility of HCMM thermal IR measurements compared with those from the NOAA/VHRR; and

   d) delineate and quantify the problems involved with measuring snow temperature from space, including sensor calibration and atmospheric effects, and relate them to present and planned earth observing satellite systems; this objective will take into consideration

and utilize the capability of HCMM for day and night thermal measurements over appropriate sites and the satellite's eight-day repeat cycle.

2) Determine if and how HCMM measurements can be incorporated with other satellite data, such as NOAA/VHRR and/or Landsat, into an overall snow hydrology program related directly to snowmelt runoff prediction.

3) Develop an approach to automated data processing of combined visible and thermal infrared satellite acquired data to provide information of interest and use to the snow hydrologist.

2. CONSIDERATIONS IN THE INTERPRETATION OF SATELLITE THERMAL IR DATA

A number of factors must be taken into consideration in the interpretation of satellite thermal IR data for measuring snow surface temperature, as well as for delineating snow extent. The delineation of a snow boundary may depend on the detection of relatively small radiative temperature differences; similarly, variations of only a few degrees in the temperature across a snow surface may be significant in terms of the snowpack condition. Among the factors that must be considered are the effects of the emissivity of the surface and atmospheric attenuation. Other factors that influence the measurement of snow surface temperature include the characteristics of the sensor, both in terms of the sensitivity and the field-of-view, and the sensor calibration. Finally, when comparing satellite measurements with ground-based temperature data, the inherent differences in the two types of measurements must be taken into account. The considerations in the interpretation of satellite data are discussed in the earlier report by Barnes et al. (1974), and in papers such as Barnes and Price (1980), Dozier (1980), and Frampton and Marks (1980).

2.1 Physical Parameters

2.1.1 Emissivity

The emissivity of snow approximates a black body in the 10.5 to 12.5 μm atmospheric window, the wavelength of the HCMR thermal IR channel. In laboratory experiments using an emissivity box, Shafer and Super (1971) found that the emissivity of snow in the 8 to 14 μm interval ranged from 0.966 to 0.989, with an average value of 0.978 for all types of snow surfaces examined. From aircraft measurements, Griggs (1968) found a mean emissivity of 0.99 for a melting snow surface. Therefore, within the accuracy of the satellite measurements snow may be considered to emit as a black body.

In contrast to snow, a forested or non-forested surface that is not snow covered may have an emissivity of 0.95 or less. In using satellite data to delineate a snow boundary, therefore, the differences in

emissivity can be a factor. Similarly, when the field-of-view of the radiometer includes partial snow cover, variations in emissivity may exist over the area being viewed.

In the study by Barnes et al. (1974) calculations were made to ascertain the apparent decrease in surface temperature (i.e., the reduction in equivalent black body temperature as "seen" by the satellite) that could be caused by a decrease in emissivity from 1.0 to 0.9. These calculations showed that the apparent decrease in temperature caused by assuming an emissivity of 1.0 when the actual value is 0.9 could be as much as 4-6°K, depending on the air temperature and atmospheric transmission. Therefore, a difference of only a few degrees in the actual temperature of the snow surface (emissivity near 1.0) and the ground (emissivity less than 1.0) could be masked in the satellite measurements because of the difference in emissivity. Fortunately, in most instances the terrain near the edge of the snowpack probably has an emissivity greater than 0.9.

2.1.2 Atmospheric Attenuation

Useful observations of the Earth's surface were, of course, not possible from HCMM in either the visible or thermal IR channels when cloud cover existed. Even without clouds, however, atmospheric attenuation affects thermal IR measurements of the surface temperature. The HCMR thermal IR channel was designed to measure in the 10.5 to 12.5 μm spectral band, where the atmosphere is nearly transparent. Nevertheless, some absorption does occur in this "atmospheric window" region due to the presence of water vapor, atmospheric gases, and aerosols, causing the radiative temperature measured by the satellite to be lower than the actual temperature of the surface. Corrections for the attenuation by water vapor, which is the most significant absorber in the 10.5 to 12.5 μm window region, are discussed in papers by Cogan and Willand (1976) and Barnes and Price (1980), among others.

As discussed in the above papers, the correction for atmopsheric attenuation may be defined as the difference between the ground surface temperature (T_s) and that inferred from the measured IR radiance (T_B) when looking at an angle Θ with respect to nadir through a cloud-free atmosphere. This correction can be estimated through numerical integration

of the equation of radiative transfer. As discussed later in the report, two approaches were used to estimate the atmospheric effect for the cases analyzed. The results of the calculations, which used actual meteorological sounding data, indicated that the corrections for snow surfaces at higher elevations, with a relatively dry atmosphere, are generally of the order of no more than 1°-2°K.

2.2 Satellite Sensor and Orbital Characteristics

The sensor and orbital characteristics of the HCMM are described in a report on the Heat Capacity Mapping Experiment equipment and data calibration (Murphy et al., 1978), the Heat Capacity Mapping Mission User's Guide (NASA, 1979), and the paper by Barnes and Price (1980). The HCMR summary data sheet from the User's Guide is shown in Table 2-1, and the spectral response curves for the two channels are shown in Figure 2-1. As mentioned previously, the improved sensor sensitivity (NEΔT) and field-of-view of HCMR as compared to the VHRR were advantages with regard to the use of the HCMM data for snow hydrology studies.

The HCMM orbit was selected to have a 16-day repeat cycle, with a shorter five-day period of approximate repeats over a selected ground point (NASA, 1979). This particular orbit resulted in satellite day/night coverage patterns at least once every 16 days at approximately 12-hour intervals for all latitudes poleward of 35 degrees. It was possible, therefore, to obtain registered data for the diamond-shaped area of overlap between the day and night HCMM passes for 12-hour or in some instances 36-hour intervals. The procedures for registration of the day/night "pairs" are described in the User's Guide (NASA, 1979). Precisely registered day/night data sets had not been available previously from other satellite systems.

2.3 Sensor Calibration

The procedure and methodology for calibrating the HCMR thermal IR channel are described in detail in the paper by Barnes and Price (1980). In addition to the internal calibration procedure, atmospheric and surface truth data from an instrumented ground-calibration site at White Sands, New Mexico, were used to obtain an external calibration during the early

Table 2-1 Heat Capacity Mapping Radiometer (HCMR) Summary Data Sheet

Orbital altitude = 620 kilometers

Angular resolution = 0.83 milliradians

Resolution = 0.6 km x 0.6 km at nadir (infrared)

0.5 km x 0.5 km at nadir (visible)

Scan angle = 60 degrees (full angle)

Scan rate = 14 revolutions/second

Sample rate = 1.19 samples/resolution element at nadir

Sampling interval = 9.2 microseconds

Swath width = 716 kilometers

Information bandwidth = 53 KHz/channel

Thermal channel = 10.5 to 12.5 micrometers; NEDT = 0.4°K at 280°K

Usable range = 260° to 340°K

Visible channel = 0.55 to 1.1 micrometers; SNR = 10 at ~1% albedo

Dynamic range = 0 to 100% albedo

Scan mirror = 45 degree elliptical flat

Nominal telescope optics diameter = 20 cm

Calibration = Infrared: View of space, seven-step staircase electronic calibration, and blackbody calibration once each scan.

Visible: Pre-flight calibration assumed valid.

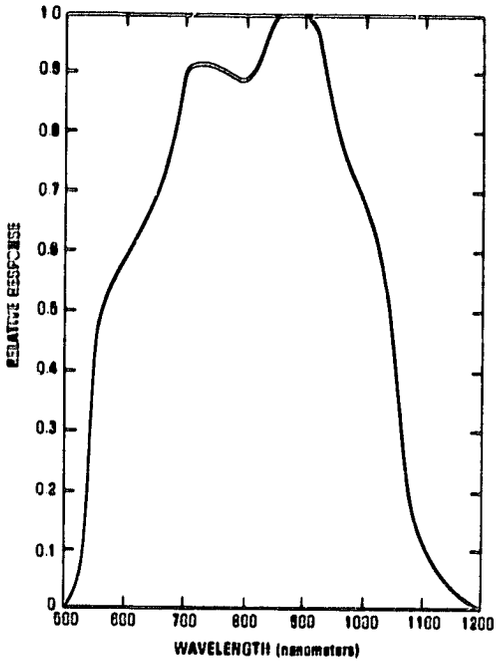

HCMR spectral response, channel 1.

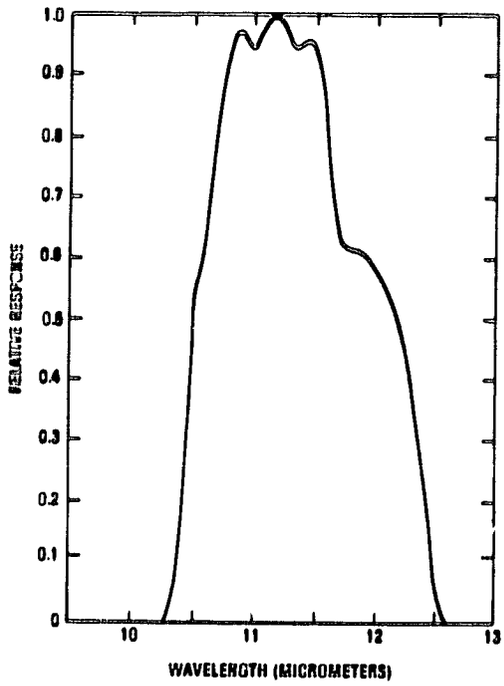

HCMR spectral response, channel 2.

Figure 2-1 Spectral Response Curves for the HCMM Heat Capacity Mapping Radiometer (HCMR) Visible (1) and Thermal IR (2) Channels (from Barnes and Price, 1980).

part of the mission. Based on an evaluation of data from five satellite passes during May and June 1978, a decision was made to offset the prelaunch calibration values by -5.5°C in order to force agreement between the satellite and surface measurements. This offset was subsequently applied to all standard processed HCMM data.

Further comparisons were carried out for data acquired during October and December 1978 and February 1979. These comparisons indicated an offset of approximately +5°C, in the direction opposite to the already applied correction. Thus, the later results suggested that the prelaunch calibration of the thermal channel should not have been modified. The variability of the comparisons between the satellite and surface measurements must be considered when using the HCMM data to determine absolute snow surface temperature.

2.4 Comparisons Between Satellite Data and Temperatures Measured at Shelter Height

When examining satellite thermal measurements of the surface temperature over broad areas, the only source of comparative data may be the standard temperatures measured at shelter height. When the standard temperature data are used, possible differences between the actual surface temperature and the shelter temperature at about 2 m above the surface must be taken into account. Geiger (1965) discussed the variation of temperature with height over a snow surface. He found that on a cold winter day, the temperature at shelter height (200 cm) was only slightly lower than that immediately above the surface (10 cm); at night, however, a strong inversion existed with the value at 10 cm being some 7°K lower than that at 200 cm. During melting, the snow surface remained at 273°K, but the air immediately above was as much as 10°K warmer because of the effects of solar radiation and the advection of warm air; at the same time the shelter reading was about 278°K.

Edgerton et al. (1968), in a study of microwave measurements over a snow covered ice surface, acquired temperature readings at a height of about 5 cm above the surface and at the antenna height, representative of the free air. On a relatively warm day, the readings at both heights were approximately 284°K; during the subsequent night the reading at the antenna height dropped to about 263°K, whereas the 5 cm reading dropped

to 256°K. Shafer and Super (1971), in their study of aircraft-acquired data, found that the radiometric measurements generally agreed within 2.5°K with nearby shelter temperatures. The exception was an instance when a strong inversion existed, where the maximum difference was 5.8°K.

Based on the measurements reported by these investigators, it appears that during the day snow surface and shelter temperatures generally will be roughly the same (difference < about 1°K). However, during a condition of melting snow the shelter temperature may be 5°K higher than the surface value. At night under a cloud-free and calm, or nearly calm, atmosphere an inversion may develop causing the snow surface to be 5° to 10°K colder than the atmosphere at shelter height.

2.5 The Field-of-View Problem

Even with the improved field-of-view of the HCMR as compared to the VHRR, errors in the surface temperature measurements could arise because the 600 m pixel may include a non-uniform surface. The radiation from the non-uniform surface would then be averaged by the radiometer. For example, a partially snow covered surface on a warm day, as could occur during the spring snowmelt period, would also contain trees and bare rock surfaces, both of which could have temperatures considerably higher than the temperature of the actual snow surface. The non-uniform field-of-view can also be a significant problem in areas of rough terrain, where elevation changes rapidly.

3. DESCRIPTION OF STUDY AREAS

Four study areas were originally selected for the investigation of the application of HCMM thermal data to snow hydrology. The four areas, shown on the map in Figure 3-1, are: (1) the southern Sierra Nevada in California; (2) the Salt-Verde Watershed in central Arizona; (3) the Cascade Mountains in Washington; and (4) the Upper Columbia Basin in Idaho and Montana. The California and Arizona sites were selected as the primary study areas, with the other two areas to be used if there was not an adequate data sample for the primary areas (that situation could have occurred if HCMM had operated only during the late spring and summer, when the snowpack had been depleted in the more southern areas).

During the period of operation of HCMM, an adequate data sample was collected for the two primary study areas; no data analysis was carried out, therefore, for the two secondary study sites. The hydrologic importance of snowpack accumulation in both the California and Arizona areas is well documented. Moreover, previous studies have shown that these are regions where satellite observation is particularly useful because of a lower frequency of cloud cover than in more northern regions. The specific characteristics of the two areas, which have significant differences with regard to terrain, forest cover, and snowfall, are described in the following sections.

3.1 Sierra Nevada (California)

The characteristics of the Sierra Nevada vary considerably over the northern and southern extents of the mountain range. The location of the major river basins of the Sierras is shown in Figure 3-2. The southern area represents the high elevations of the Sierra Nevada where snow cover is relatively stable, and where up to 75 percent of the annual runoff occurs during the April to July snowmelt period. Approximately three-fourths of the San Joaquin Basin is above 2,000 meters (6,500 feet) in elevation, while about half of the Kings Basin is above 2,500 meters (8,200 feet). The altitude of the Kern Basin ranges from about 750 meters (2,460 feet) to more than 4,000 meters (13,120 feet); Mt. Whitney, the highest point (4,418 meters [14,465 feet]) in the 48 states is in the Kern Basin. The Kaweah and Tule Basins are both lower in elevation,

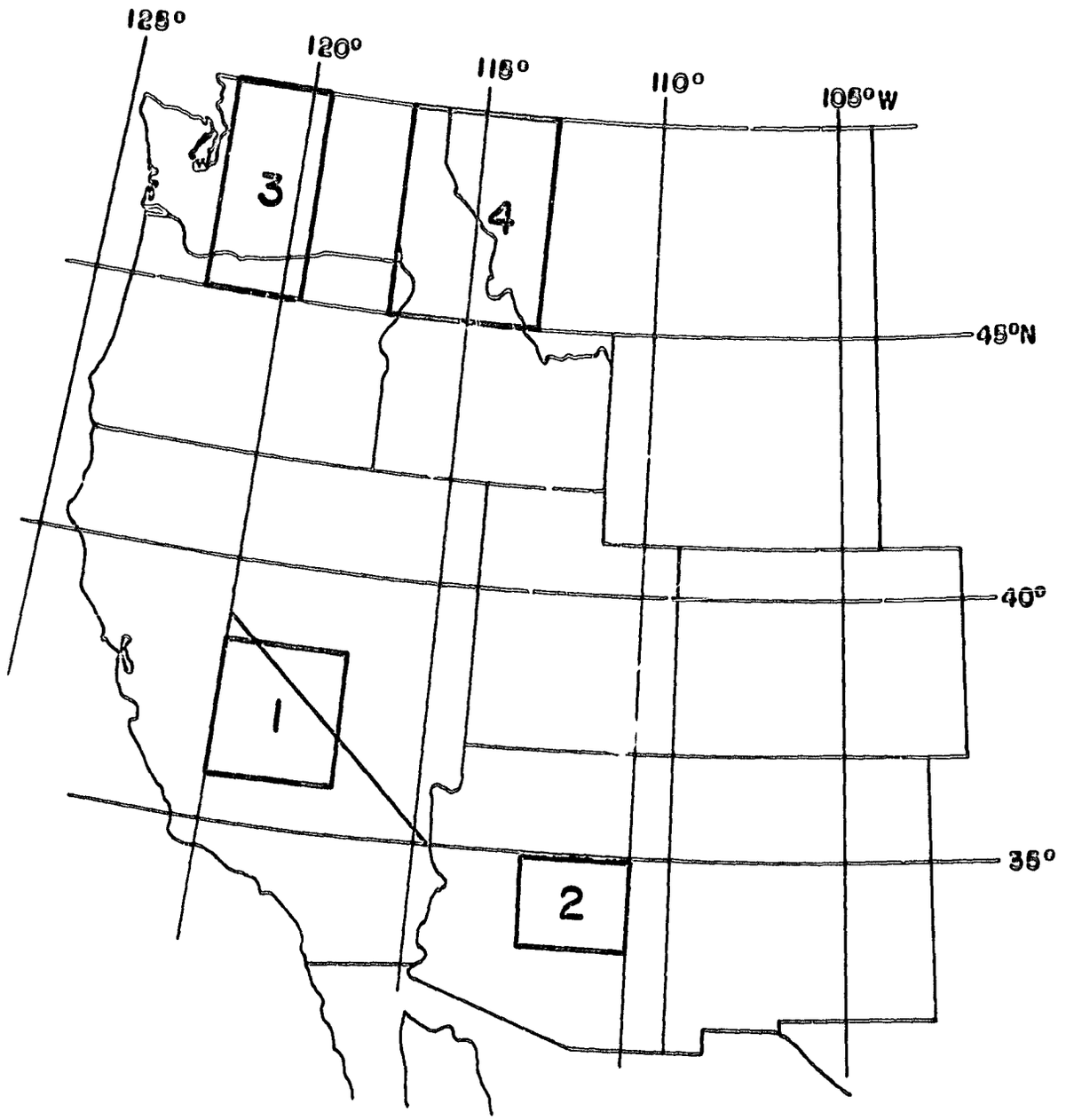

Figure 3-1 Map Showing locations of four original study areas: (1) the southern Sierra Nevada in California; (2) the Salt-Verde Watershed in central Arizona; (3) the Cascade Mountains in Washington; and (4) the Upper Columbia Basin in Idaho and Montana.

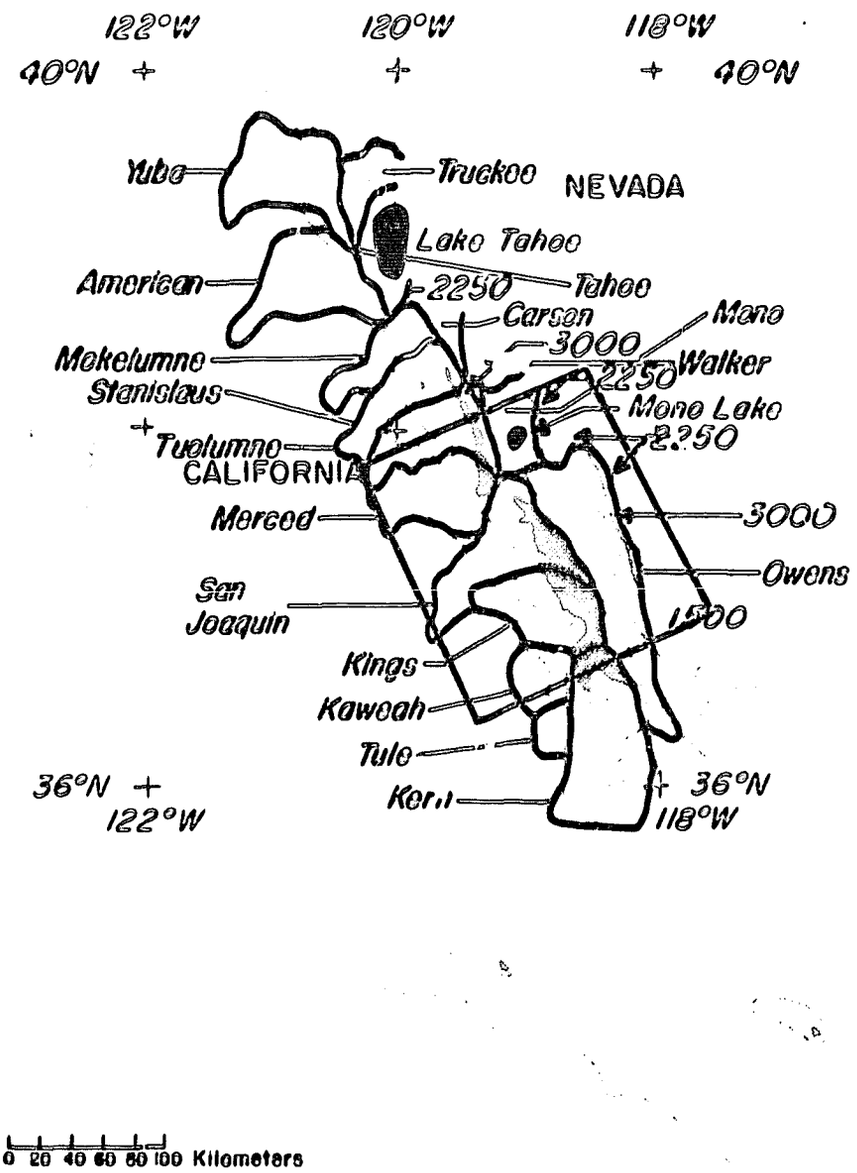

Figure 3-2 Map showing river basins in Sierra Nevada Study area. Elevation contours are in meters. The area for which most analyses were carried out is outlined.

with the entire Tule Basin lying below 2,250 meters (7,380 feet).

The precipitation characteristics of the southern area are described by Rango et al. (1979). The average annual precipitation at the 2,750 meter (9,000 foot) elevation in the Kings River Basin is about 890 millimeters (35 inches). Precipitation measurements made along the frontal slope at the western side of the basin appear to be representative of, or at least proportional to, precipitation at the higher elevations, although some minor variations may occur. In the Kern River Basin, precipitation varies considerably with elevation and location within the basin. At 2,750 meters (9,000 feet), average annual precipitation along the Great Western Divide exceeds 890 millimeters (35 inches), while at the same elevation along the Sierra crest, precipitation may be as low as 410 millimeters (16 inches). Precipitation, snowpack accumulation, and snow cover appear much more variable over the Kern Basin than over the Kings Basin.

The northern half of the Sierras is characterized by lower elevations and more transient areas of snow cover; in this area, 45 percent of the annual runoff occurs during the April to July snowmelt period. The sub-basins vary in size from 100 square kilometers (38 square miles) to 16,000 square kilometers (6,400 square miles). Use of the sub-basins allows cross-checks between adjacent and nearby basins when cloud cover, missing imagery, or other factors contribute to loss of data from a specific basin or portion of the study area on any given day. Average annual precipitation amount in the northern study area (the combined Sacramento and Feather Basins) is about 990 millimeters (39 inches).

Land use charts depict the Sie as as consisting primarily of "forest and woodland, mostly ungrazed", with some "forest and woodland, grazed". In a slightly different classification scheme, Anderson (1963) designates the higher elevation as "Alpine" and "Commercial Forest". In this scheme, a narrow band of "lower Conifer Zone" borders the commercial forest zone along the western slope of the Sierras, with the lower elevation designated as "Woodland-Brush-Grass Zone". Despite the apparent abundance of forest-covered land, Court (1963) points out that in total area, the Kings River Basin is only 28% forested; furthermore, trees are so sparce in the forested area that only about 17% of the basin is covered by the tree canopy. For the Sierras as a whole, Court reports that 76% of the area is exposed to the sky.

3.2 Salt-Verde Watershed (Arizona)

The Salt-Verde watershed, which comprises the Arizona study area and includes about 34,000 square kilometers (13,000 square miles) in central Arizona, and ranges from 400 to 3,900 meters (1,325 to 12,670 feet) above mean sea level, is shown in Figure 3-3.

Three separate drainage basins, the Salt, Verde, and Tonto, comprise the watershed, and runoff from these basins flows into six reservoirs on the Salt and Verde Rivers. These reservoirs are operated by the Salt River Project to provide hydroelectric power, and municipal, industrial, and irrigation water to more than one million people and 250,000 acres of land. They have a combined storage capacity of approximately 2.5 cubic kilometers (two million acre-feet).

The Salt-Verde watershed is indicated on land usage charts to consist of "forest and woodland, grazed" or "open woodland, grazed", with the predominant growth in the forested areas being Ponderosa Pine. The growth in other areas consists of Juniper Zones and grasslands.

The Arizona snowpack is extremely variable from year to year because of its location at the southern edge of the continental snowpack, and rapid snowmelt can occur at lower elevation areas at anytime during the snow season. The annual precipitation amount generally ranges from 250 to 650 millimeters (10 to 25 inches).

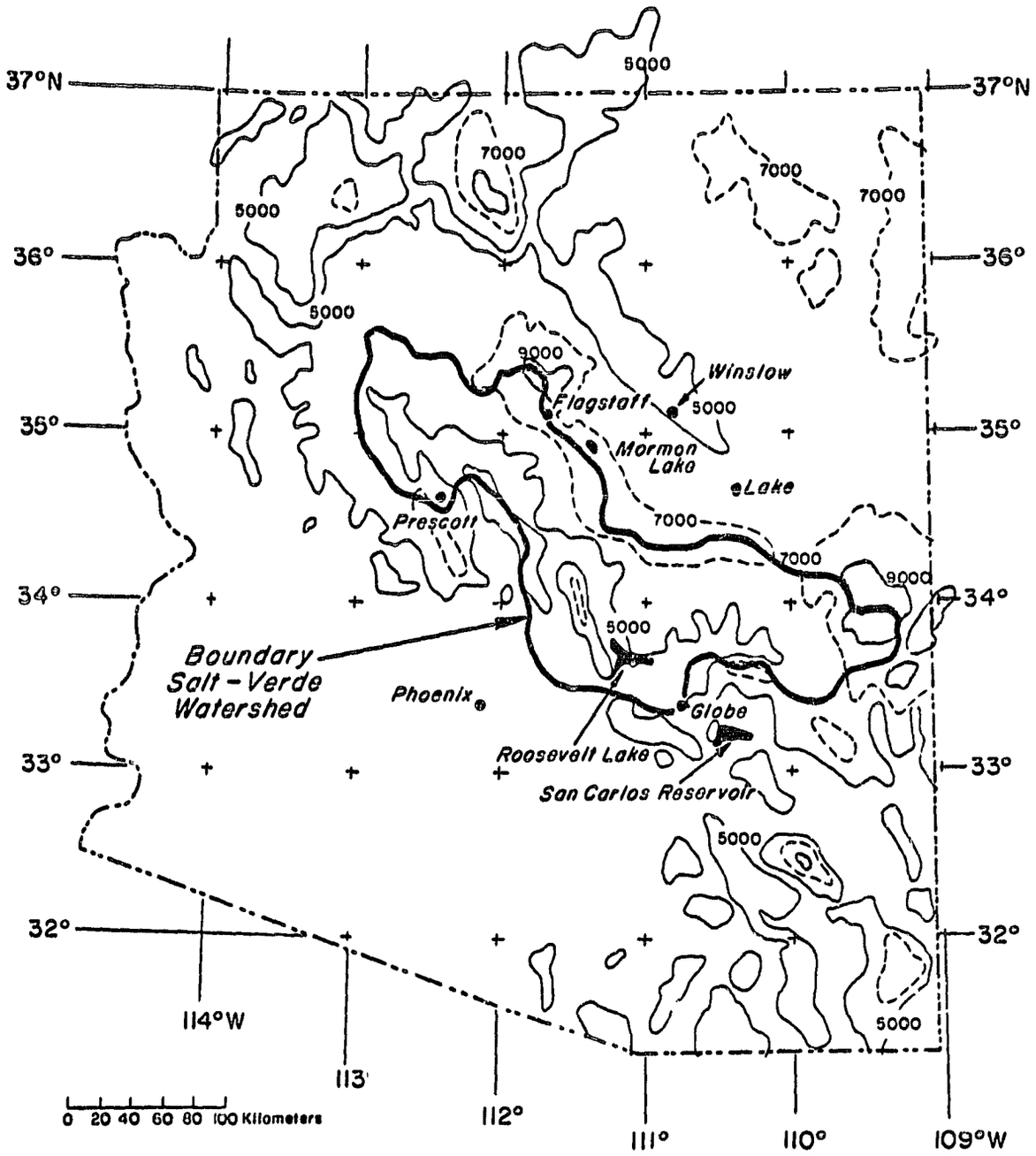

Figure 3-3 Map showing Salt-Verde Watershed, Arizona Study Area. Contours for 1500 m (5000 ft.), 2100 m (7000 ft.), and 2700 m (9000 ft.) are indicated.

4. DATA SAMPLE

4.1 HCMM Data

Standard processed HCMM images were received on a routine basis during the investigation for all four study areas. In total, images for more than 150 HCMM scenes were received, with the daytime scenes including both the visible and thermal IR images, and the nighttime scenes only the thermal IR. Of this total sample, several scenes were not useable because of substantial cloud cover, data noise, or the area of coverage being outside the specified study area. Nevertheless, a considerable number of the scenes covering the secondary study areas or areas outside those specified for the investigation were essentially cloud-free; these data were not analyzed, however, because of the adequate data sample available for the primary study areas.

Several excellent quality, cloud-free scenes were collected by HCMM for the Arizona and California study areas. Because the snowpack in the Arizona mountains had been depleted by the time HCMM began to collect data in early May 1978, the data sample for that area is from the winter and spring of 1979. The Sierras data sample is from the late spring and early summer of 1978, as well as the 1979 snow season. The scenes selected for analysis are listed in Table 4-1.

TABLE 4-1

HCMM DATA SAMPLE FOR PRIMARY STUDY AREAS

Salt-Verde Watershed - Arizona		Southern Sierra Nevada - California	
Date	Type of Data	Date	Type of Data
9 Feb 79	Day VIS and IR	29 May 78	Night IR
15 Feb 79	Day VIS and IR	30 May 78	Night IR
24 Mar 79	Day VIS and IR	30 May 78	Day VIS and IR
4 Apr 79	Day VIS and IR	31 May 78	Day VIS and IR
15 Apr 79	Day VIS and IR	17 Jul 78	Night IR
		17 Jul 78	Day VIS and IR
		3 Apr 79	Night IR
		4 Apr 79	Night IR
		5 Apr 79	Day VIS and IR

Additional data products were acquired for the scenes selected for analysis, including positive and negative transparencies and Computer Compatible Tapes (CCT's). As seen in Table 4-1, only daytime HCMM passes were available for the Arizona study area (because of power limitations and other constraints, fewer nighttime passes were read out during 1979). For the Sierras study area, however, three cases with day/night coverage were available. For these cases, therefore, the day/night registered data products, including temperature difference (ΔT) and apparent thermal inertia (ATI) images and CCT's, were also acquired. Both 12-hour and 36-hour day/night pairs were available for the May 1978 case; only the 12-hour pair was available for the July 1978 case, and a 36-hour pair for the April 1979 case.

Another day/night data set (14 May 1978) was also received late in the study period, but was not analyzed because of the extensive analysis of the 29-31 May case, carried out earlier in the study. In addition, several other scenes were received for the Sierras study area that could provide useful snow data despite partial cloud cover (i.e., 20 January day/night, 31 March day, and 27 April day; all in 1979). These scenes were not used because the investigation was concentrated on the completely cloud-free day/night data sets listed in Table 4-1.

4.2 Supporting Aircraft Data

Data from three supporting U-2 aircraft day/night missions over the Sierras study area and one day/night mission over the Arizona study area were used in the investigation. On the 1978 flights, the aircraft carried the HCMR, a two-channel instrument essentially identical to the instrument flown on the spacecraft. On the 1979 flights, the aircraft carried the improved resolution High Altitude Multispectral Scanner, although for the purposes of this investigation data from only one visible channel and the thermal IR channel were used. Naturally, the data from the U-2 aircraft crossed only a small portion of each overall study area. A summary of the U-2 data is given below in Table 4-2.

TABLE 4-2

SUPPORTING AIRCRAFT (U-2) DATA

Sierras Area (Kings River Basin)

a. HCMR Instrument day/night mission (flights 78-033/034) 31 May/1 June 1978 day/night mission (flights 78-035/036) 19/20 July 1978	b. High Altitude Multispectral Scanner night/day mission (flights 79-029/030) 4 April 1979

Arizona Area (Salt/Verde Watershed)

High Altitude Multispectral Scanner	night/day mission (flights 79-029/030) 4 April 1979

4.3 Surface Truth Information and Other Satellite Data

Because the purpose of the investigation was to examine snow surface temperatures measured by the HCMM thermal IR radiometer over relatively broad study areas, it was not feasible to collect specialized surface truth information. The comparative meteorological and snow data were derived, therefore, from standard sources, such as meteorological charts, state climatological data summaries, aerial snow survey charts, snow course measurements, and the SNOTEL (snow telemetry) network.

Ground-based observations of snowpack conditions were available from the Salt River Project Office for some locations in the Salt-Verde Watershed during the 1979 snowmelt season. A set of surface temperature data for the Dusy and Palisade Basins of the Middle Fork of the Kings River in the southern Sierra Nevada was available for 5 and 6 April 1979. This data set, which consisted of surface radiant temperatures measured with a hand-held radiant thermometer and wet- and dry-bulb air temperatures, was collected by the University of California at Santa Barbara as part of a snow research program.

In addition to the use of surface truth information to assess the snow cover conditions, HCMM visible channel images were used as the principal means to determine snow cover extent for comparison with the

thermal patterns mapped from the IR data. Interpretation of the images was accomplished through use of well-established snow-mapping techniques described in the handbooks by Barnes and Bowley (1974) and Bowley et al. (1979).

NOAA VHRR (Very High Resolution Radiometer) thermal IR channel imagery was also acquired to determine the relative resolution utility as compared to the HCMM. Similarly, a limited sample of the higher resolution Landsat imagery (Bands 5 and 7) was acquired for comparison with the HCMM data.

5. DATA PROCESSING METHODS

5.1 HCMM Imagery

Images for the scenes selected for analysis were acquired in both positive and negative transparency formats as well as the original hard-copy positive prints. Initially, the analysis was performed directly from the 1:4 million scale prints and refined where necessary using the somewhat better quality transparencies. In some cases, enlarged prints were produced from the negative transparencies. The enlargements, at a scale of approximately 1:1 million, facilitated the analysis for scenes in which the snow extent was limited such as during April in the Arizona study area. Since the objectives of the investigation were directed more toward the analysis of the HCMM digital data rather than the imagery, extensive reprocessing of the images was not undertaken. Examples of HCMM visible and thermal IR images are presented in Sections 6 and 7.

5.2 HCMM Digital Tape Data

Data in the digital tape format (CCT's) were acquired for all HCMM scenes selected for analysis. Although the tapes contained data from both the visible and thermal IR channels, only the thermal IR data were processed and analyzed for this investigation. Two programs were developed to process the digital data; one program was designed to print out the data in a format suitable for hand analysis, and the other was designed to produce an automated mapping of the IR temperature contours. These two programs were also adapted for use in processing the thermal IR tapes from the U-2 aircraft flights. The programs are shown schematically in Figure 5-1 and are described in the following sections.

5.2.1 Print Program

The "print" program was developed to (a) convert HCMM digital counts within selected areas to degrees Celsius, and (b) convert the temperatures into alpha-numeric characters, which are printed out scan-line by scanline. The resulting printout is at a scale easier to work with than would be a printout of actual temperature values. Table 5-1 lists the alphanumeric characters associated with the corresponding Celsius temperatures.

TABLE 5-1

ALPHANUMERIC CODE USED IN PRINT PROGRAM

Character	°C	Character	°C
-	T<-13	1	1
M	-13	2	2
L	-12	3	3
K	-11	4	4
J	-10	5	5
I	-9	6	6
H	-8	7	7
G	-7	8	8
F	-6	9	9
D	-5	V	10
E	-4	W	11
C	-3	X	12
B	-2	Y	13
A	-1	Z	14
Blank	0	.	15
		+	T>15

5.2.2 Contour Program

The "contour" program was developed to extract and display specified temperature values over selected areas of the HCMM image. This unique program uses a raster to vector conversion to compute and output exact pixel (x) and scanline (y) positions of the desired temperature values or any other desired contour thresholds that are stored sequentially in raster format. A plot program then drives a CRT plotter for displaying the vectors created by the raster-to-vector program at the exact scale of the HCMM imagery. Registration lines are also plotted to be used for registration of the contours within the image; it is possible, therefore, to overlay the thermal contours on the visible image.

The system to produce the automated contouring of HCMM thermal data is shown in Figure 5-1. The structure of a typical HCMM image showing the critical dimensions used for scaling the plotted vectors is indicated. Modifications to the "RASVEC" program were made to process the data from the U-2 High Altitude Multispectral Scanner in the same manner. Examples of the outputs of these two programs are shown in Sections 6 and 7.

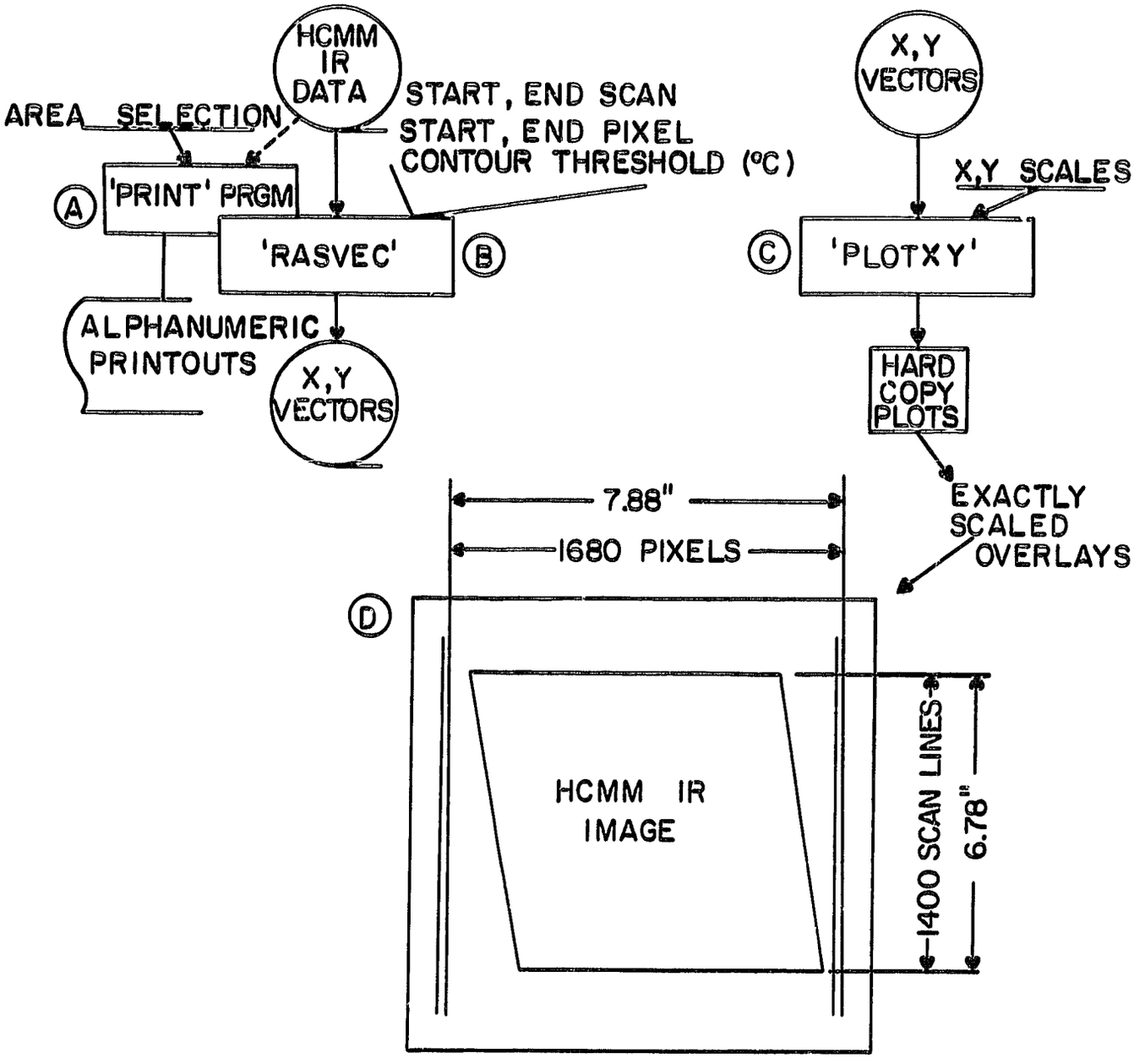

Figure 5-1 Schematic Diagram of Print and Automated Contouring Programs for HCMM Thermal IR Digital Data (CCT's)

5.3 Atmospheric Correction

Corrections for atmospheric attenuation, as discussed in Section 2.1.2, were calculated for selected dates of the HCMM overpasses using actual meteorological sounding data from stations in the Southwest. The calculations were made initially using the program "RADTRA", developed by Rangaswamy and Subbarayudu (1978). The resulting atmospheric corrections for two representative soundings and various surface temperature values are shown in Table 5-2.

For comparison with the corrections obtained using the RADTRA program, some of the corrections were also calculated using a software program in which an atmospheric opacity computation is combined with a radiative transfer model that includes atmospheric multiple scattering effects. This program, termed "VISIR", was developed by Burke et al. (1978). The program allows for a selection of various types of atmospheres or a user-prescribed atmosphere, such as actual sounding data. The VISIR corrections are also shown in Table 5-2.

TABLE 5-2

CORRECTIONS FOR ATMOSPHERIC ATTENUATION (NADIR VIEW ANGLE)

Station	Elevation (above sea level) in meters	Surface Temperature (°K)	Temperature Correction (surface-satellite in °K) RADTRA	VISIR
A	1312	273	-0.3	-0.2
		278	0	-0.1
		283	0.2	-
		289	0.5	-
B	1487	273	0.1	1.3
		278	0.3	1.6
		283	0.5	-
		289	0.8	-

Station A: Winnemucca, Nevada
Station B: Winslow, Arizona
Calculations made using upper air sounding data for 30 May 1978 (00 GMT)

The results of the calculations indicate the atmospheric corrections to be relatively small. The corrections using the RADTRA program are less than 1°K and the corrections using the VISIR program less than 2°K. The

slight negative corrections (i.e., the satellite measured temperature greater than the actual surface temperature) probably are caused by lower surface temperatures (to represent snow cover) being used with an overall warmer sounding; a negative correction in reality would be very unlikely except, perhaps, if a strong temperature inversion existed over the surface. Since the snow cover within the Arizona and California study areas is generally at a higher elevation than the stations used for the calculations, the amount of water vapor in the atmosphere over the snow would be even less and the corrections even smaller than those calculated. The correction for atmospheric attenuation does not appear to be a significant problem, therefore, in the interpretation of HCMM thermal IR measurements of snow surface temperature.

6. DATA ANALYSIS FOR ARIZONA STUDY AREA

6.1 Analysis of Imagery

Visible and thermal-infrared imagery of snow cover on the Salt-Verde watershed of central Arizona were analyzed for the daytime passes of 9 and 15 February, 24 March, and 4 and 15 April 1979. These data represented the best cloud-free samples viewing most, or all, of the watershed. No useful nighttime infrared imagery was available. The daytime observations on these dates show a gradual depletion of the snow cover in the watershed, from a maximum in areal extent in early February, to a nearly complete disappearance of the snowpack by 15 April. Figures 6-1 through 6-10 show the visible and corresponding thermal infrared HCMM images for each of the above dates.

In each of the visible images the areal extent of the highly reflectant snow cover is very well defined. In the thermal infrared images the darker tones represent the lower temperatures associated with the snow cover, and these boundaries correlate closely to those observed in the visible data. The snow-covered area in the February visible images (Figures 6-1 and 6-3) displays considerable variation in reflectance resulting from forest cover and vegetation effects. This is typical of colder, dryer snowfalls that do not cling to vegetation. The March and April visible images (Figures 6-5, 6-7 and 6-9), however, display a much more uniform, high reflectance throughout the snow-covered area. These are typical of recent wet snowfalls that cling to vegetation, or of deeper snow amounts in a melting condition. Some of the variation in snow brightness observed in the February images compared to the March and April data, may also be the result of darker processing of the images.

The thermal infrared images display variations in reflectance only on the image of 9 February (Figure 6-2), where the brightest areas in the corresponding visible image are displayed considerably darker in the infrared than the grayer areas associated with forest cover and vegetation. The snow boundary is very well defined in each of the corresponding infrared images, as the warmer, lower elevation desert areas have a uniformly very bright signature.

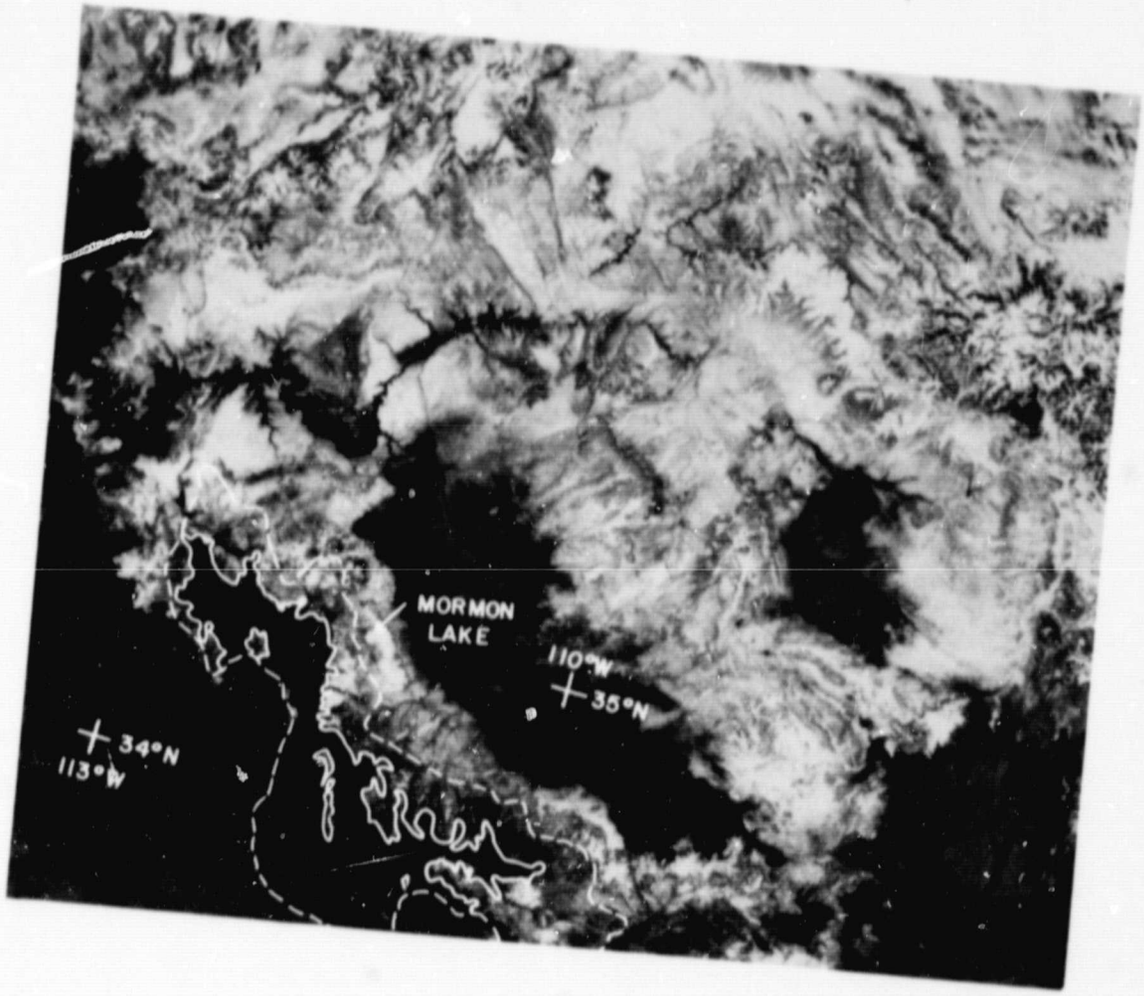

Figure 6-1 HCMM visible image (I.D. 0289-20200-1) of 9 February 1979, showing snow cover extent over the Salt-Verde watershed (outlined) of central Arizona.

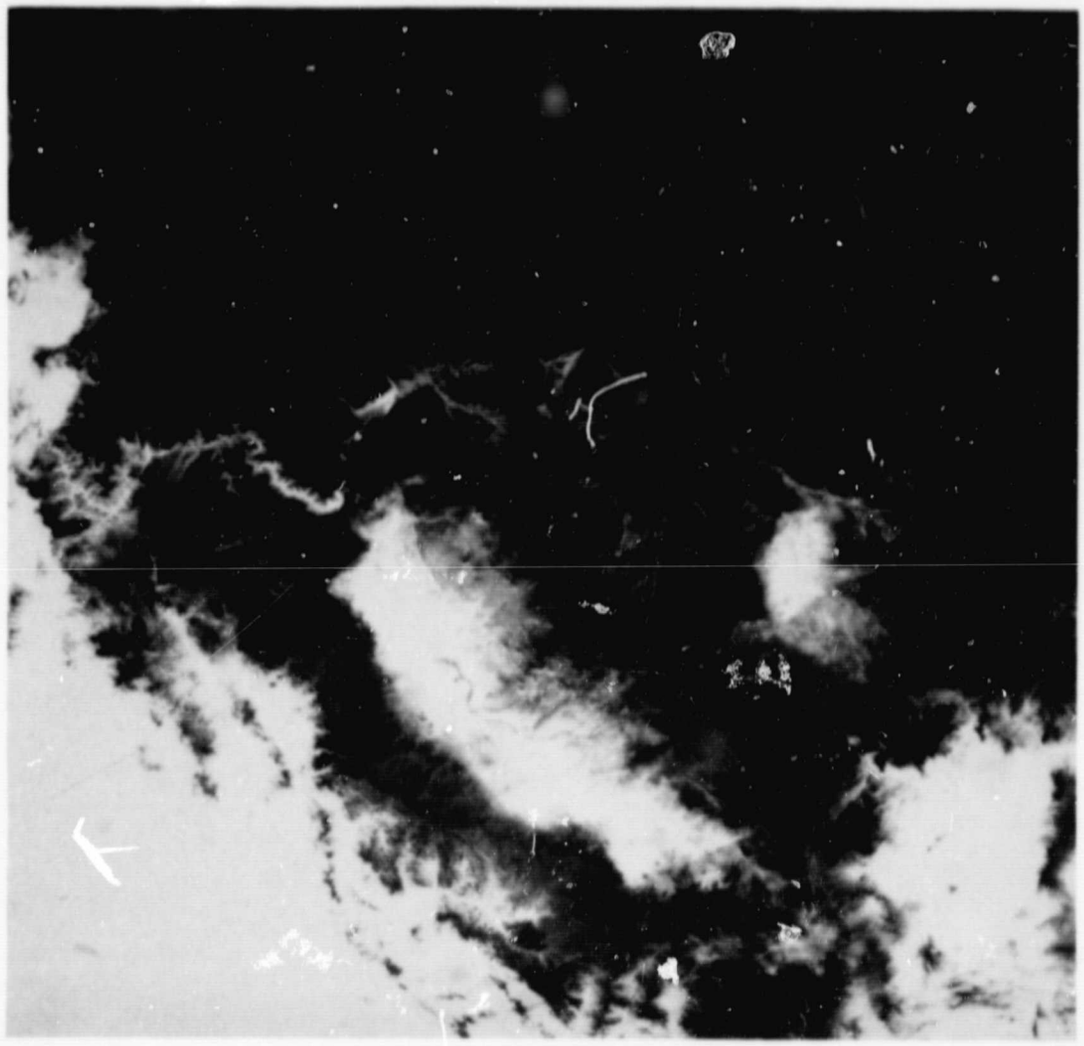

Figure 6-2 HCMM infrared image (I.D. 0289-20200-2) of 9 February 1979, showing thermal pattern of snow cover over the Salt-Verde watershed of central Arizona.

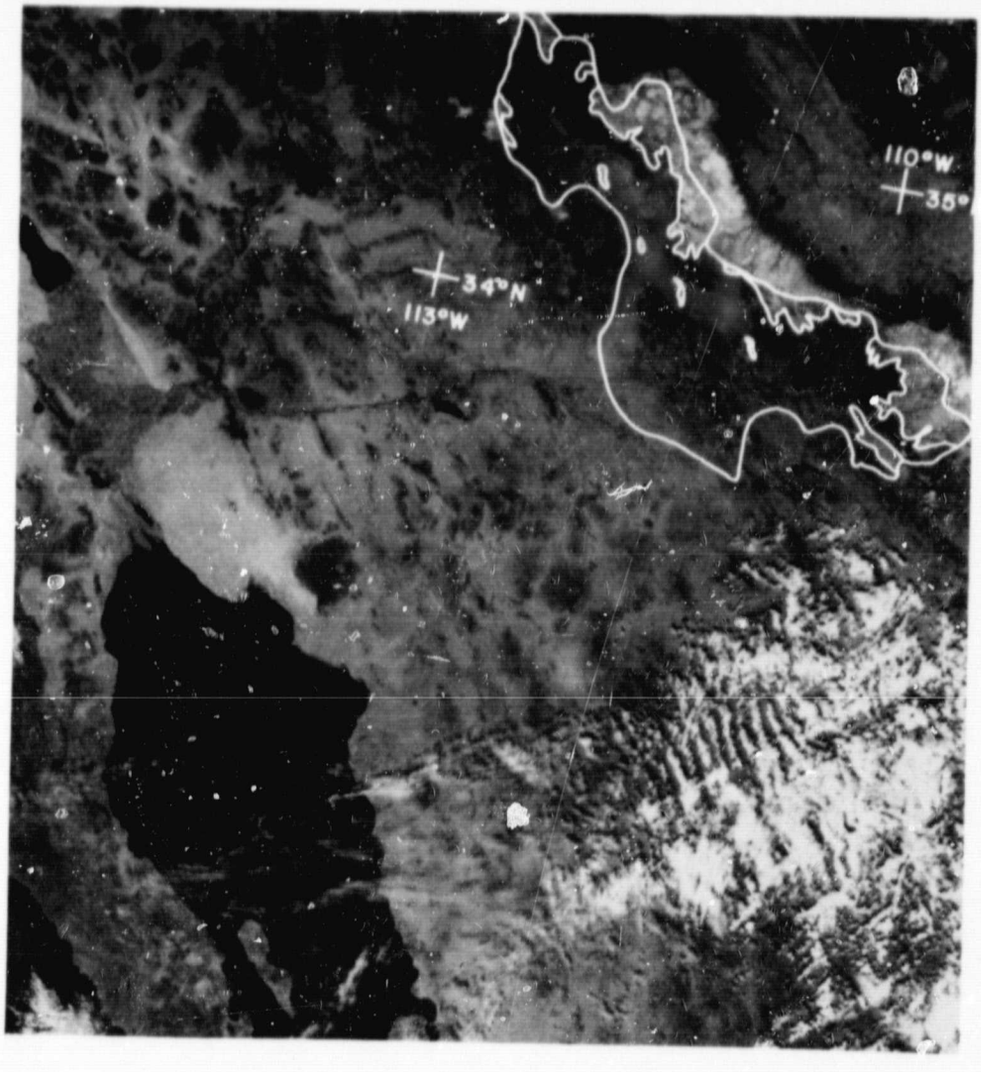

Figure 6-3 HCMM visible image (I.D. 0295-20300-1) of 15 February 1979, showing snow cover extent over the Salt-Verde watershed (outlined) of central Arizona.

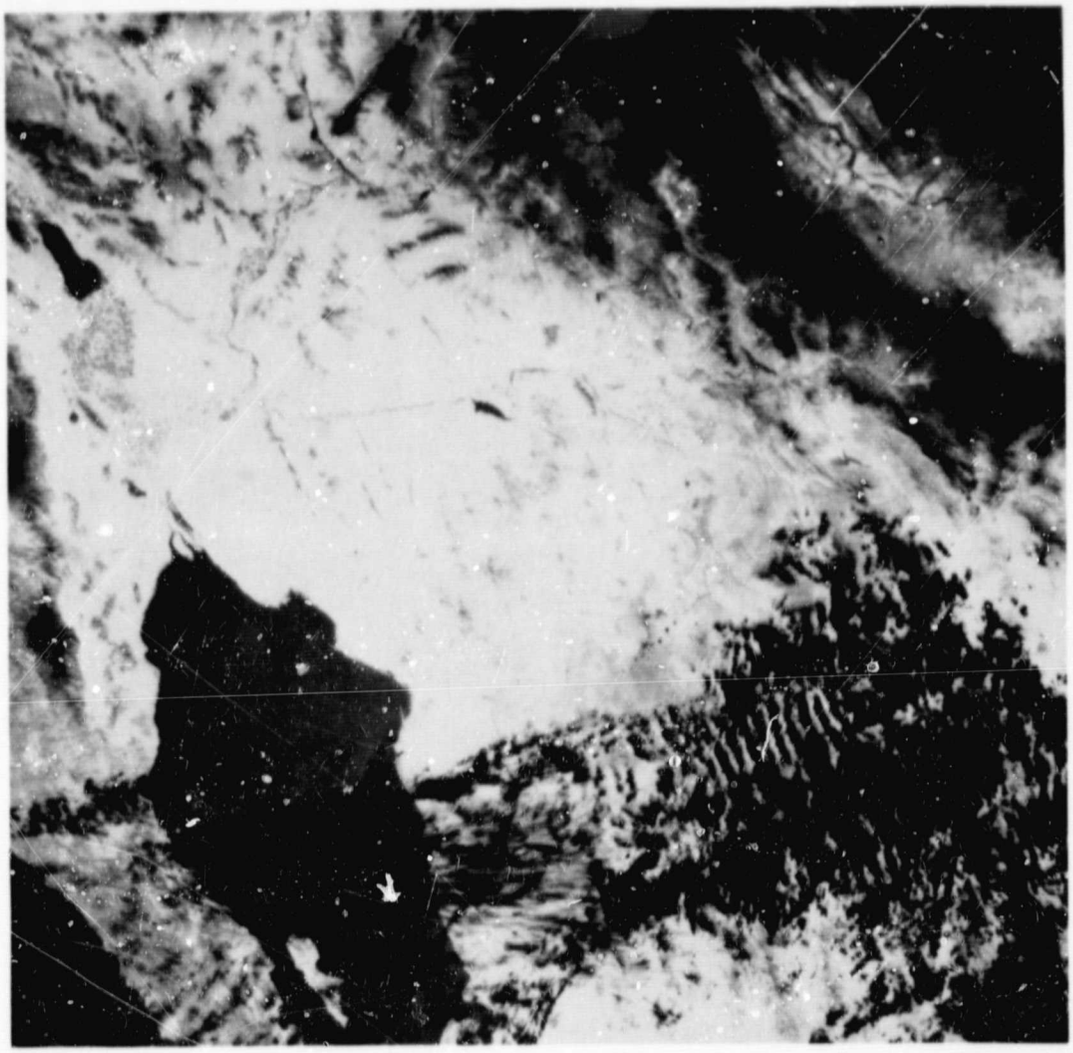

Figure 6-4 HCMM infrared image (I.D. 0295-20300-2) of 15 February 1979, showing thermal pattern of snow cover over the Salt-Verde watershed of central Arizona.

Figure 6-5 HCMM visible image (I.D. 0332-20190-1) of 24 March 1979, showing snow cover extent over the Salt-Verde watershed (outlined) of central Arizona. Arrows denote high water runoff in Gila River.

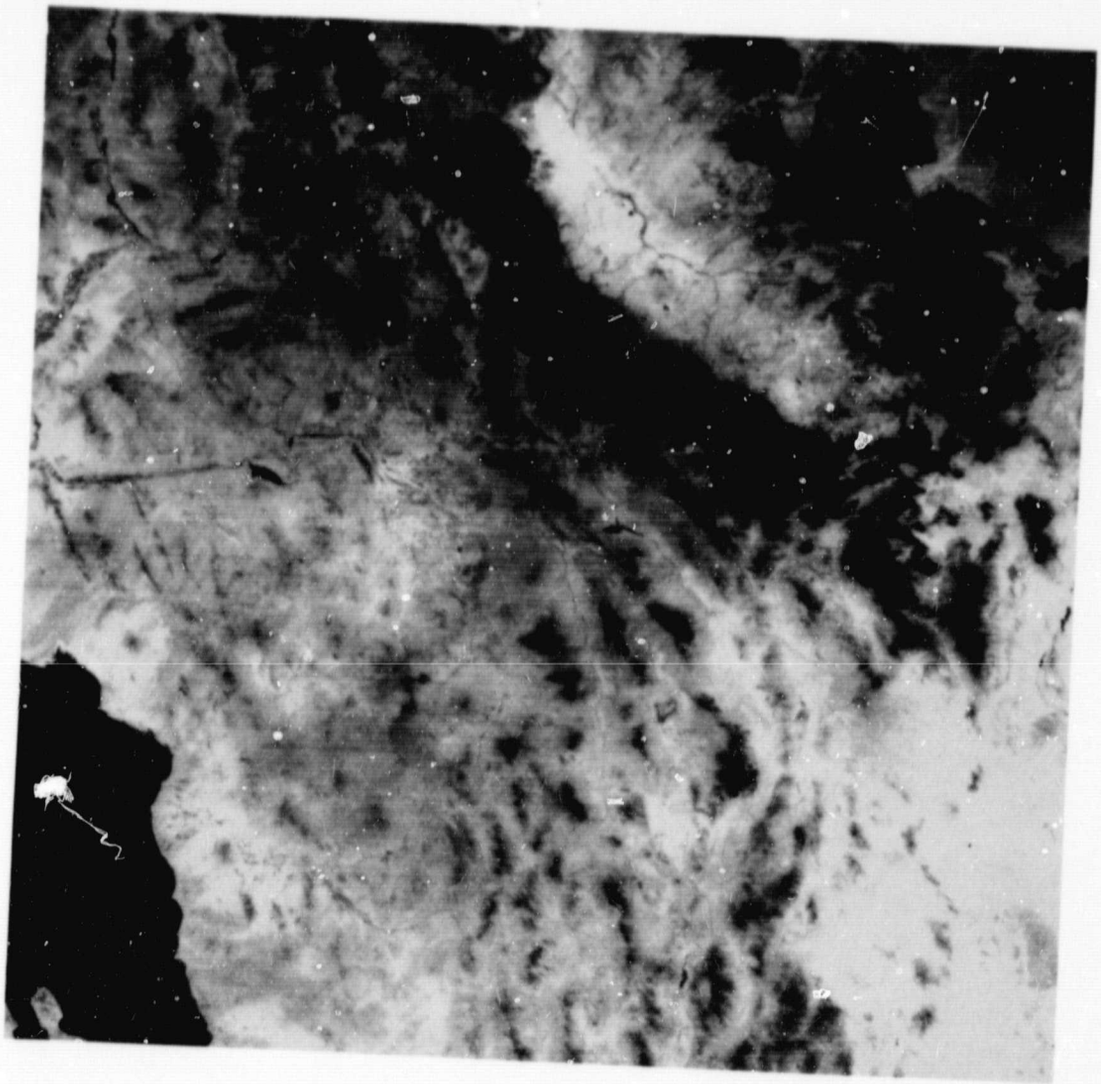

Figure 6-6 HCMM infrared image (I.D. 0332-20190-2) of 24 March 1979, showing thermal pattern of snow cover over the Salt-Verde watershed of central Arizona.

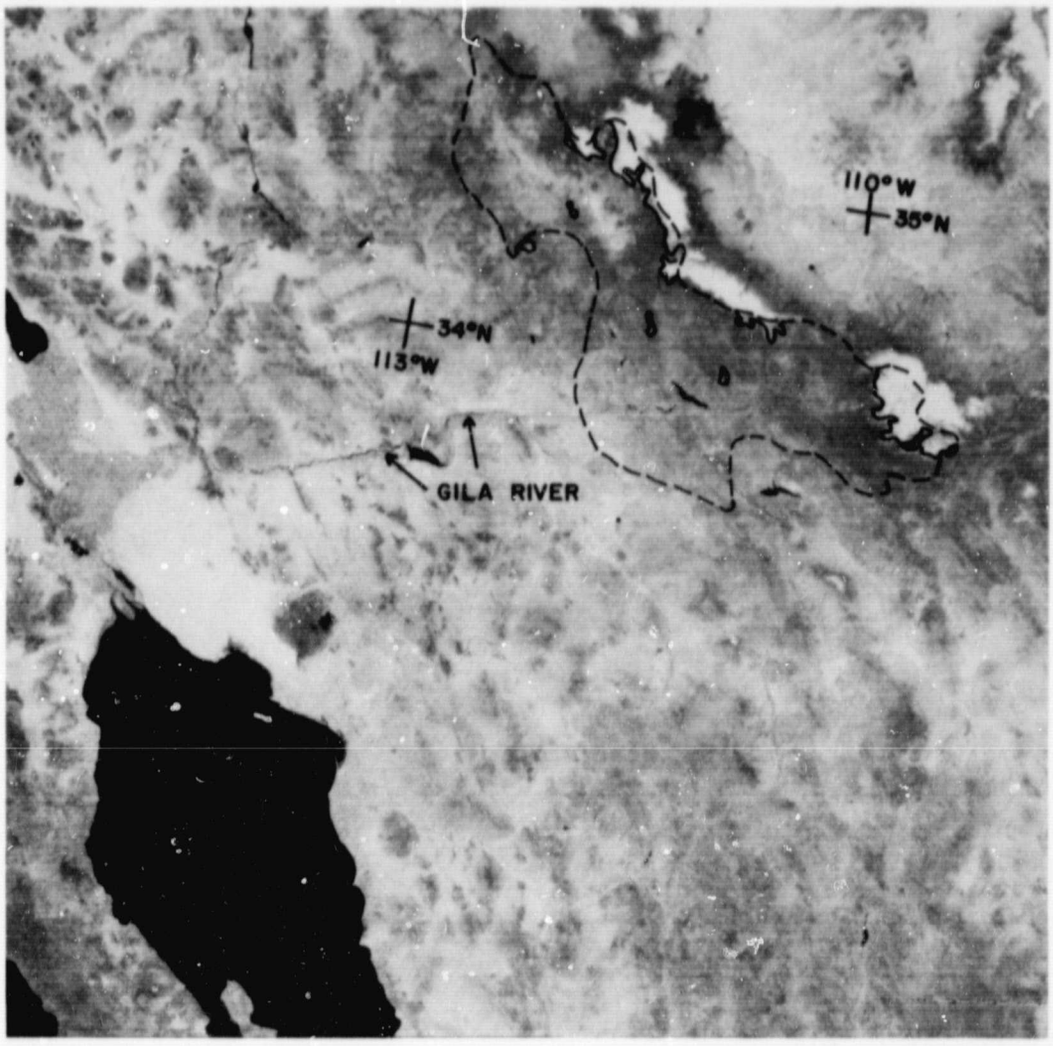

Figure 6-7 HCMM visible image (I.D. 0343-20230-1) of 4 April 1979, showing snow cover extent over the Salt-Verde watershed (outlined) of central Arizona. Arrows denote high water runoff in Gila River.

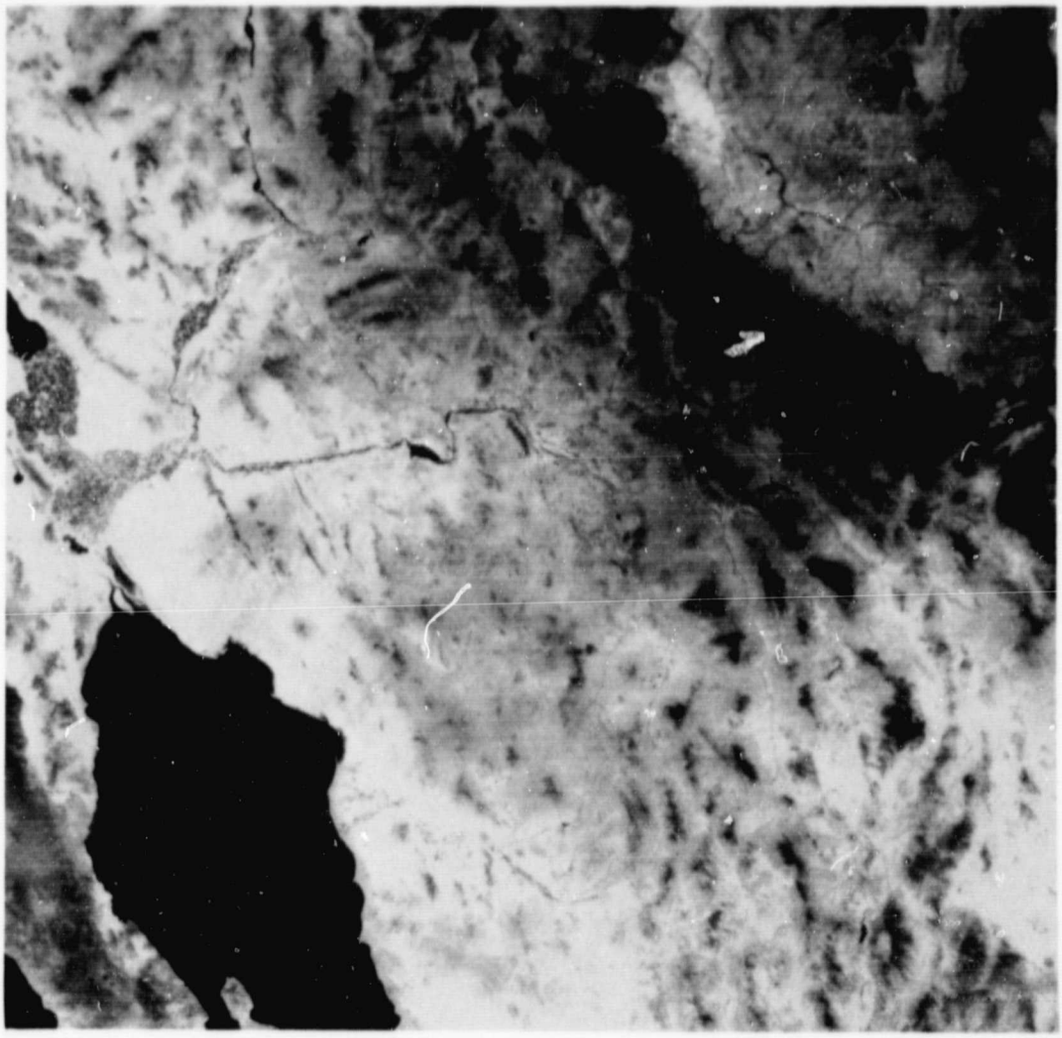

Figure 6-8 HCMM infrared image (I.D. 0343-20230-2) of 4 April 1979, showing thermal pattern of snow cover over the Salt-Verde watershed of central Arizona.

Figure 6-9 HCMM visible image (I.D. 0354-20270-1) of 15 April 1979, showing snow cover extent over portion of the Salt-Verde watershed (outlined) of central Arizona.

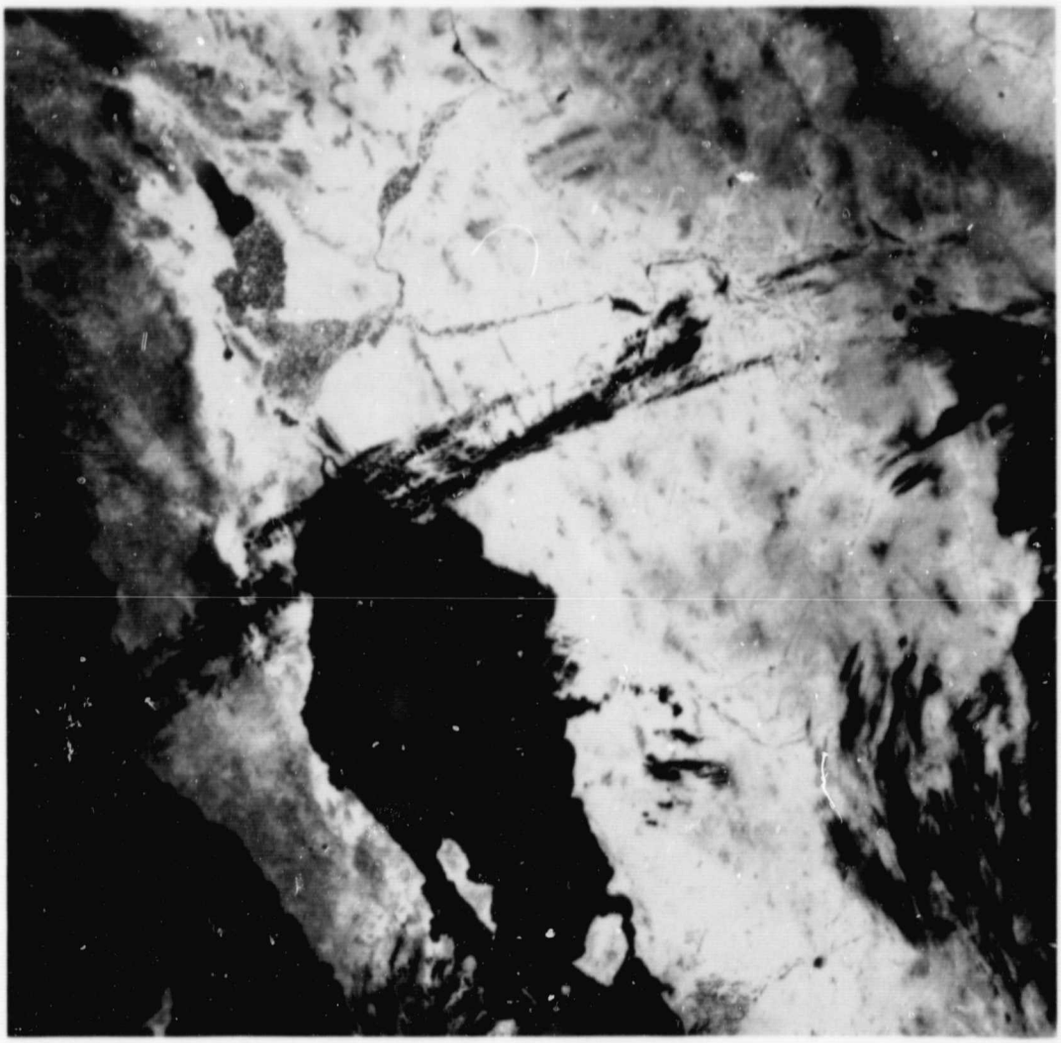

Figure 6-10 HCMM infrared image (I.D. 0354-20270-2) of 15 April 1979, showing thermal pattern of snow cover over portion of the Salt-Verde watershed of central Arizona.

Comparison of the images for 24 March, 4 April and 15 April shows that considerable melting of the snow cover occurred over the three-week period. Also, considerable water can be seen in the Gila River in these images due to the high runoff. The most rapid depletion of the snow cover occurred in the region west and north of Mormon Lake, and in the area southeast of the Mogollon Rim. Figure 6-11 shows the rapid retreat of the snowline as outlined from the HCMM visible images of 24 March, 4 April and 15 April.

6.2 Analysis of Thermal Infrared Data Using Printouts

The HCMM digital data (CCT's) were processed for each of the five cases discussed in Section 6.1. The "print" program, defined in Section 5.2, produced alpha-numeric data printouts, which were analyzed by hand. The results of these analyses are as follows:

(a) 9 February 1979

Of the five Arizona cases, the maximum areal snow extent was observed on this date. Throughout the study area, the 0°C isotherm correlates very closely to the observed snow boundary. Within the snowpack, minimum temperatures range from -5°C to -8°C. These minimum temperatures appear to correlate very well with the isolated areas of maximum brightness observed in the visible image for this date. The areas of maximum brightness are, therefore, some 5° to 8° colder than the less reflective snow-covered areas.

(b) 15 February 1979

Although the snow-cover extent is substantially less on this date, the 0°C isotherm still corresponds very closely to the snowline observed in the visible image. Minimum temperatures across the snowpack have increased slightly and now range from -4°C to -7°C; however, there still appears to be close agreement between the location of the minimum temperatures and the isolated areas of maximum snow brightness in the visible image for this date.

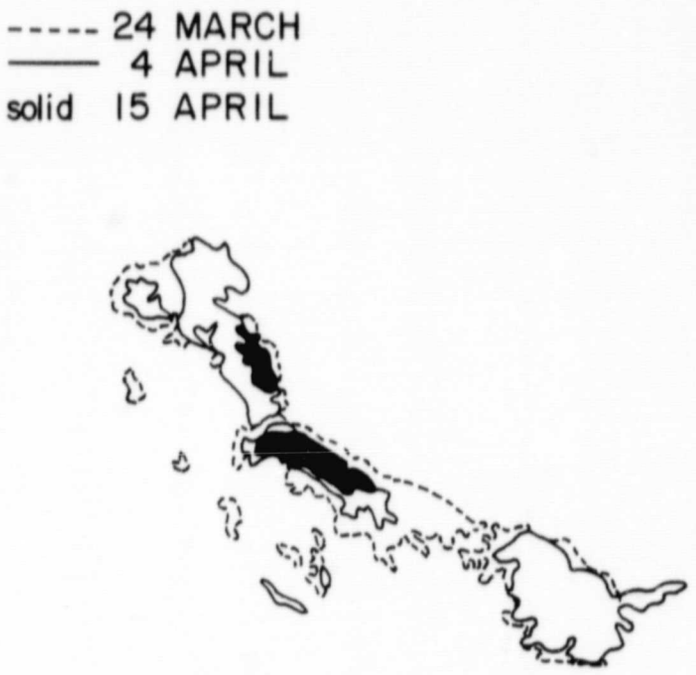

Figure 6-11 Diagram showing rapid retreat of the snow cover over central Arizona mountains as mapped from HCMM visible images of 24 March, 4 April and 15 April 1979.

(c) 24 March 1979

Analysis of the digitized data printout reveals a slight warming trend throughout the snowpack. The 0°C isotherm is now located slightly within the observed snow boundary, and the +2°C isotherm now corresponds closely to the boundary of the main snowpack. Temperatures of the smaller, isolated snow areas located along ridges well to the south of the main snowpack, are closer to +4°C. The minimum temperatures within the main snowpack range from -5°C to -6°C. These are located at the isolated higher elevation terrain areas; however, in this instance, little if any variation in snow brightness can be detected in the visible image.

(d) 4 April 1979

With significant melting and depletion of the snowpack now occurring, significant warming of the remaining snow cover is displayed in the analysis of the digital data. The snow boundary on this date correlates closely to the +5°C isotherm throughout the snowpack. The 0°C isotherm is, however, located very close to the +5°C isotherm along the higher elevation areas of the Mogollon Rim and also along the northern edge of the snowpack surrounding the Mt. Baldy area located in the eastern end of the Salt River Basin. The minimum temperatures within the snowpack in the Mt. Baldy area range from -5°C to -7°C; elsewhere, they range from -2°C to -3°C.

(e) 15 April 1979

The remaining snow cover displays a continued warming trend in the digital analysis on this date. The snow boundary along the Mogollon Rim corresponds closely to the +5°C isotherm, while the northern boundary of the snowpack in this region correlates more with the +7°C to +8°C isotherm. A small isolated pocket of minimum temperature (-1°C to -2°C) within the remaining snow cover, corresponds to an area of maximum brightness (non-forested) observed in the visible image. The temper-

ature of the snow boundary located west of Mormon Lake also appears closer to the +7°C to +8°C isotherm, whereas the temperature of Mormon Lake, which appears to be ice free, is -2°C to -3°C.

The relationships between observed IR temperatures and areas of rapid snow cover depletion during the period from 24 March to 15 April were also examined. The temperature of the snow-covered area that was observed on 24 March but was no longer observed on the 4 April image, due to rapid melting, ranged from about -2°C to +2°C. The area of snow cover observed on 4 April that had melted prior to the 15 April HCMM observation, had temperatures ranging from about 0°C to +5°C.

A sample of a portion of the alpha-numeric IR data printout for 4 April is shown in Figure 6-12; the area shown is outlined in Figure 6-7. The heavier contour represents the 5°C isotherm, which closely fits the observed snow boundary.

6.3 Automated Contour Plotting

The contour plotting program discussed in Section 5.2 was developed to extract and display specified isotherms over selected areas of a single HCMM image. The selection of the specific isotherms to be contoured was based on the analysis of the alpha-numeric data printouts. The contours were plotted at the same scale as the imagery and then duplicated on transparent acetate overlays for more accurate comparison with the satellite-observed snowlines.

This contour plotting program shows considerable promise as a technique suitable for automated processing of snow cover temperature data. It would eliminate the tedious procedure of hand analysis of over-sized computer printouts for comparison with the much smaller scale imagery. A possible procedure would be to have the automated contours plotted for every 2°C at the scale of the HCMM images. It would then be a simple matter to overlay transparencies of the contour plots directly over the imagery and define the temperature of the snow boundary. Comparison between areas of minimum snow cover temperatures and snow brightness levels would also be easily derived.

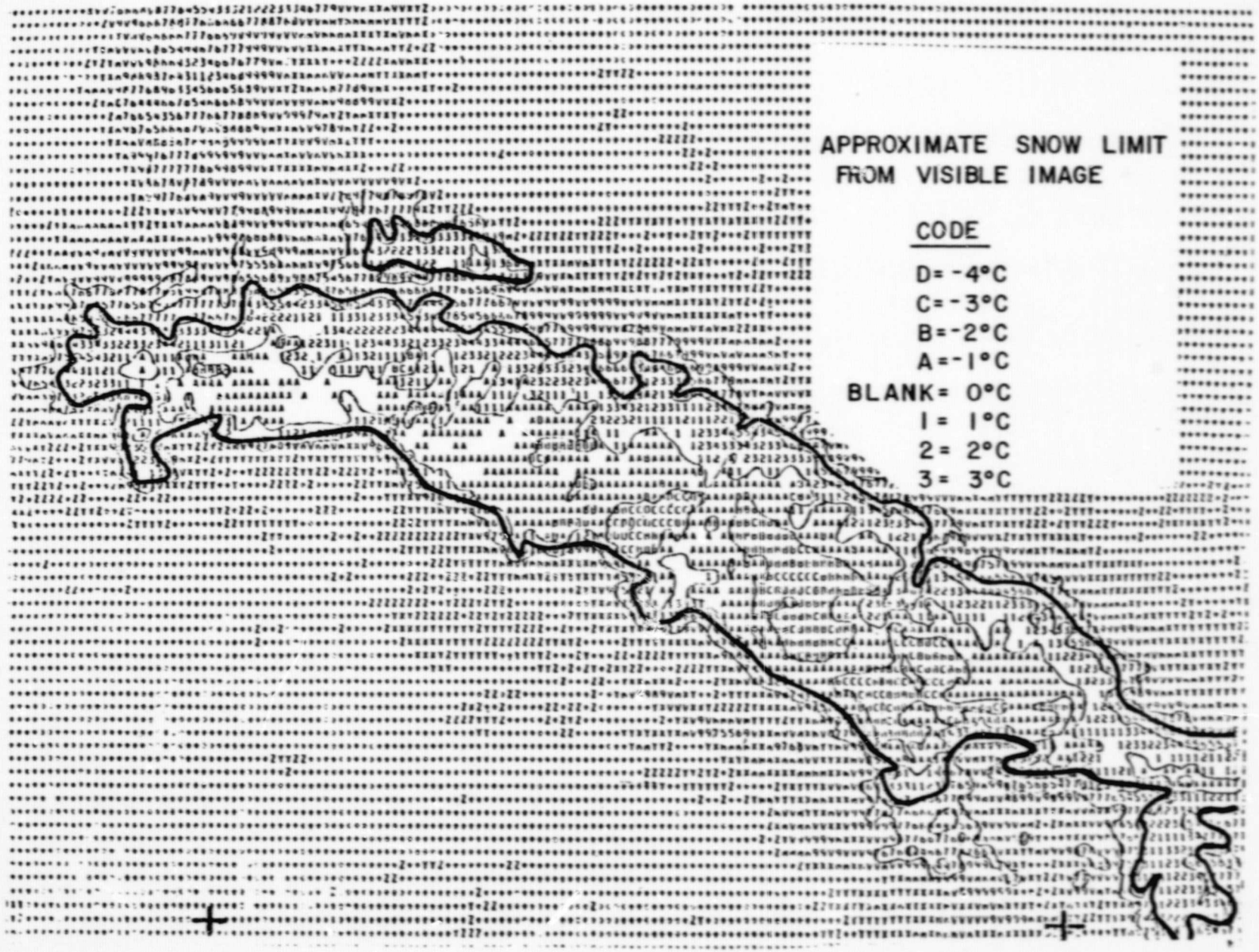

Figure 6-12 Sample of a portion of the alphanumeric IR data printout for 4 April 1979. The heavy dark line represents the approximate snow line as mapped from the corresponding HCMM visible image. Note the close correlation with the +5°C isotherm.

Examples of the contour plotting program are shown in Figure 6-13. The contours shown for 15 February (a) and 24 March (b) represent the 0°C threshold. This isotherm closely fits the observed snow boundary in the visible image for 15 February (Figure 6-3); however, on the 24 March image (Figure 6-5) this 0°C isotherm is located slightly inside the observed snow boundary due to a slight warming trend. The contours shown for 4 April (c) and 15 April (d) represent the +5°C threshold. This isotherm corresponds closely to the entire snow boundary observed on 4 April (Figure 6-7). On 15 April, however, the 5°C isotherm fits only along the snow boundary located along the Mogollon Rim (southern border of larger snow area).

6.4 Comparison of HCMM and U-2 Temperatures

Thermal infrared digital data from the U-2 High Altitude Multispectral Scanner flown over the Arizona study area on 4 April 1979 was processed for a selected portion of the Salt-River Watershed. The data from this daytime flight has been compared with the corresponding HCMM data for that date.

The results of the comparison of the thermal IR band temperatures measured by the U-2 High Altitude Multispectral Scanner for a number of locations over the rapidly melting snow cover, with temperatures for these same locations displayed on the corresponding daytime HCMM pass, indicate that the U-2 temperatures were typically 5°C higher than the values analyzed from the HCMM thermal infrared digital printout. Figure 6-14 shows the comparison between the HCMM and U-2 data for the region near Mogollon Rim in the Central Arizona Mountains. The area shown in the U-2 visible image (above right) is outlined in the corresponding HCMM visible image shown below. Automated contour plots were processed at the same scale as the U-2 and the HCMM images. The +10°C isotherm (top left) closely matches the boundary shown in the U-2 image, while the +5° isotherm (bottom left) fits the snow boundary shown in the HCMM image.

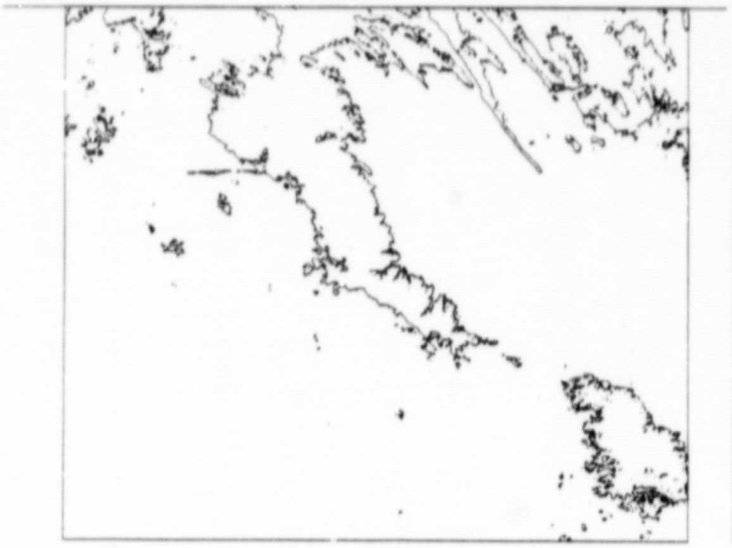

15 February 1979; 0°C threshold

(a)

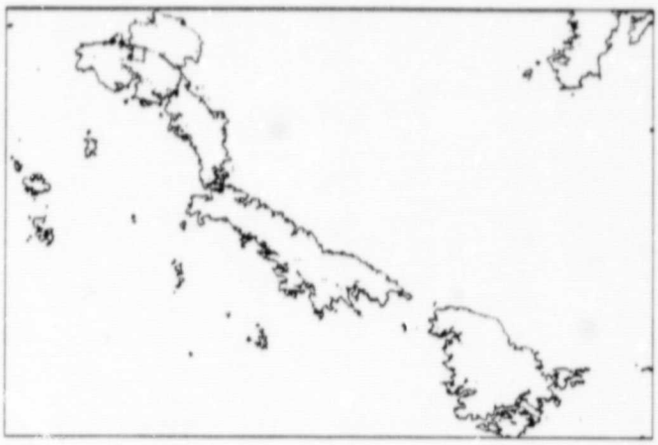

24 March 1979; 0°C threshold

(b)

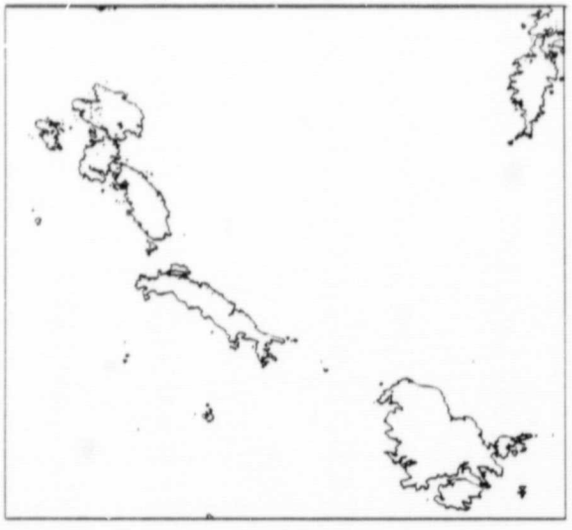

4 April 1979; 5°C threshold

(c)

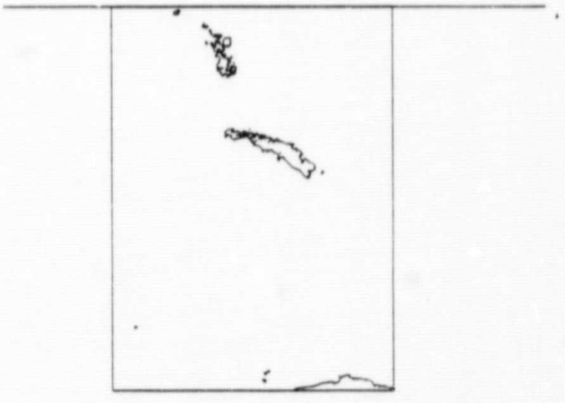

15 April 1979; 5°C threshold

(d)

Figure 6-13 Examples of contour plotting program for snow over central Arizona mountains. The 0°C isotherm is shown for 15 February and 24 March (a and b), and the 5°C isotherm is shown for 4 and 15 April (c and d).

(a) U-2 IR data, 10°C isotherm

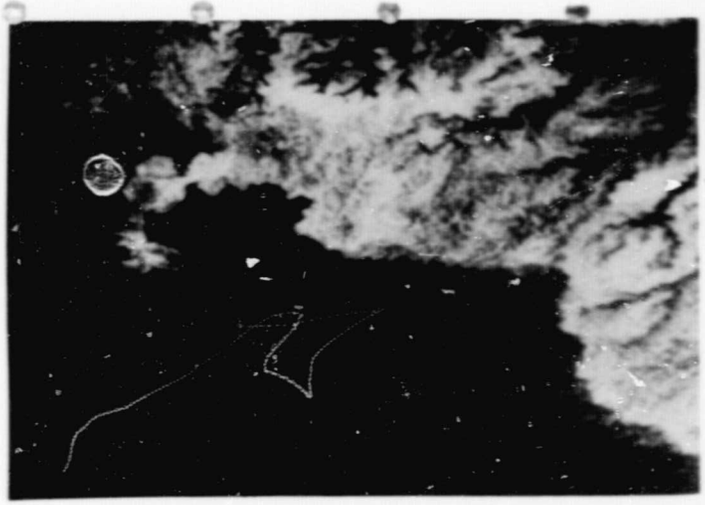

(b) U-2 day visible image

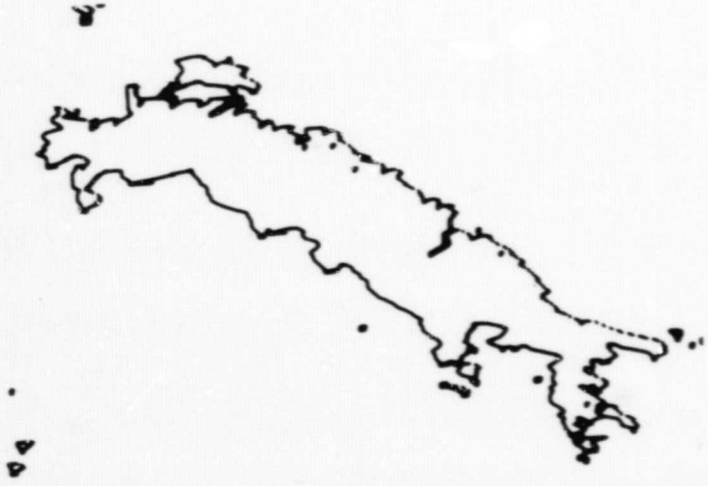

(c) HCMM day IR, 5°C isotherm

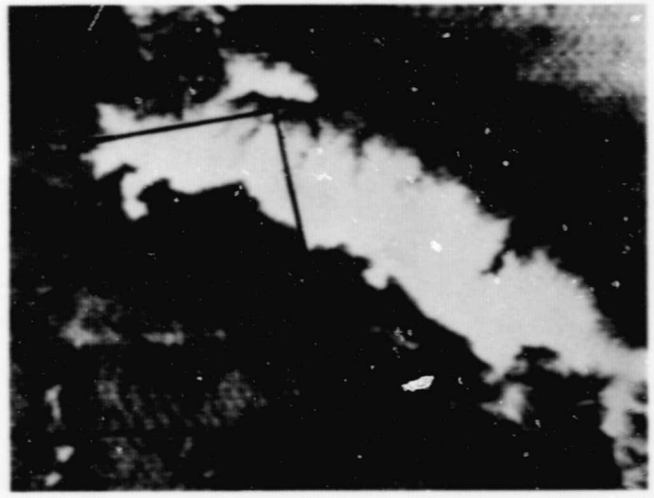

(d) HCMM day visible image (area of U-2 image outlined)

Figure 6-14 Comparison between HCMM visible image (below right) and U-2 visible image (above right), and automated contour plots (10°C for U-2 and 5°C for HCMM) processed at the same scale as the images. The area shown in the U-2 image is outlined on the HCMM image.

The following table shows a sample of the temperature differences between the daytime U-2 and daytime HCMM for the locations indicated on the U-2 contour plot shown in Figure 6-14. These results tend to substantiate the findings of other investigators that with the offset that has been applied to all HCMM data, based on the early White Sands calibration, the HCMM values may, in fact, actually be 5°C too low.

TABLE 6-1

HCMM/U-2 COMPARISON FOR ARIZONA STUDY AREA

Area	Mean HCMM Temperature	Mean U-2 Temperature	Temp. Difference (U-2 minus HCMM)
A	0°C	+5°C	+5°C
B	-1°	+4°	+5°
C	-1°	+4°	+5°
D	-2°	+2°	+4°
temp at snowline*	+5°	+10°	+5°

*snowline mapped from visible data

6.5 Correlation Between IR Temperatures and Other Data

Considerable ground truth information was acquired for the Arizona test site. The data were obtained from a number of sources including the Soil Conservation Service (Phoenix Office), the Watershed Division of the Salt River Project, and the monthly Climatological Data Booklets published by NOAA. These data included snow course measurements, aerial survey maps, snow-extent maps derived from GOES satellite images, SNOTEL data, and daily maximum and minimum air temperatures.

The major snowfalls across the Central Arizona Mountains during the February through April period occurred during the following dates:

Dates	Snow Amount
February 1 + 2	6 to 22 inches
March 19 to 22	5 to 30 inches
March 29 to 30	trace to 16 inches
April 10 to 12	trace to 16 inches

The actual snow depths, as well as snow boundaries across the Salt-Verde watershed at the times of the HCMM observations, are shown in Figure 6-15. There does not appear to be any correlation between reported snow depths and either the reflectance in the visible image or the temperature in the IR image; the observed variations in reflectance and temperature are, therefore, due primarily to the effects of forest cover.

Examination of daily maximum and minimum air temperatures during the major snow melt period of 24 March to 15 April, showed that daily minimum temperatures ranged from near freezing (0°C) to a few degrees below freezing near the 1500 m (5000 ft) elevation. At this same elevation, daily maximum temperatures ranged from about 10°C to 20°C. At elevations near the 2250 m (7500 ft) level, maximum readings ranged from about 5°C to 15°C with daily minimum temperatures ranging from 0°C to -10°C. Throughout this period of snow depletion, therefore, the snow surface apparently underwent a daily melting refreezing cycle. Figures 6-16 and 6-17 display the daily maximum and minimum temperatures for two stations located within the snow-covered area.

Correlative Landsat imagery available for two dates close to the dates of the HCMM images was acquired for comparison of the snow features. Figure 6-18 shows the Landsat MSS-5 band (0.6 - 0.7 μm) image of 1 April 1979. Overall comparison with the HCMM image of 4 April (Figure 6-7) shows that the Landsat image displays considerably more gray-scale variation across the snow extent. This is partly due to the better resolution of the Landsat data (∿80 m) and also to the actual processing of the imagery. The Landsat image displays a higher contrast between the snow-covered and the snow-free terrain than the HCMM image displays. As a result, forested terrain within the snow-covered area can be detected in the Landsat image but not in the HCMM image.

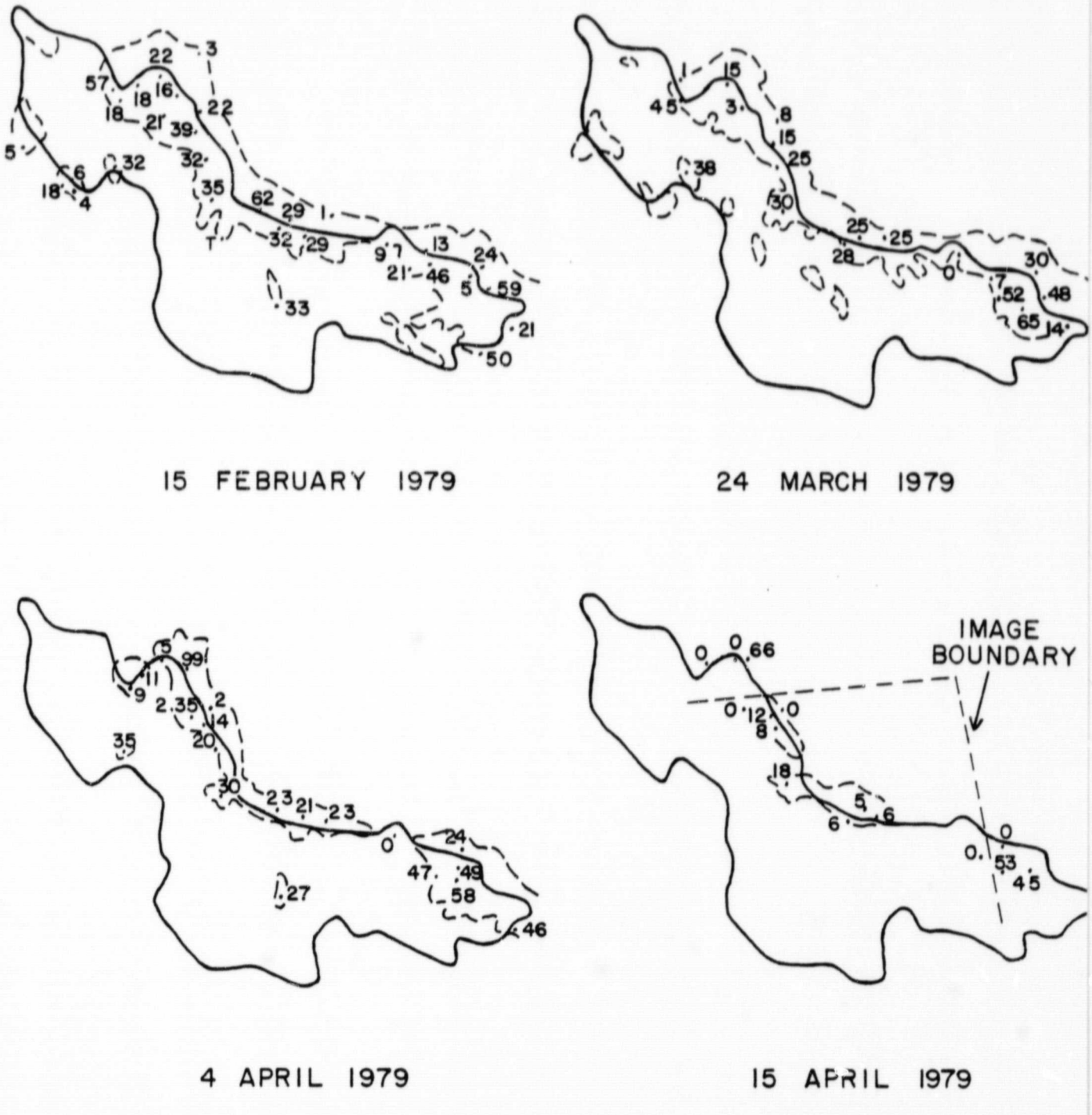

Figure 6-15 Maps of Salt-Verde watershed (solid line) showing reported snow depths (inches) and locations of snow lines (dashed lines) for 15 February, 24 March, 4 April and 15 April 1979.

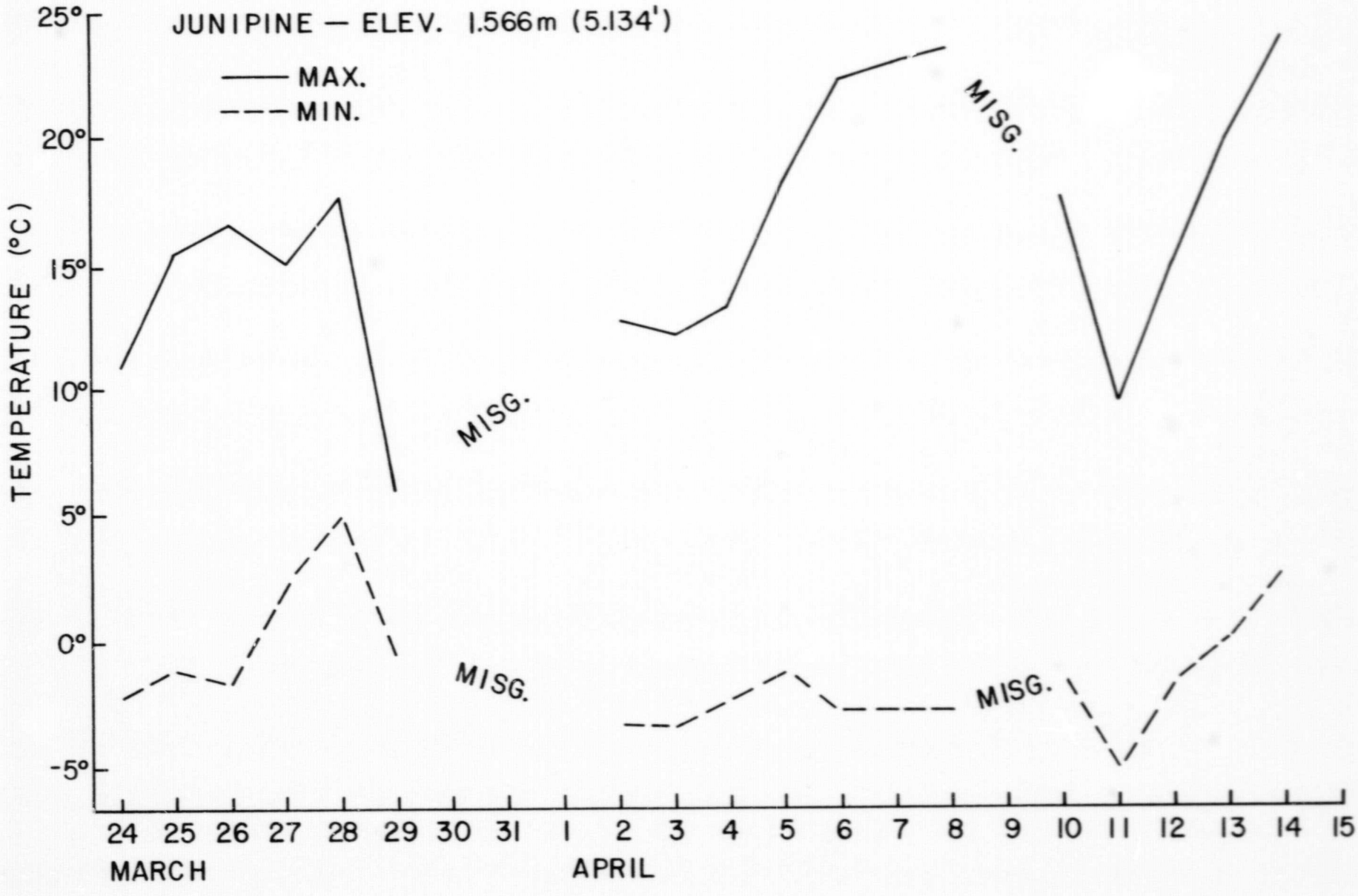

Figure 6-16 Graph showing daily maximum and minimum temperatures at Junipine (Elev. 5,134') for period from 24 March through 15 April 1979.

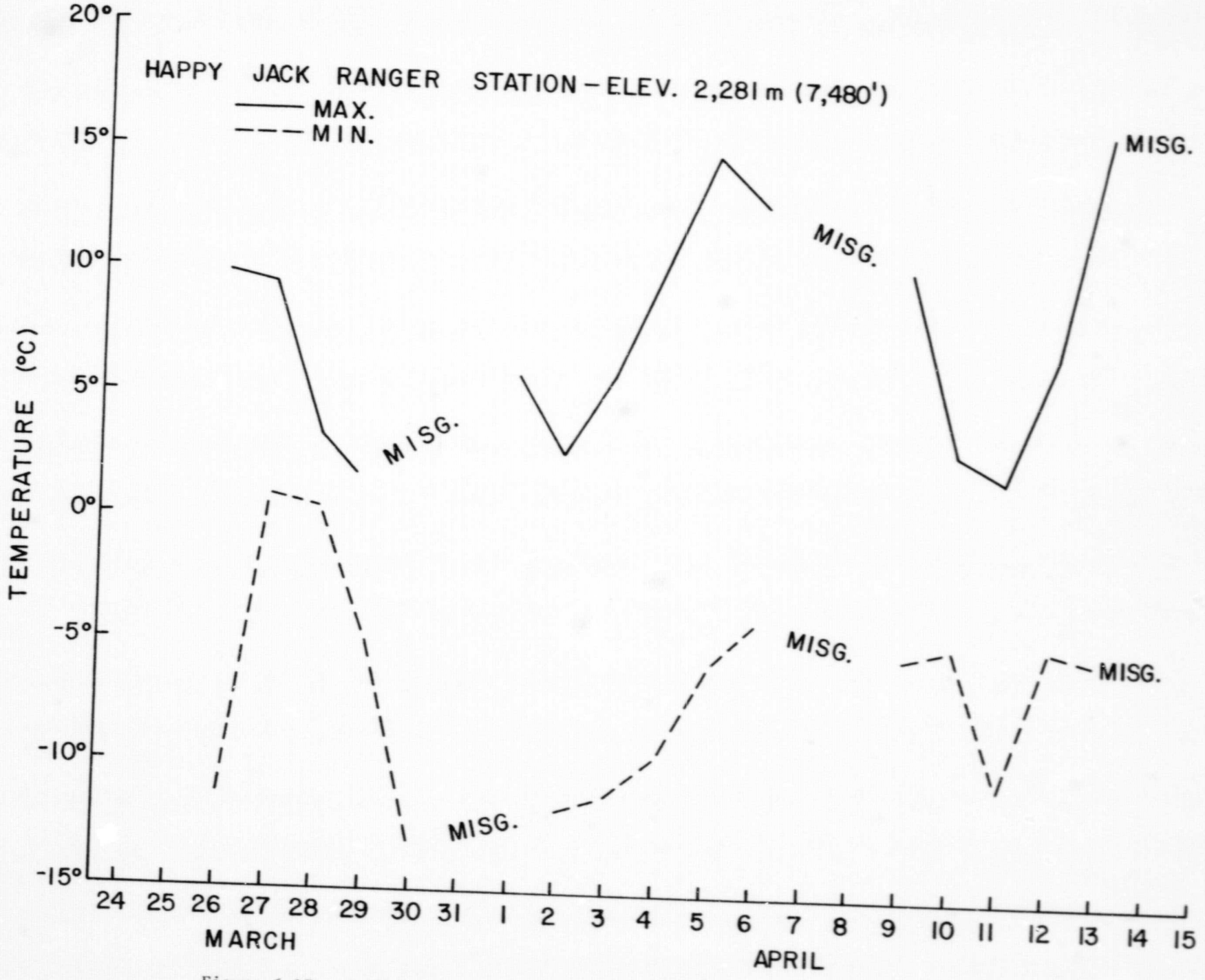

Figure 6-17 Graph showing daily maximum and minimum temperatures at Happy Jack Ranger Station (Elev. 7,480') for period from 24 March through 15 April 1979.

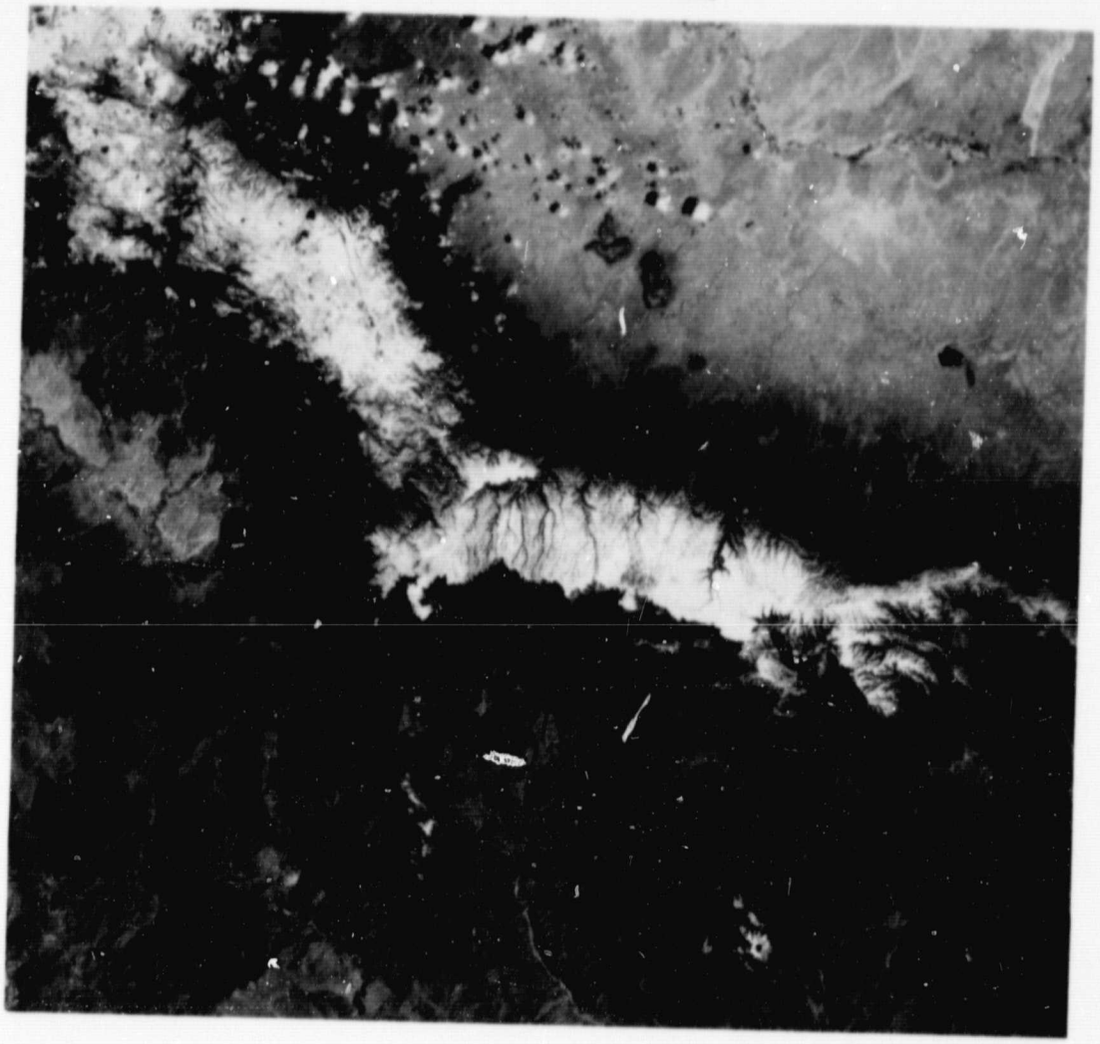

Figure 6-18 Correlative Landsat-3 image (MSS-5) of 1 April 1979 showing considerably more detail and gray-scale variation across the snow extent than the 4 April HCMM image.

7. DATA ANALYSIS FOR SIERRAS STUDY AREA

From the overall sample of potentially useful data for the Sierras study area, described in Section 4, three cases were selected for analysis. These cases (late May 1978, mid-July 1978, and early April 1979) were selected because of the availability for each case of both daytime and nighttime cloud-free HCMM passes. Moreover, for each case, U-2 data were also collected over a portion of the study area either on or near the dates of the HCMM passes. The data available for analysis in each of the three cases, including imagery from other satellites, are listed in Table 7-1. The analyses are described in the following sections.

7.1 May 1978 Case

7.1.1 Analysis of HCMM Imagery

An excellent set of HCMM data were collected over the Sierras study area at the end of May 1978, approximately one month after the satellite went into operation. During a three-day period, four HCMM passes (two nighttime and two daytime) provided essentially cloud-free coverage of the southern Sierras. The data set consists of the nighttime passes on 29 and 30 May and daytime passes on 30 and 31 May. The HCMM images from these passes are shown in Figures 7-1 through 7-3.

The daytime visible and thermal IR images of 30 and 31 May are shown in Figures 7-1 (a and b) and 7-2 (a and b), respectively. The visible images indicate that a substantial snow cover still exists in the southern Sierras at the end of May. The Sierras snowpack in the spring of 1978 was, in fact, above normal and was slow to melt because of abnormally cool weather. Snowmelt runoff, however, was less than had been forecast, mainly because much of the snowmelt went to recharge the ground water, which had been depleted over the past two dry years.

Aerial snow surveys were flown over the southern Sierras snowpack by the Corps of Engineers about every 10 days from the end of April through early July. The snow-covered area of the Kings River Basin was mapped on 22 May as 1256 km^2 (785 mi^2) and on 2 June as 1152 km^2 (720 mi^2); the equivalent snowline elevations for the two dates would be 2490 m (8300 ft) and 2580 m (8600 ft), respectively, making the snowline

TABLE 7-1

DATA SAMPLE FOR SIERRAS STUDY AREA

Case	DATA AVAILABLE FOR ANALYSIS					
	HCMM		U-2	Other Satellite		
1. May 1978	29 May	Night IR	(HCMR)	27 May	Landsat	
	30 May	Night IR	31 May (Flight 33) - Day	30 May	NOAA VHRR	
	30 May	Day VIS, IR	1 June (Flight 34) - Night	31 May	NOAA VHRR	
	31 May	Day VIS, IR				
	30-31 May	36 hr ΔT				
	30 May	12 hr ΔT				
2. July 1978	17 July	Night IR	(HCMR)	20 July	Landsat	
	17 July	Day VIS, IR	19 July (Flight 35) - Day			
	17 July	12 hr ΔT	20 July (Flight 36) - Night			
3. April 1979	3 April	Night IR	(High Altitude Multispectral	5 April	NOAA AVHRR	
	4 April	Night IR	Scanner)			
	5 April	Day VIS, IR	4 April (Flight 79-029) - Day			
	4-5 April	36 hr ΔT	4 April (Flight 79-030) - Night			

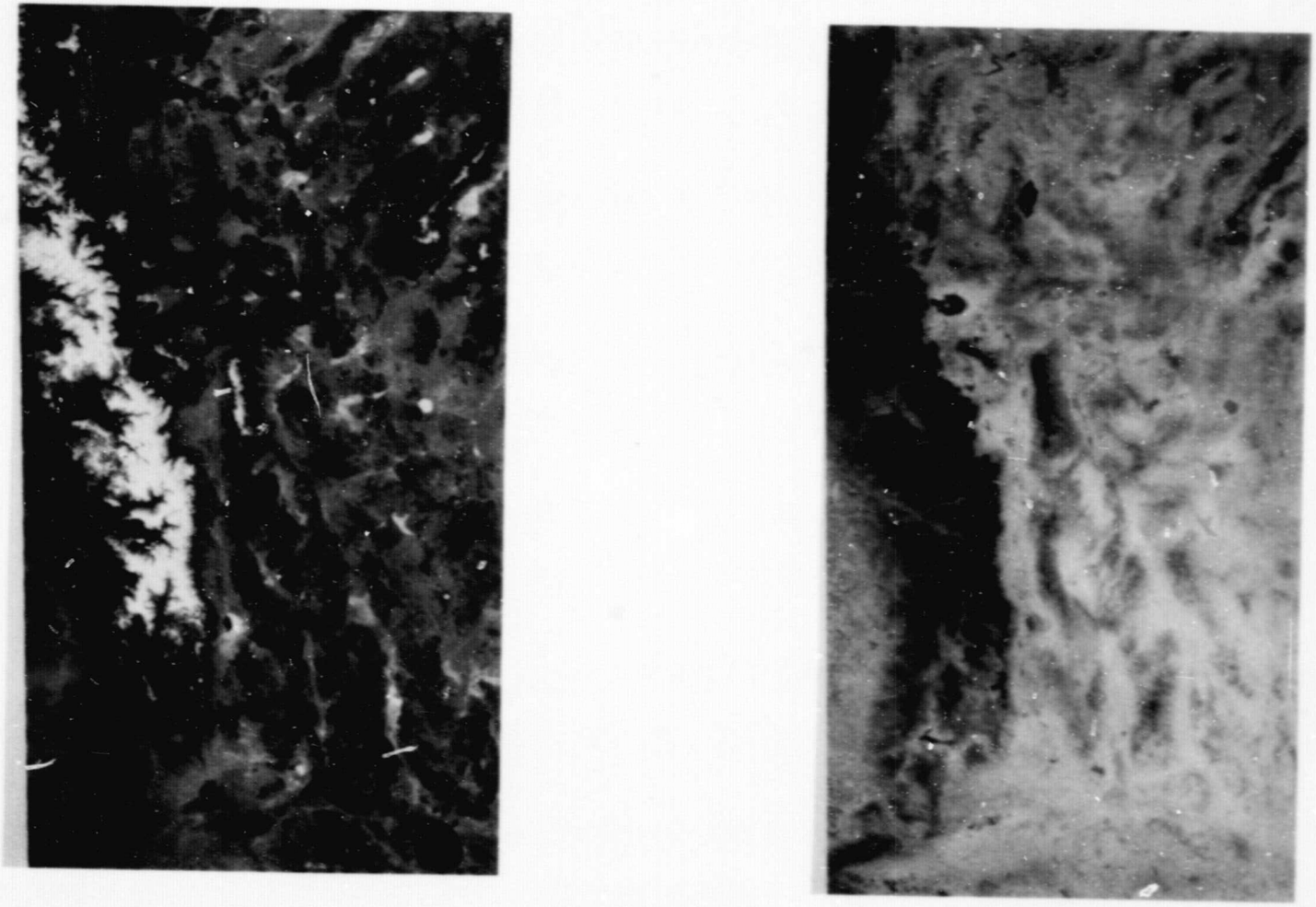

(a) (b)

Figure 7-1 HCMM visible image (a) and corresponding daytime IR image (b) for 30 May 1978, showing snow cover in the Sierra Nevada study area (Image ID Numbers: (a) 034-21140-1 and (b) 034-21140-2).

(b)

(a)

Figure 7-2 HCMM visible image (a) and corresponding daytime IR image (b) for 31 May 1978, showing snow cover in the Sierra Nevada study area (Image ID Numbers: (a) 035-21310-1 and (b) 035-21310-2).

elevation during the 29-31 May period about 2550 m (8500 ft). Although the continuous snowline was mapped at this level, some patchy snow cover still existed at lower elevations. For example, a station at the 2020 m (6735 ft) level reported a snow depth of 30 cm (12 in) on 31 May. New snow had also fallen over parts of the area on the 24th and 25th.

In the visible images (Figures 7-1a and 7-2a) the snowpack in the higher elevation, non-forested areas displays a uniform high brightness level, whereas the snow located within lower elevation, densely forested areas along the western slope of the Sierras has a mottled, gray-white appearance. A few cellular clouds can also be detected in the image of 31 May (Figure 7-2a).

On both dates, the corresponding thermal IR images (Figures 7-1b and 7-2b) display an almost uniformly dark pattern (lower temperatures), the extent of which almost exactly fits the snowline as mapped from the visible images. It appears, therefore, that the temperatures of the snow surface are significantly lower than those of the surrounding snow-free terrain, with the difference being sufficient for the snowline to be distinctly delineated. It is difficult in the IR images, however, to detect variations in temperature within the snow-covered area, such as the reflectance variations seen in the visible images.

The nighttime IR images of 29 and 30 May, shown in Figures 7-3a and 7-3b, display distinct variations in gray-tone level across the Sierras snowpack. The snow in the higher elevation, non-forested areas appears uniformly darker (colder) than the snow located along the densely forested, lower elevation areas along the western slope. Comparison with the visible images of 30 and 31 May shows that in some locations the boundary of the area of lowest temperature (darkest tone) fits the snowline closely, as was the case with the daytime images. In other locations, however, the nighttime thermal pattern does not define the snowline. Moreover, in the nighttime image, lighter toned gray levels are observed along the western slopes of the Sierras and at the extreme southern extent of the snowpack; the presence of these lighter gray-tone levels in areas shown to be snow-free (in the visible image) is apparently also the result of nighttime radiational cooling, which reduces the temperature contrast between the snow cover and the non-snow-covered terrain. Thus, the snow cover extent appears to be depicted better in the daytime than in the nighttime thermal IR images.

(a)

(b)

Figure 7-, HCMM nighttime IR images of 29 May (a) and 30 May 1978 (b), showing snow cover in the Sierra Nevada study area (Image ID Numbers: (a) 033-10040-3 and (b) 034-10220-3).

7.1.2 Comparison Between HCMM and Other Satellite Imagery

In addition to the HCMM data, Landsat and NOAA VHRR images were also available in late May, providing an opportunity to compare the resolutions of the respective sensor systems. A Landsat-2 scene, viewing a portion of the southern Sierras from Mono Lake southward to the northern part of the Kern River Basin, is shown in Figure 7-4. At the 80 m resolution of Landsat, considerably more detail along the snow line can be mapped than is possible with HCMM; also variations in reflectance associated with forest effects can be mapped in greater detail. Nevertheless, comparison of the Landsat and HCMM images reveals that the overall snow-cover extent can be mapped nearly as accurately from the 500 m resolution HCMM data as from the 80 m resolution Landsat data, even though the fine-scale variations in the snow line cannot be detected.

Comparative NOAA-5 thermal IR images are shown in Figure 7-5 (a and b). Figure 7-5a is the daytime IR image for 30 May and Figure 7-5b is the daytime IR image for 31 May (note that the VHRR IR data are displayed the reverse of HCMM, with lighter tones signifying lower temperatures). The improved quality and resolution of the corresponding HCMM images is apparent. The areas of lowest temperature were mapped from the corresponding HCMM and VHRR thermal IR images of 31 May, as shown in Figure 7-6 (a and b). Although the overall patterns appear similar, the lower resolution (1 km) of the VHRR image provides somewhat less detail than the HCMM data in defining the snow extent.

7.1.3 Analysis of HCMM Digital Data

HCMM digital IR data were processed initially in the printout format for all four passes during the 29-31 May period. Subsequently, several automated temperature contour plots were also generated.

Hand analysis of the digital printout for the 29 May nighttime pass indicates that the snow line, as mapped from the visible image, and defined in most areas by the dark gray tone in the IR images, is generally delineated by the 0°C isotherm. Further comparisons with the imagery show that the boundary of the darker tones, which represent the snow at the non-forested higher elevation terrain, closely correspond to the -7°C isotherm. The lowest temperatures observed within the solid

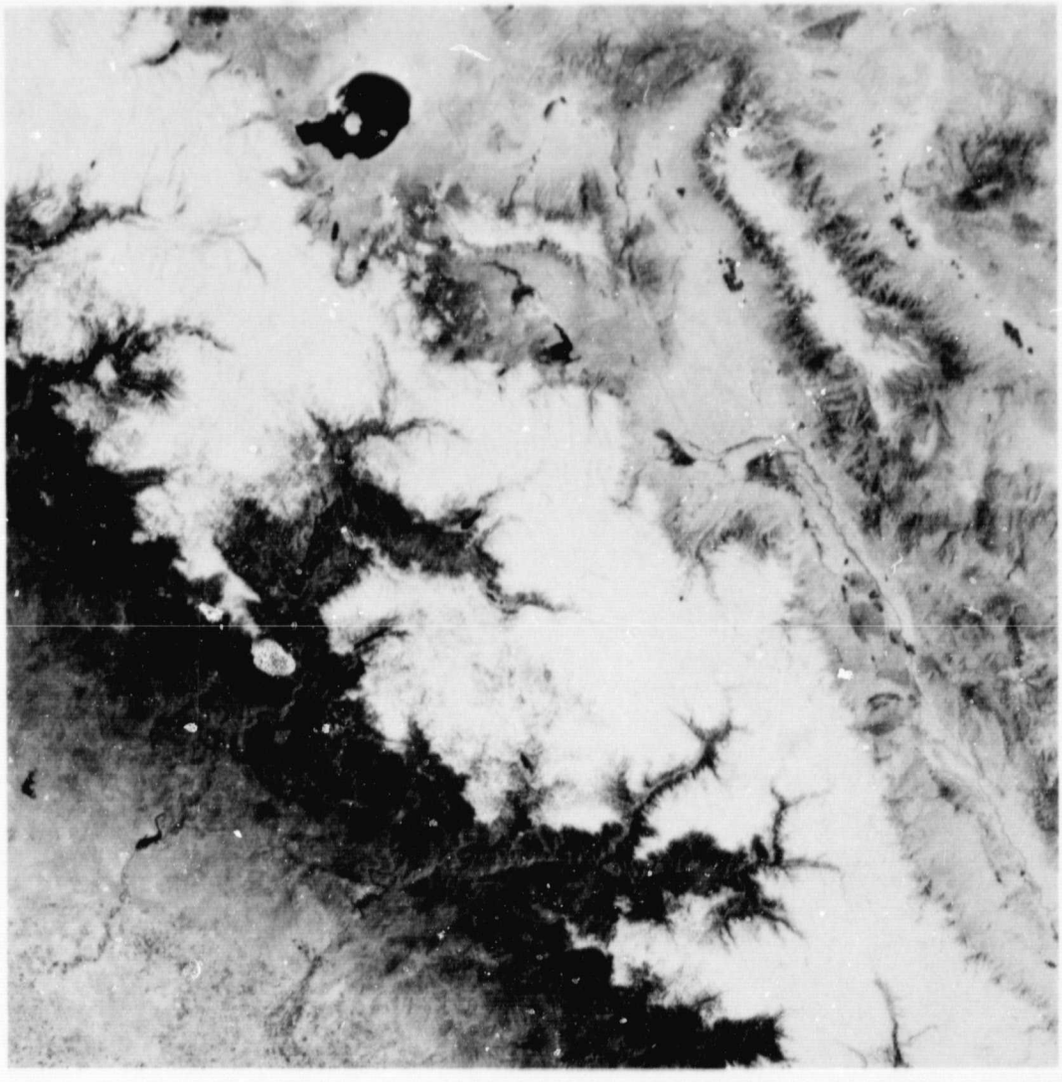

Figure 7-4 Correlative Landsat-2 image (MSS-5) of 27 May 1978, viewing a portion of the southern Sierras from Mono Lake southward to northern portion of Kern River Basin.

(b)

(a)

Figure 7-5 Comparative NOAA-5 VHRR daytime thermal IR images showing the Sierras snow cover on 30 May (2) and 31 May (b) 1978 (note that in these images, the lower temperatures are displayed in brighter tones).

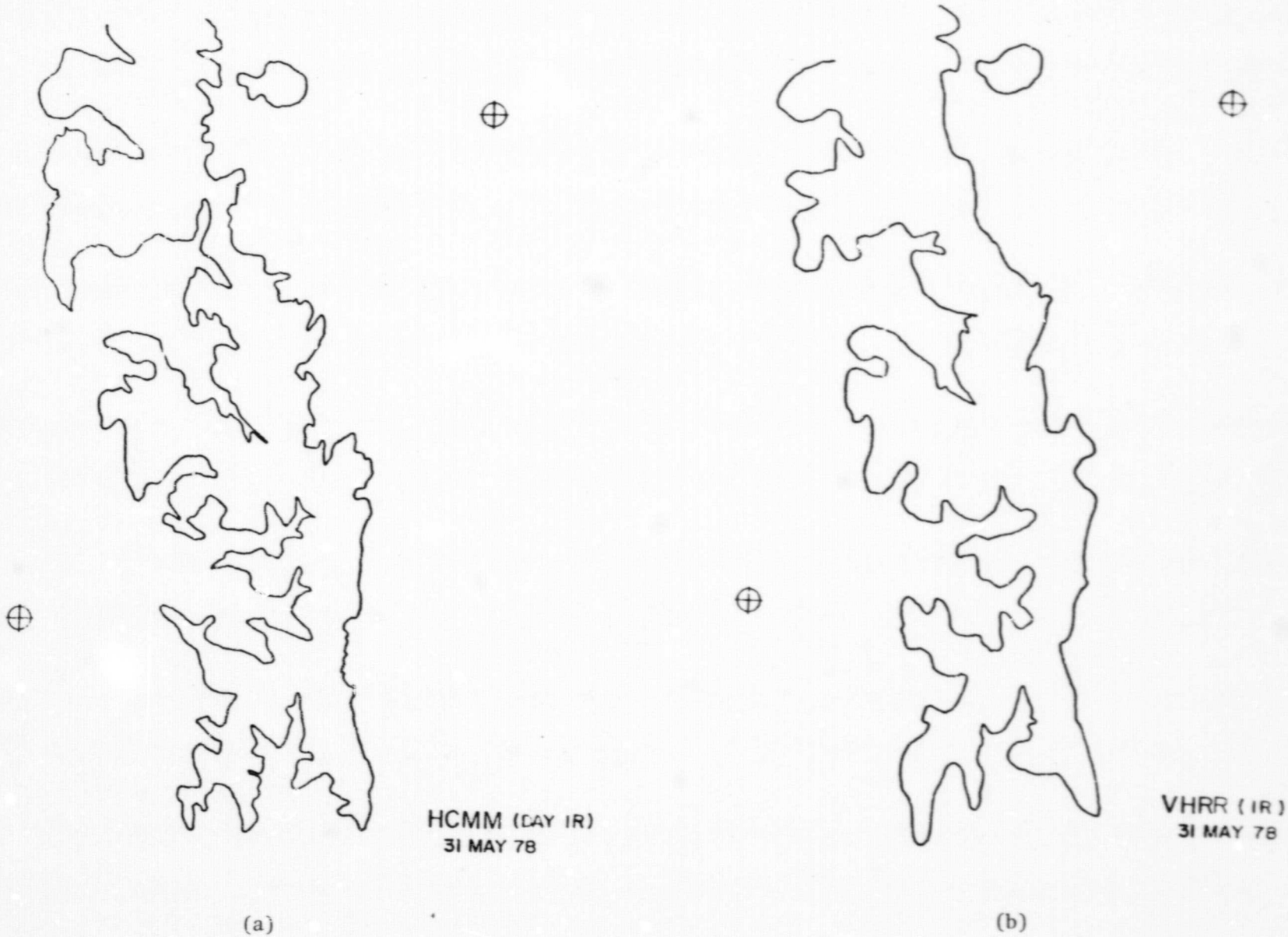

Figure 7-6 Apparent snow cover boundary as mapped from the HCMM day IR image of 31 May (a) and the NOAA/VHRR IR image (b) also of 31 May.

darker toned areas range from about -9°C to -11°C; these minimum temperatures likely define the highest elevation ridges of the Sierras. Temperatures within the lighter gray-toned areas associated with the densely forested areas generally range from about -1°C to -3°C.

The temperature of the snow boundary is also fairly well defined by the 0°C isotherm in the 30 May night IR digital analysis. However, the overall temperatures within the higher elevation snowpack are indicated to be slightly lower. The boundary of the darkest tone areas representing the higher elevation, non-forested terrain is better represented in this case by the -8°C isotherm, whereas the lowest temperatures within the solid dark area now range from about -10°C to -13°C. Also, the areal extent of these minimum temperatures at the higher elevation terrain appears to have about doubled in size from the previous night.

Analysis of the IR digital products for the daytime passes of 30 and 31 May shows the temperature of the snow boundary generally averaging near +10°C. A strong temperature gradient exists between non-snow-covered terrain and the snow boundary, with temperature spreads ranging anywhere from about 15° to 20°C at the actual snow line. The temperature of the snow surface at the snow line varies considerably along the entire snow boundary, ranging from about +3°C to +15°C; therefore, although the snow line can be readily located because of the sharp temperature gradient, the actual temperature of the snow boundary is somewhat more difficult to determine in the daytime IR data.

The outer boundary of the more solid, highly reflective snow cover at the higher elevation, non-forested terrain closely corresponds with the 0°C isotherm on both days, with minimum snow cover temperatures within these brighter areas ranging from -4°C to -5°C. The temperature of the snow remaining in the lower elevation, densely forested areas along the west slope ranges from about +1°C to +12°C.

The IR temperatures of the snow boundary, the snow within forested areas, the boundary of higher elevation snow, and within the higher elevation snow are summarized in Table 7-2 for the four HCMM passes. The results of the analysis indicate that the temperatures are very consistent over the two nighttime and the two daytime passes. The average differences between the nighttime and daytime values are also shown in the table. It appears that the temperature difference is less at the

TABLE 7-2

SUMMARY OF HCMM THERMAL IR TEMPERATURES FOR 29-31 MAY

Target	Nighttime IR		Daytime IR		Night/Day
	29 May	30 May	30 May	31 May	Temp Difference
snow boundary	0°C	0°C	∿10°C	∿10°C	∿10°C
snow within forested areas	-1°C to -4°C	-1°C to -4°C	12°C to 1°C	12°C to 1°C	7°C to 16°C
boundary of higher elevation snow	-7°C	-8°C	0°C	0°C	7°C to 8°C
minimum temp within higher elev snow	-9°C to -11°C	-10°C to ≤13°C	-4°C to -5°C	-4°C to -5°C	∿5°C to 8°C

higher elevations than for the lower elevation snow within the more heavily forested areas.

A number of contour plots of temperature thresholds were also generated for the May HCMM data to compare isotherms selected from the hand analyses with the snow extent mapped from the visible imagery. These plots were prepared at the same scale as the imagery to allow clear acetate copies to be overlayed directly onto the images. Examples of two plots, the 0°C isotherm contour and the -9°C contour for the 30 May nighttime IR data, are shown in Figure 7-7 (a and b). The 0°C isotherm closely matches the snow boundary, and the -9°C contour agrees closely with the observed boundary of the darkest tone in the corresponding image, which represents the extent of the higher elevation, non-forested snow cover.

7.1.4 Comparison with Reported Temperatures and U-2 Data

California Climatological Data gives daily maximum and minimum temperatures for the few reporting stations located within the Sierras study area. These stations are located mostly at about the 2000 m level, near the lower extent of the snowpack at the end of May. One station is at a considerably higher elevation (3700 m); although this station (White Mountain 2) is located in the White Mountains just east of the main Sierra Range, it is the only reporting station that does give an indication of temperatures near the highest levels of the Sierras.

As discussed earlier (Section 2.4), air temperatures recorded at standard shelter height can only be used in a very general comparison with snow surface temperatures. During snowmelt periods, when daytime air temperatures are well above freezing, the snow surface temperature may be 5-10°C lower than reported air temperatures; differences of at least that much can also be expected at night. For purposes of comparison with the HCMM IR temperatures, therefore, an average correction of 7°C was applied to the maximum and minimum reported temperatures, which should occur at approximately the times of the daytime and nighttime HCMM passes.

The reported temperatures at the lower elevation stations did not show much variation over the three-day period, and were quite consistent

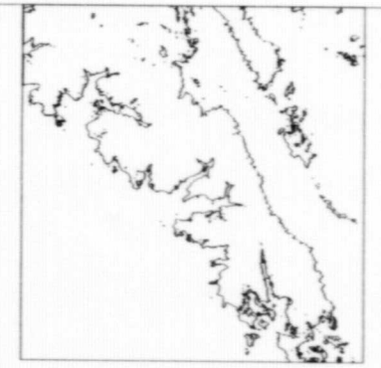

30 May 1978; 0°C threshold

(a)

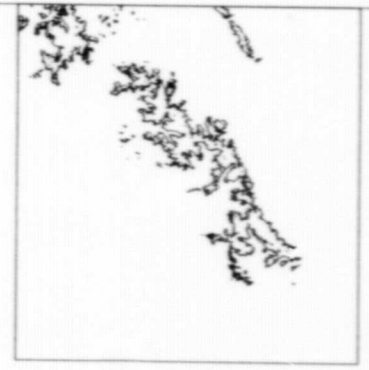

30 May 1978; -9°C threshold

(b)

Figure 7-7 Examples of automated contour plots for HCMM 30 May night IR data. The 0°C isotherm (a) and the -9°C isotherm (b) are shown.

from station to station; the actual reported temperatures were about 20-22°C for the daily maximums and 1-7°C for the minimums. The White Mountain station reported considerably lower temperatures; on the 29th and 30th, the maximums were about 7°C and minimums -3°C, whereas on the 31st the minimum was -14°C and the maximum only +3°C.

Applying the 7°C correction, the daytime snow surface temperatures at the lower elevations can be considered to be in the range of 13° to 15°C and at the high elevations in the range of -4° to 0°C; the nighttime temperatures can be considered to be in the -6° to 0°C range for lower elevations and about -10°C at the higher elevations. Comparing these temperature values with the IR temperatures measured by HCMM (Table 7-2), it appears that the HCMM measurements are consistently lower. In general, the difference seems to be of the order of 5°C, except for the nighttime temperatures at the highest elevations, where the difference is smaller.

As listed in Table 7-1, U-2 flights across the study areas were made on 31 May (day) and 1 June (night). These data were processed and an attempt was made to locate the corresponding area covered in the U-2 data with the HCMM data. Although the general area could be located, it was not possible to match specific geographic features. Furthermore, the U-2 temperatures over the Sierras appeared to be much too high. For example, the temperatures in the nighttime data ranged between 2° and 14°C; no temperatures lower than 2°C were found. These temperatures are considerably higher than the snow surface temperatures estimated from the station reports and much higher than the HCMM temperatures. Because of these difficulties, the U-2 data for this case were not used. Subsequent U-2 data were used in the analysis of the July 1978 and April 1979 cases.

7.1.5 Analysis of Temperature Difference (ΔT) Imagery and Digital Data

Day/night registered data sets were processed for both a 12-hour and a 36-hour interval for the May case. The 12-hour data set was processed from the night and day HCMM passes of 30 May, and the 36-hour data set was processed from the 30 May night pass and the 31 May day pass. The temperature difference (ΔT) images for these data sets were

processed with the smaller ΔT values displayed in darker tones. Hence, water bodies are generally the darkest-tone features in the images; cloud patterns are also displayed as black.

The overall gray-tone patterns of the 12-hour ΔT and 36-hour ΔT images for 30 and 31 May shown in Figure 7-8 (a and b), are very similar to the patterns displayed in the day IR images. In the ΔT images, however, the gray levels defining the snow cover extent appear considerably lighter in tone, and lack broad variations in gray level throughout the snowpack. The smallest values of ΔT (darker tones) fit closely with the lowest temperatures indicated in the day IR data and hence represent the snow-covered terrain.

In the digital ΔT printouts corresponding to these images, the ΔT values represent the actual differences between the night IR and day IR values, with the differences for nearly all pixels being positive (i.e., day IR minus night IR value). The analysis of ΔT digital data across the higher elevation snow cover indicates fairly consistent temperature differences of from 6-18°C. This agrees fairly well with the temperature differences observed in the manual analysis of the day and night IR passes. The ΔT values over the non-snow-covered, lower elevation terrain areas are significantly higher, ranging from about 18-45°C.

7.2 July 1978 Case

7.2.1 Analysis of HCMM Imagery

Because of unusually cool weather during the late spring and early summer of 1978, the snowpack in the Sierras study area melted more slowly than normal. In order to monitor the snowmelt behavior for potential flood danger, the Corps of Engineers flew aerial snow surveys over the southern Sierras later into the summer than would normally be the case. The latest flight was made on 6 July, at which time the snowpack in the Kings River Basin was reported to exceed the snowpack at the corresponding date in 1969, the previous greatest snowpack on record. On 6 July, the snow line elevation in the Kings River Basin was estimated to be at the 3000 m level (just below 10,000 ft). Even as late as 17 July, the date of the HCMM day/night data set, substantial snow still remained at high elevations in the Sierras.

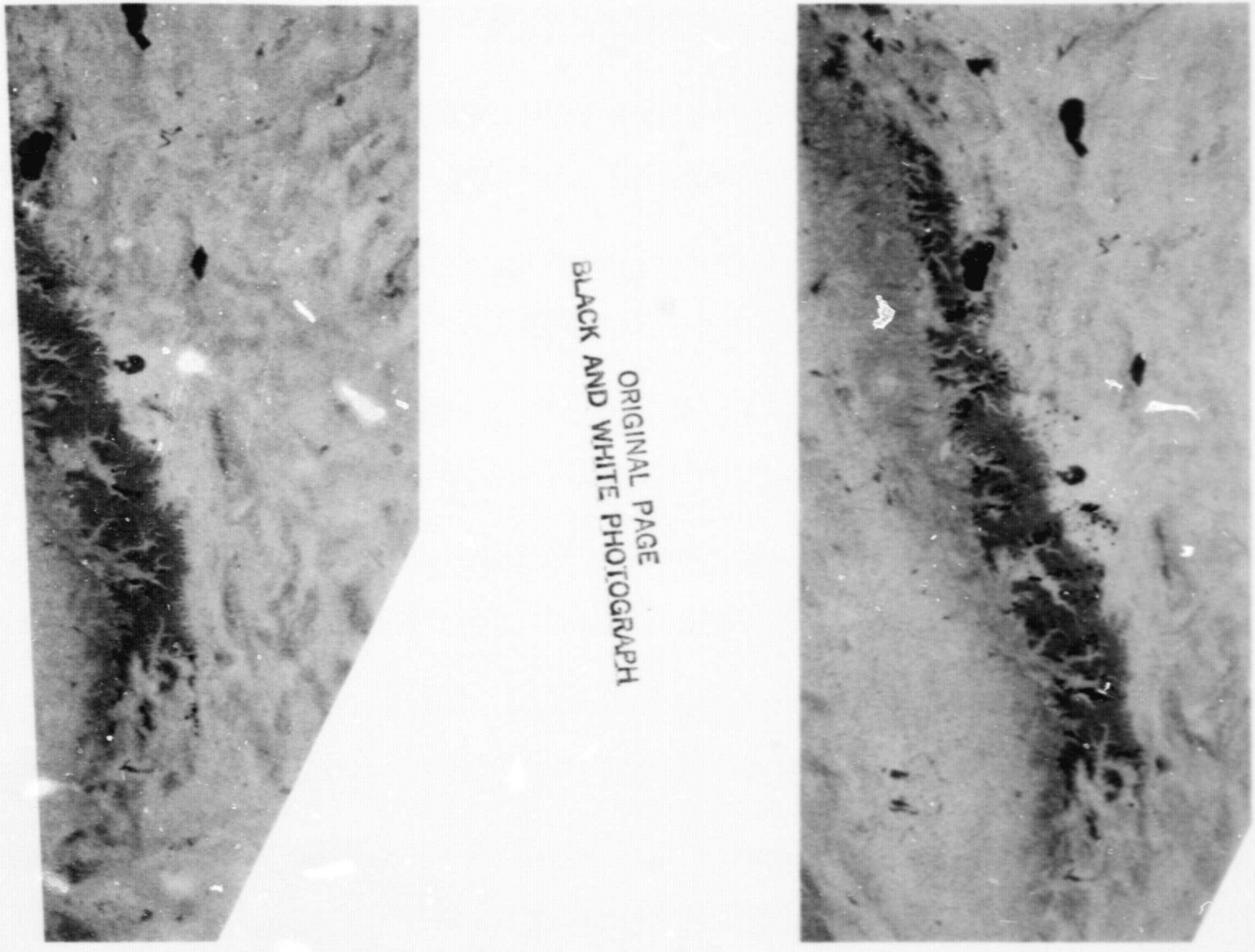

ORIGINAL PAGE
BLACK AND WHITE PHOTOGRAPH

(a) (b)

Figure 7-8 HCMM temperature difference (ΔT) images for Sierras study area May 1978 case: (a) 12-hour ΔT (30 May day - 30 May night); (b) 36-hour ΔT (31 May day - 30 May night).

The HCMM imagery for 17 July is shown in Figure 7-9 (a to c), where Figure 7-9a is the day visible image, 7-9b the day IR image, and 7-9c the night IR image. These images can be compared to the late May images shown in the previous section. Although the snowpack for mid-July is well above normal, a significant decrease in snow extent between the two dates is readily apparent. In addition to the lesser snow extent, the brightness of the snow in the July visible image is also considerably less than the brightness in the May images; the lower brightness appears to be due in part to the photographic processing of this particular image (Figure 7-9a), which is very dark overall.

The daytime IR image (Figure 7-9b) is of considerably better quality than the corresponding visible image, such that water bodies and other features are much more clearly depicted. An area of uniformly dark tone (lowest temperatures) in the IR image fits very closely to the snow cover mapped from the visible image. Enlarged maps of the snow line derived from each image are shown in Figure 7-10 (a and b). In most areas, the IR image (Figure 7-10b) indicates slightly less snow extent than the visible image (Figure 7-10a).

In the IR image, the non-snow-covered western slopes of the Sierras appear as a medium gray tone somewhere between the dark (cold) snow cover and the brighter (warmer) desert basins and agricultural valleys. This indication of lower temperatures along the western slopes is probably the result of the moderating effect of higher elevation terrain and forest canopy.

Analysis of the night IR image (Figure 7-9c) indicates a considerably broader extent of darkest tones, which extend well outside the snow-covered area depicted in the daytime images. In fact, the extent of the darkest tones in this image corresponds more closely to the extent of the medium gray tones observed in the day IR image; the observed differences are likely due to the effect of the daytime heating and nighttime radiational cooling over the mountain terrain.

7.2.2 Comparison Between HCMM and Landsat Imagery

A cloud-free Landsat scene of the southern Sierras on 20 July is shown in Figure 7-11a, and the snow extent mapped from Landsat is shown in Figure 7-11b. Because of the higher Landsat resolution, certain

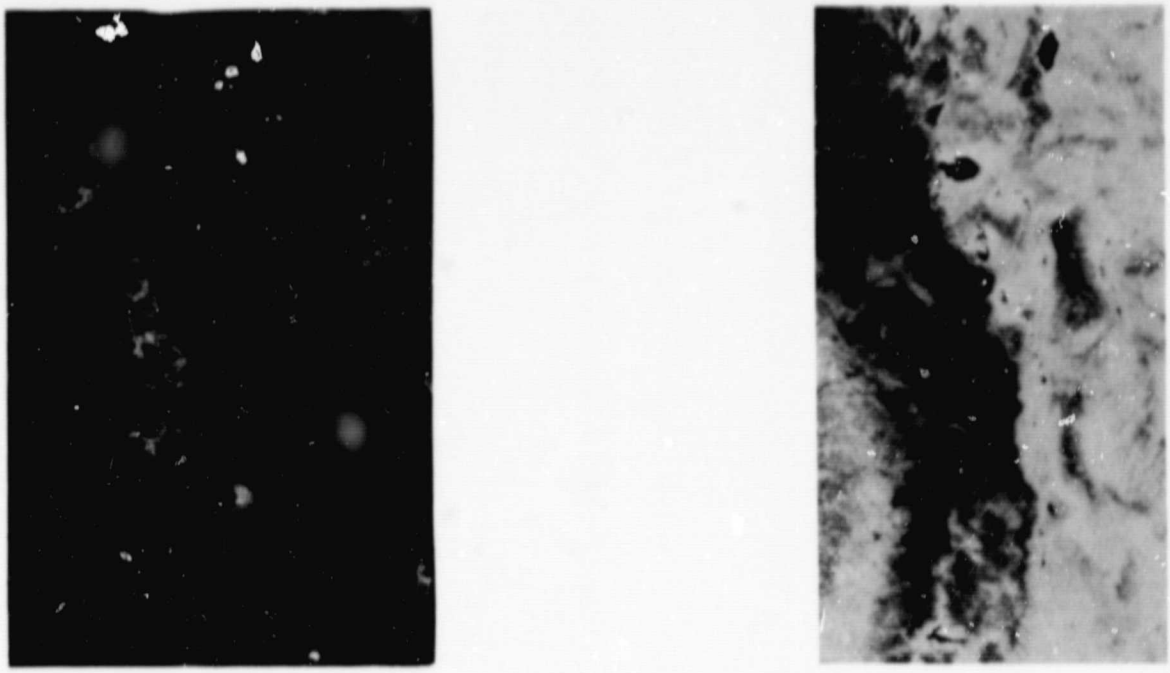

(a) (b)

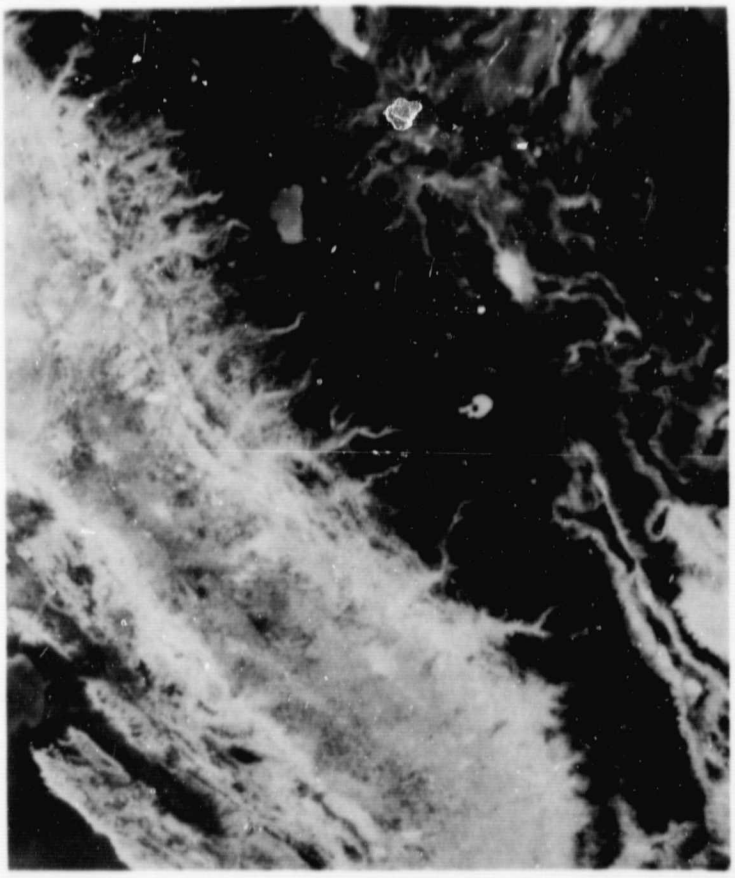

(c)

Figure 7-9 HCMM daytime visible image (a), daytime IR image (b), and nighttime IR image (c) of 17 July 1978, showing above normal snowpack in the Sierras study area (Image ID Numbers: (a) 082-21080-1; (b) 082-21080-2, and (c) 082-10160-3).

(a)

(b)

Figure 7-10 Maps showing the Sierras snow line for 17 July mapped from the HCMM day visible (a) and day IR (b) images.

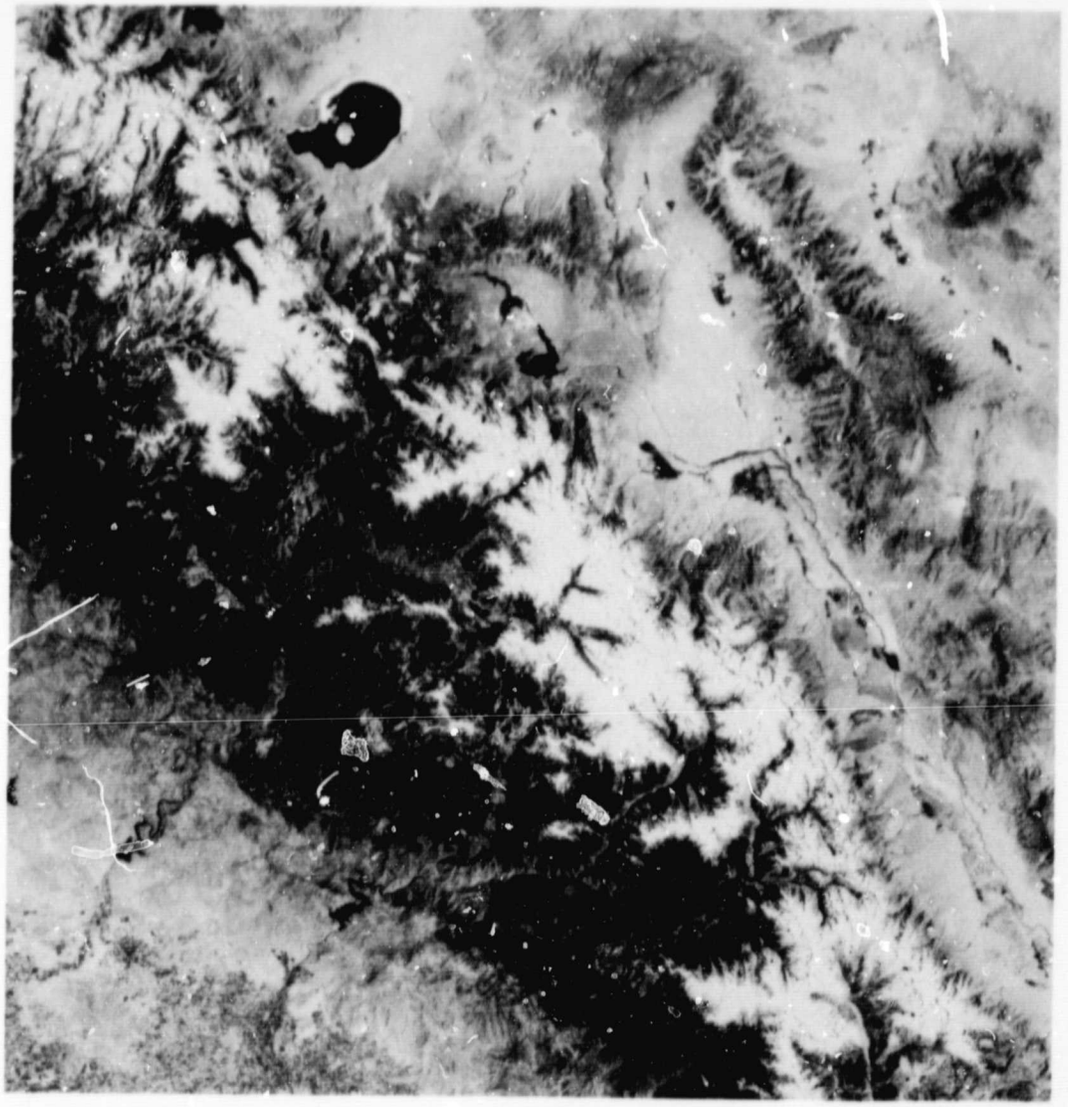

ORIGINAL PAGE
BLACK AND WHITE PHOTOGRAPH

Figure 7-11a Correlative Landsat-2 image (MSS-5) of 20 July 1978, showing considerably more small detail in the Sierras snow cover extent than observed in the 17 July HCMM image.

Figure 7-11b Map showing snow line mapped from 20 July Landsat-2 image. Note that although finer detail is apparent in the Landsat image, the overall snow boundary corresponds closely to the snow extent mapped from the HCMM image (Figure 7-10a).

features not visible in the HCMM image can be detected; for example, numerous small lakes, which are no longer frozen, can be seen within the snow-covered terrain of the southern Sierras. When transferring the snow line from a Landsat image, however, it is difficult to map all of the fine detail apparent in the image. Thus, as was also found in the May case, the overall snow line mapped from the lower resolution HCMM image (Figure 7-10a) matches closely with the snow line mapped from the Landsat image (Figure 7-11b).

7.2.3 Analysis of HCMM Digital Data

Both the daytime and nighttime thermal IR digital data on 17 July were processed and analyzed. For this case, the data were processed only in the printout format. The snow line derived from the daytime visible image was mapped onto the printouts to determine the snow line temperature threshold and snow surface temperatures.

For the daytime data, the snow line fits closely with the +15°C isotherm. The IR temperatures within the snow-covered terrain range as low as +4°C, with isolated minimum values of -2°C. The overall average temperature of the snow is about +7°C. The digital data indicate a fairly distinct boundary between snow with temperatures generally between 7° and 15°C and snow at the highest elevations with an average temperature of 4-5°C. The temperatures of the non-snow-covered terrain along the western slopes of the Sierras is as high as 27°C.

In the nighttime data, the snow line is generally delineated by the 0°C isotherm, with snow cover temperatures ranging between 0° and -9°C; the average snow temperature is about -5°C. However, non-snow-covered areas immediately surrounding Mono Lake, which appear very dark in the night IR image (Figure 7-9c), also have temperatures from 0° to -4°C, undoubtedly the result of radiational cooling during the early morning hours.

7.2.4 Comparison of HCMM Digital Data with U-2 Data and Reported Temperatures

Digital IR data from the U-2 HCMR were also analyzed for a portion of the study area. These data were from flights made across the Kings River Basin south of Mono Lake in the vicinity of Lake Crowley (see Figure 7-9c, where Lake Crowley is readily detectable in the nighttime HCMM image). The U-2 flights were made on 19/20 July. The comparative data (shown in Table 7-3) indicates the HCMM IR temperatures to be consistently lower than the U-2 temperatures; the differences range from 5-16°C.

The only other correlative temperature data for this period are the standard station reports from California Climatological Data. These data do not give actual surface-measured temperatures, but as discussed in the May case, it is possible to derive a general estimate of the temperatures over the snow-covered terrain from the station reports. The reports indicate very little change in temperature during the period from 17 to 20 July, so the two to three day difference between the HCMM and U-2 measurements should not be significant.

The highest elevation station (White Mountain 2, at an elevation of 3700 meters) reported maximum daytime temperatures of 13-15°C and minimum nighttime temperatures of 2-4°C. Stations at lower elevations, just below the snow line, reported temperatures generally in the range of 20-22°C during the day and minimums of about 4°C at night. No stations reported temperatures below freezing at anytime during the period.

These reports indicate that the snowpack was in a melting condition at all elevations during both day and night. In the May case, although daytime temperatures were above freezing at most stations during the day, the nighttime readings were well below freezing. In July, therefore, it is probable that the snow surface temperature remained near 0°C at night. During daytime, if the snow surface temperature is assumed to be 5-10°C lower than the air temperature (as discussed in the analysis of the May case), then the surface temperature should be in the range of 10-15°C.

Compared to these temperatures, the HCMM thermal IR temperatures again appear to be of the order of 5°C too low, consistent with the previous findings. Also, the reported temperatures indicate that the

TABLE 7-3

COMPARISON OF SURFACE TEMPERATURE MEASUREMENTS (°C)
FOR HCMM AND U-2 HCMR DIGITAL IR DATA

Sample Point	HCMM (17 July 1978)		U-2 (19/20 July 1978)		Temperature Difference	
	Day	Night	Day	Night	Day	Night
Lake Crowley	+13°	+11.5°	+29°	+20°	+16°	+8.5°
Temperature at snow line	+15°	0°	+20°	+7°	+5°	+7°
Snow cover (average temperature)	+7°	-5°	+18°	+8°	+11°	+13°

U-2 measurements may be somewhat too high (in particular, the temperatures of Lake Crowley seem to be too high; moreover, the 9°C difference between the day and night measurements is also puzzling). Taking into account a probable error in the U-2 data, then a HCMM error of about -5°C seems quite reasonable; this error is in agreement with the previous findings both for the Arizona analysis and analysis of the May case.

7.2.5 Analysis of Temperature Difference (ΔT) Imagery and Digital Data

The overall gray-tone pattern of the 12-hour ΔT image for 17 July is very similar to the pattern in the day IR image. Except for water bodies, the smallest values of ΔT (darker tones) fit closely with the lowest daytime temperatures and hence are over the snow-covered terrain.

In the digital ΔT printout, Mono Lake can be readily detected, since it has distinctly smaller values of ΔT than the surrounding terrain (including the island in the lake). The ΔT values for the lake are consistently <5°C. In nearly all areas, the ΔT associated with the snow line is consistently between 15° and 20°C. All values over snow cover are less, with several values being between 0° and 5°C. The ΔT values over non-snow-covered terrain are substantially greater, ranging generally between 20° and 40°C. The HCMM ΔT values are in fairly good agreement with the U-2 data (Table 7-3) and with the diurnal temperature range at the reporting stations.

7.3 April 1979 Case

7.3.1 Analysis of 5 April Daytime Visible and IR Imagery

The extent of snow cover over the Sierras during early April 1979 is depicted in the 5 April day visible image, shown in Figure 7-12. Variations in snow cover reflectance due to forest effects are also clearly observed on this data. The snow cover on higher elevation, non-forested terrain displays a uniformly high reflectance, whereas the snow on the lower elevation, densely forested western slopes appears as mottled gray tones. The extent of these areas of varying snow cover reflectance are outlined in Figure 7-13.

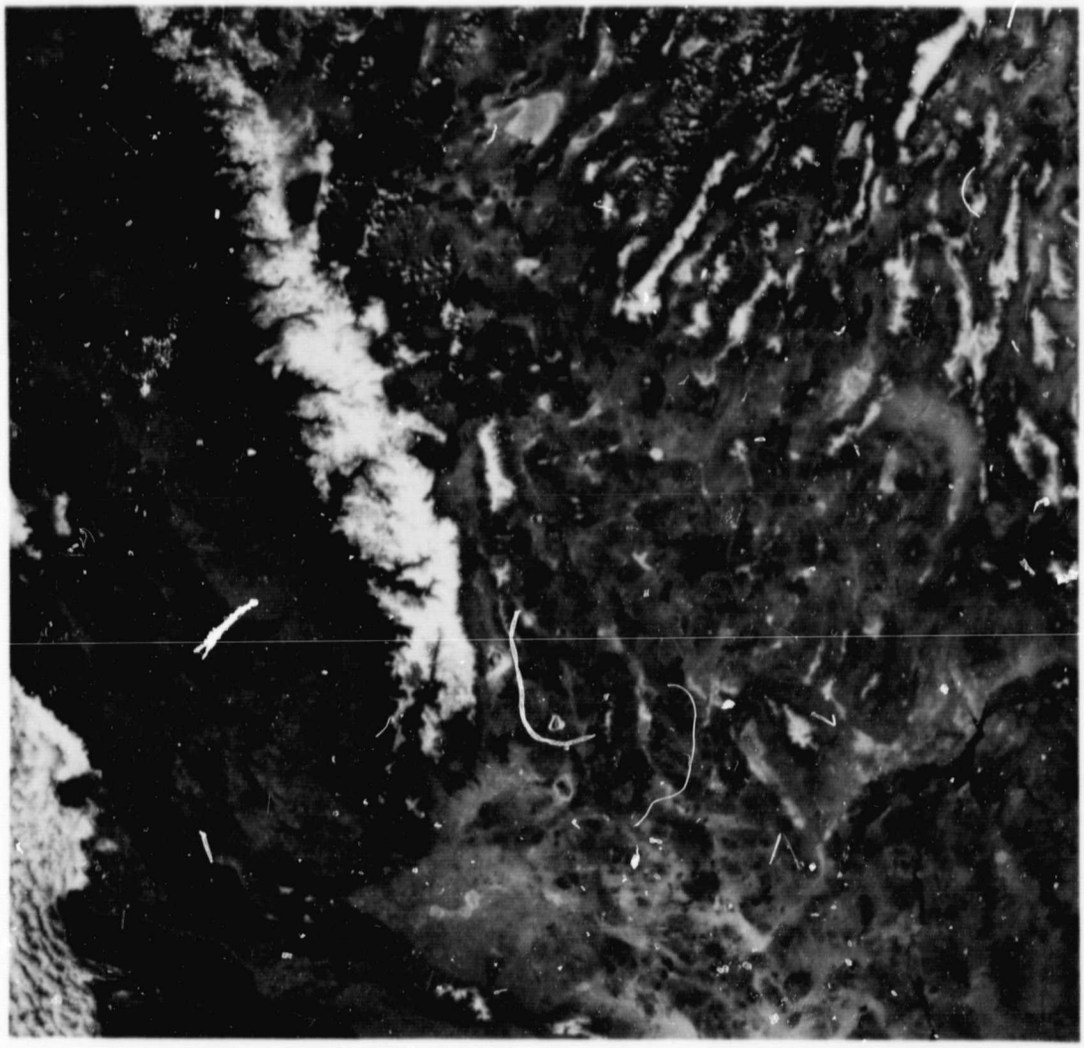

Figure 7-12 HCMM visible image of 5 April 1979, showing variations in Sierras snow cover reflectance due to forest cover effects (Image ID Number 0344-20420-1).

Figure 7-13 Map showing extent of areas of varying snow cover reflectance mapped from 5 April HCMM visible image. The mottled tone represents the extent of snow cover with a lower reflectance due to forest cover effects.

The corresponding IR image for 5 April is shown in Figure 7-14 (the images for this case, which were received late in the study period, are of exceptionally high quality). The dark (cold) pattern in the IR image agrees very closely with the overall snow extent depicted in the visible image. Very detailed thermal patterns are detectable in this image at the snow boundary along the eastern slope of the southern Sierras, as well as other areas such as the snow boundary surrounding the White Mountains (east of the Sierras along the California-Nevada border). These patterns are apparently associated with variations in temperature caused by narrow ridges with colder, north-facing slopes and warmer south-facing slopes; there is also evidence in the visible image of similar variations in the snow cover pattern.

Variations in the thermal pattern within the snow-covered area are not as readily detectable in the IR image as are the variations in reflectance observed in the visible image. However, with the aid of a strong backlight, tonal variations similar to those observed in the visible image did become apparent. There is also some evidence of cloud in the IR image obscuring Lake Tahoe and producing a fuzzy, dark pattern north of Mono Lake; although other cellular cloudiness can be seen in the upper portion of both images, the apparent cloud near Lake Tahoe and Mono Lake cannot be detected in the visible image.

7.3.2 Analysis of 5 April Daytime IR Digital Data

Analysis of the digital computer printout of the daytime IR data showed an excellent correlation between the 0°C isotherm and the overall snow cover boundary displayed in the daytime visible image. The higher elevation snow cover (solid high reflectance) is delineated in the digital analysis by the -5°C isotherm; temperatures within the higher elevation areas range between -5°C and -10°C, with some isolated areas having temperatures of -11°C to -12°C.

The lowest temperatures observed in the digital analysis were located over two mountain areas immediately west of Mono Lake. These areas exhibited homogeneous temperatures of $\leq$-13°C (the lower cutoff of the radiometer temperature range) and did not correlate well to observed geographic features in this area. Also, these features could not be detected in the visible or IR imagery. Therefore, it can only be

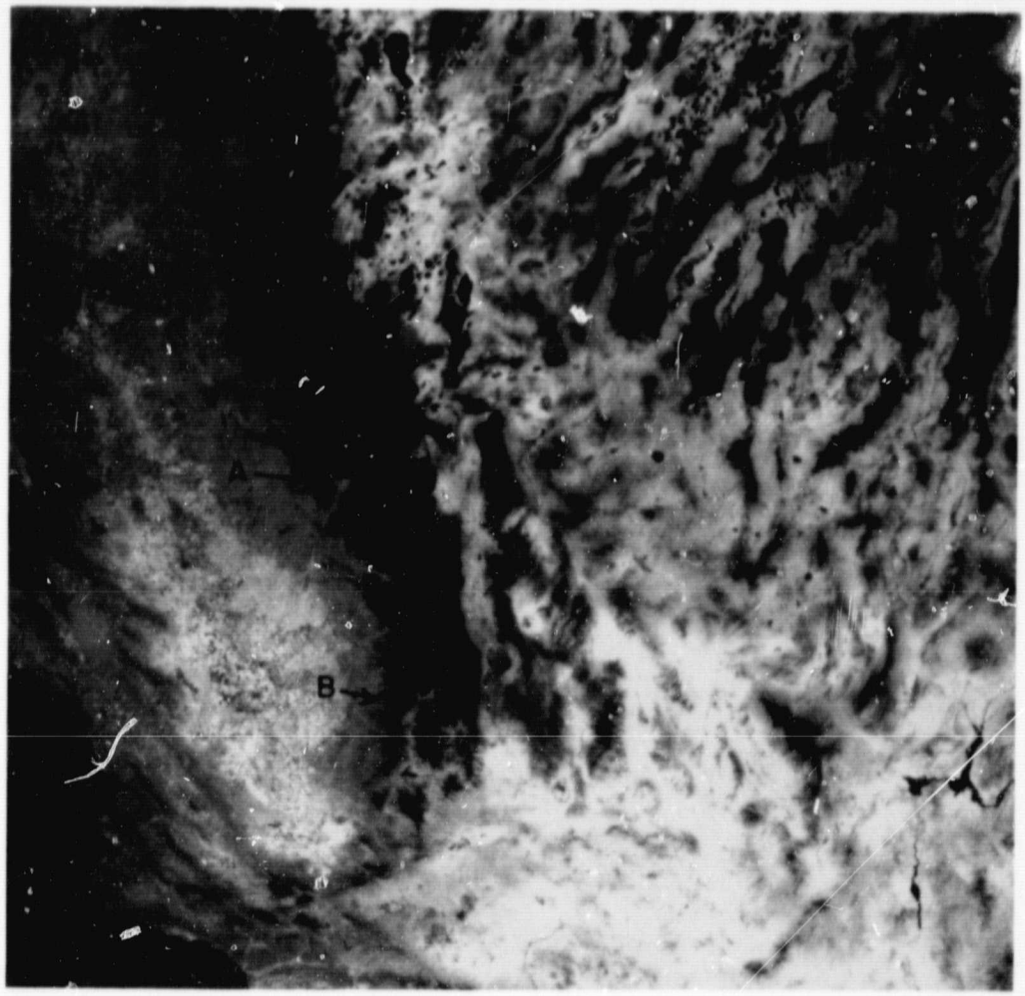

Figure 7-14 HCMM day IR image of 5 April 1979, showing close agreement with corresponding visible image in overall snow cover extent (Image ID Number 0344-20420-2).

assumed that they are representative of thin, cirriform clouds, similar to the clouds that can be seen in the IR image over Lake Tahoe and north of Mono Lake.

7.3.3 Analysis of 4 April Nighttime IR Image and Digital Data

In the nighttime IR image 36 hours earlier, shown in Figure 7-15, the southern Sierras appear in a mostly homogeneous dark tone. However, the overall boundary of the darkest-tone area does not correspond to the snow line as closely as it does in the daytime IR image. As observed in the nighttime images discussed previously, the snow line in the vicinity of Mono Lake is completely obscured because of the overall lower temperature of the surrounding terrain caused by radiational cooling.

Other ambiguities are also apparent in the 4 April image. In contrast to the pattern in the vicinity of Mono Lake, the snow extent actually appears somewhat reduced at some locations along the western and southern slopes of the Sierras. Note for example the apparent reduced snow extent observed at areas A and B in Figure 7-15, compared to the snow boundary observed at these same locations in the daytime IR image of 5 April (Figure 7-14).

The ambiguities other than those caused by radiational cooling of non-snow-covered terrain are probably associated with the processing of the images. Because of the overall lower surface temperatures at night, the curve relating temperature to gray-tone is different than the curve used for producing daytime images; this difference, of course, is why water bodies show up in dark tones in daytime images and light tones in nighttime images despite retaining essentially the same temperature. As shown in Figure 7-16, a snow surface could cool at night and yet be displayed in a lighter gray-tone than in the daytime image. Caution must be used, therefore, when interpreting snow cover in nighttime IR imagery, both because of a probable lesser temperature gradient between snow and non-snow terrain as well as differences in the display curve as compared with daytime imagery.

Analysis of the digital IR data for the 4 April nighttime scene shows the overall snow boundary defined by the -5°C isotherm, with the snow cover temperatures ranging from -5°C to $\leq$-13°C. Temperatures of the snow-free

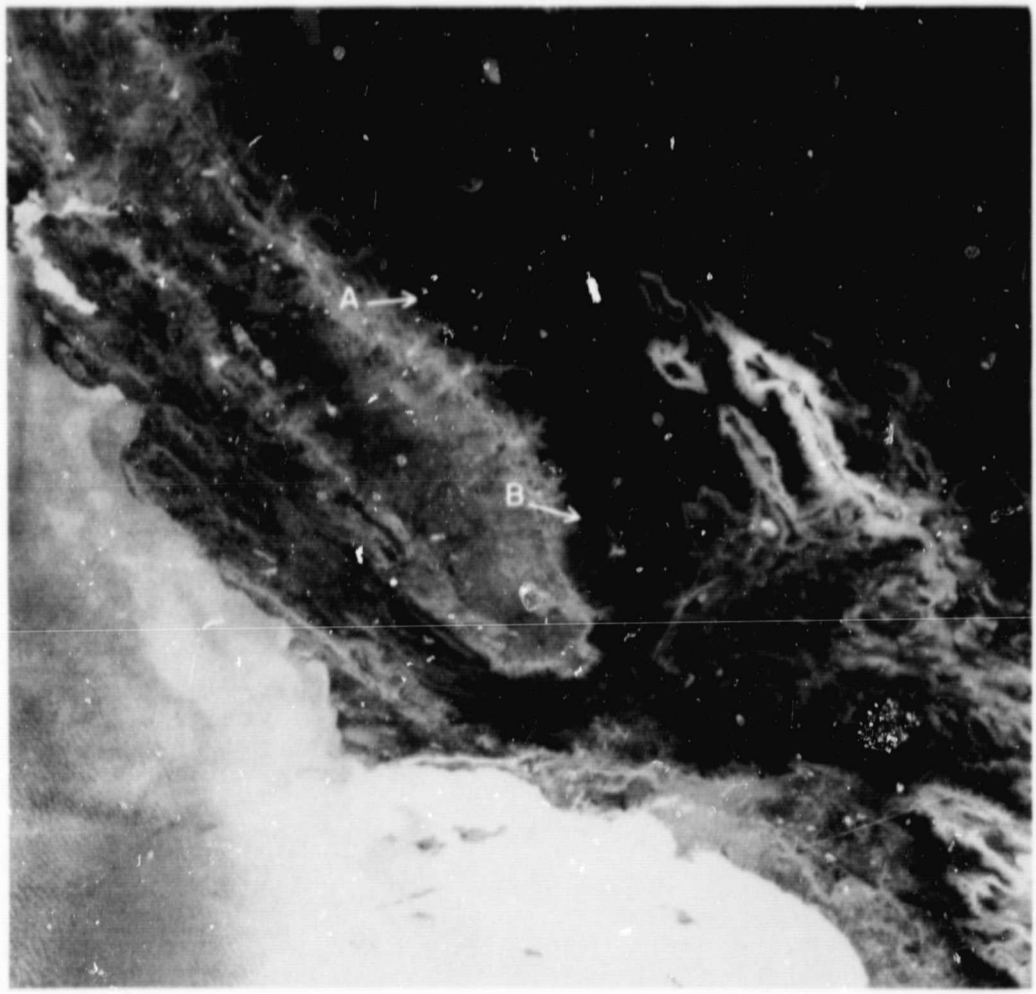

Figure 7-15 HCMM nighttime IR image of 4 April 1979, showing thermal pattern of Sierras snow cover and areas of radiational cooling. Note that the boundary of the darkest (coldest) tone does not correspond as closely to the visible snow line as does the thermal pattern in the day IR image (Image ID Number 0343-09320-3).

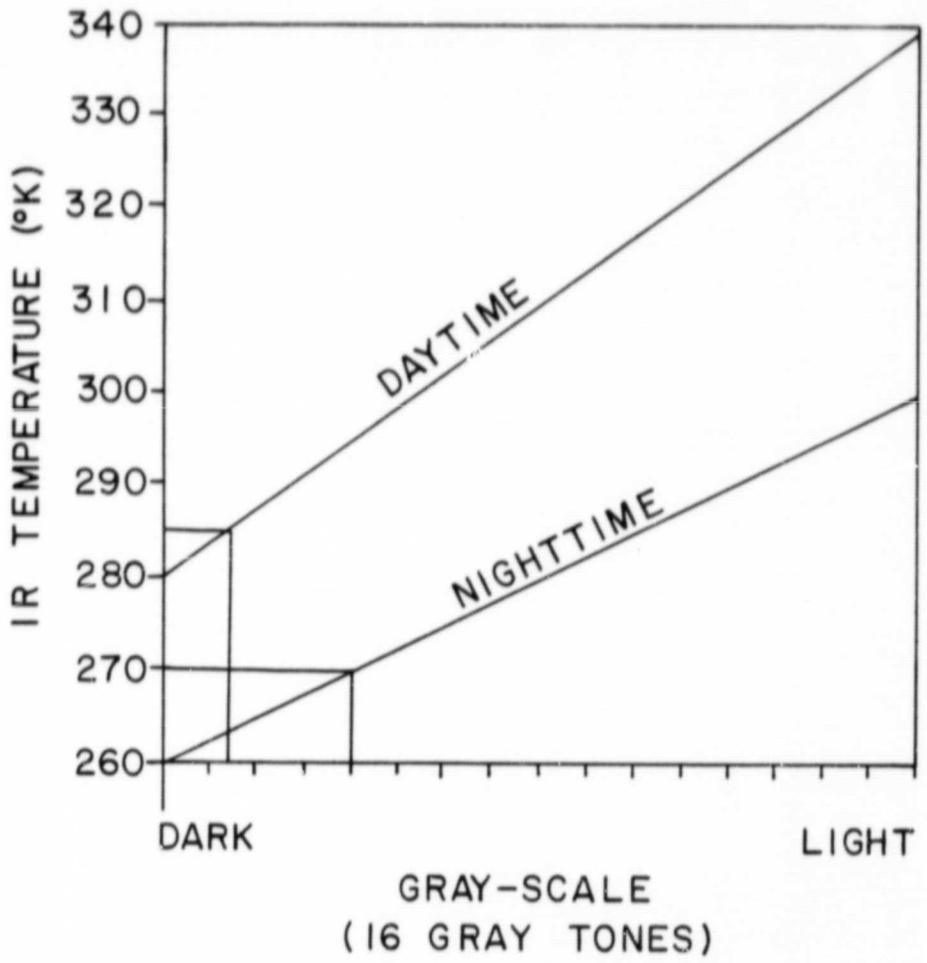

Figure 7-16 Examples of curves relating IR temperature to gray tone (not the actua. curves used in producing HCMM images). A surface with a daytime temperature of 285°K and a nightime temperature of 270°K would appear in a lighter gray tone in the nightime image.

terrain immediately adjacent to the snowpack along the western slope range from about -4°C to 0°C. In the daytime IR digital data of 5 April, these same areas have surface temperatures in the range of 1°C to 15°C; this greater temperature gradient between snow cover and snow-free terrain provides a more reliable definition of the snow boundary in the daytime IR imagery.

7.3.4 Comparison Between HCMM Data and U-2 High Altitude Multispectral Scanner Data

On 4 April 1979, both day and night IR data from the U-2 High Altitude Multispectral Scanner were collected for flights across the Kings River Basin. The thermal IR data were provided in both digital and image formats. The Multispectral Scanner is a very high resolution sensor, so it returns a large volume of data; the data volume was so large, in fact, that it was possible only to process a small amount. Also, although the sensor resolution was sufficient to identify many geographical reference points, it was difficult to locate precisely specific reference points on the corresponding HCMM data. Therefore, snow cover temperature measurements from the U-2 data were averaged over selected areas for comparison with the HCMM derived temperatures for these same general areas.

The 4 April daytime U-2 data were compared with the 5 April daytime HCMM data. Meteorological reports indicate that maximum temperatures on the 4th at mountain stations were about the same or slightly lower than on the 5th. The corresponding temperatures measured over a lake that was identifiable in both data sets and over snow show close agreement between the U-2 and HCMM measurements:

sample point	U-2	HCMM
Lake Edison	+1°	+2°
snow cover	-5.4°	-6.1°

The U-2 data acquired on the 4 April nighttime pass over the Sierras were compared with HCMM nighttime IR data also acquired on 4 April. These data were evaluated in three distinct categories; including: (1) dense snow cover at higher elevations; (2) sparse snow cover at lower

elevation; and (3) non-snow-covered terrain. The comparison of the average temperatures within each of these categories shows the HCMM temperatures to be about 5°C lower than the U-2 measurements for each of the categories:

Category	Temperature U-2	Temperature HCMM
dense snow cover	< -10°	≤ -13°
sparse snow cover	-4.3°	-9.3°C
non-snow-covered terrain	+1.5°C	-3.6°C

7.3.5 Comparison Between HCMM and Surface Temperature Measurements

For this case it was possible to compare the HCMM data with a sample of surface radiant temperature data collected by the University of California at Santa Barbara. These surface radiant temperature readings were collected on 5 and 6 April in the Dusy and Palisade Basins of the middle fork of the Kings River in the southern Sierra Nevada. The temperatures were measured by pointing the radiometer at targets consisting of "100% snow", "snow and rocks", or "snow and vegetation". Although the test sites were pinpointed on USGS quadrangle maps, it was not possible to locate the points precisely on the HCMM images or in the digital printout. The surface radiant temperatures were averaged, therefore, and compared with HCMM data averaged over a number of pixels in the same approximate area of the Sierras.

The measurements taken during the afternoon of 5 April were mostly for targets of "100% snow" or "snow with sparse trees or rocks". The average radiant temperature for 11 samples was -3.2°C (the range in values was -0.2° to -6.4°C). The average HCMM temperature for the same area was -6.2°C, or 3.0° lower than the surface measurements. Air temperatures were also measured at the test site using a sling psychrometer; the air temperature for all samples taken was a consistent 4°C, or about 7°C higher than the snow surface temperature.

As was done in the analysis of the cases discussed previously, the HCMM IR temperatures were also compared with temperatures measured at

reporting stations (at shelter height). During early April, all stations except one located within the snow-covered areas of the Sierras reported temperatures below freezing at night and well above freezing during the day. Only at the highest elevation station (White Mountain) did temperatures remain below freezing during daytime as well. Most stations reported maximum temperatures of 11-15°C on 5 April and minimums of -1°C to -7°C on 4 April; the White Mountain station reported temperatures of -1°C and -12°C, respectively. All stations reported a substantial snowpack, with depths ranging to as much as 178 cm (70 inches).

Because of the deeper snowpack in early April, the field-of-view of the radiometer should be less contaminated by non-snow features, such as exposed vegetation and bare rock, than it would be later in the spring. Thus, a difference of about 7°C between the air temperature and snow surface temperature, as was found at the Kings River test site, would also seem to be a reasonable correction to apply to the temperatures at the reporting stations. Based on this assumption, the snow surface temperature at the highest elevations would be about -8°C (5 April daytime), whereas the HCMM temperatures are -11°C to -12°C; the lower elevation snow surface temperatures would be 4-8°C, whereas the HCMM temperatures are about 0°C or slightly lower. Thus, the differences between the HCMM temperatures and assumed snow surface temperatures are consistent with the differences found at the Kings River test site. The comparisons overall indicate that the HCMM temperatures are of the order of 3-5°C too low.

7.3.6 Analysis of Temperature Difference (ΔT) Imagery and Digital Data

The gray-tone pattern of the 36-hour ΔT image for 5 April (shown in Figure 7-17) displays a very similar pattern to the overall snow cover extent observed in the day visible and day IR images. Except for the clouds and water bodies, the lowest ΔT values (darkest) fit closely to the lowest daytime temperatures, which occur over the snow cover. Two isolated areas located just west of Mono Lake appear considerably darker than the gray levels of the snow cover. The distinct appearance of these areas is indicative of the existence of clouds in either the

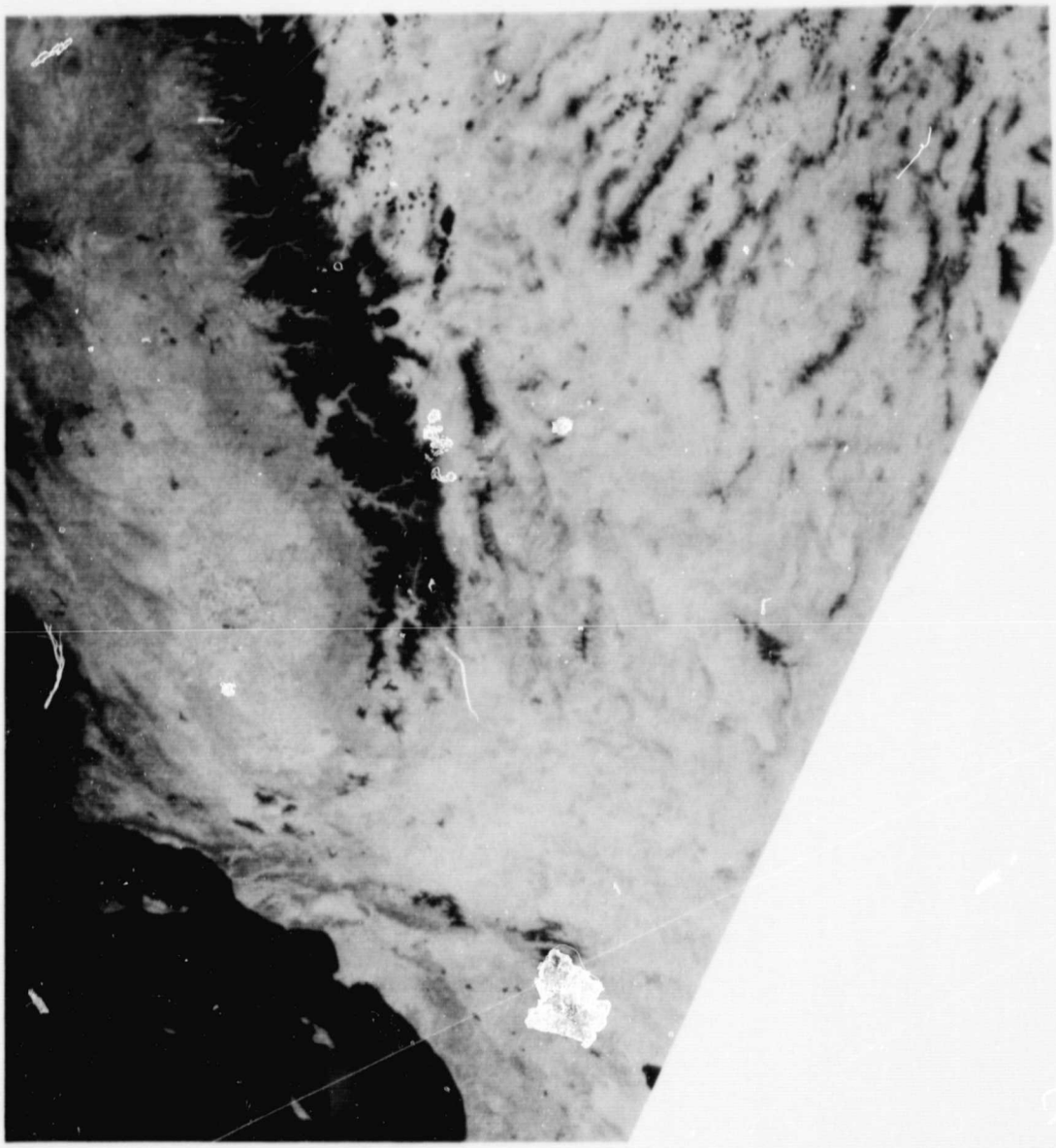

Figure 7-17 HCMM 36-hour temperature difference (ΔT) image (5 April day - 4 April night), showing similar pattern to the overall snow cover extent as observed in the corresponding day visible and day IR images.

daytime or nighttime data (note also the dark areas partially obscuring Lake Tahoe), even though clouds are not readily apparent in either the visible or IR images; this confirms the assumption made earlier based on the low temperatures observed in these areas in the analysis of the daytime digital data.

Some variations in gray-tone are also observed in areas that are snow-covered, but cloud-free. Slightly darker gray levels occur on the non-forested, higher elevation terrain areas, indicating that the day/night temperature differences were not as great over the maximum elevation terrain areas, as those prevailing over the lower elevation snow-covered areas.

In the digital printout, the entire snow line boundary is consistently at or near a ΔT of 15°C. All values over the snow cover are less than 15°C, with several higher elevation areas being between 0° and 5°C. This is consistent with the location of the darker tones observed in the ΔT image. The ΔT values over non-snow-covered terrain are substantially greater than 15°C, whereas the ΔT values over Mono Lake are very small as compared to those of the surrounding terrain including the snow cover. The ΔT values observed at the snow line and over the snowpack are consistent with values found in the analysis of the other Sierras cases.

7.3.7 Cursory Analysis of Apparent Thermal Inertia (ATI) Imagery

Analysis of apparent thermal inertia (ATI) data was not an original objective of the investigation since the concept of thermal inertia does not have a readily apparent application to snow hydrology. Nevertheless, ATI images were received along with the ΔT images for the day/night data sets. Although the ATI patterns in the images for the May and July 1978 cases are not of high contrast, the patterns displayed in the April 1979 case are very well defined. The ATI image for the 36-hour data set of 4-5 April is shown in Figure 7-18.

A cursory analysis of this ATI image, as well as the images for the other cases, indicates that the Sierras snow cover is readily apparent. The tonal patterns within the snow-covered area vary between very bright tones, medium gray-tones, and very dark tones. Clouds and water bodies (large lakes and Pacific Ocean) display the highest brightness levels.

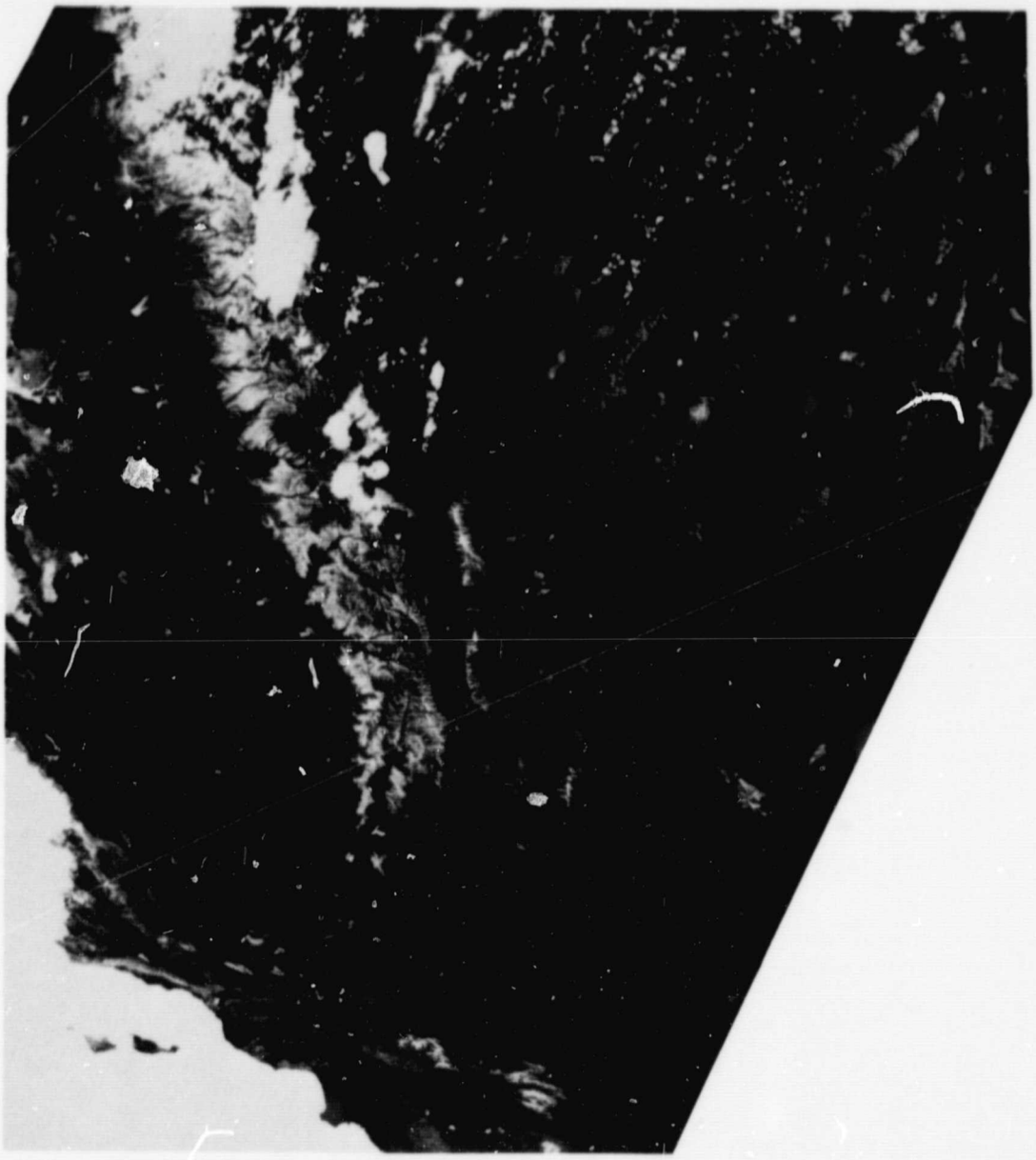

Figure 7-18 Apparent thermal inertia (ATI) image for the 36-hour data set of 4-5 April 1979. Note the brighter tones outlining the snow cover boundary of the lower elevation western slopes, and the darker tones representing the colder higher elevation snow.

The location of the brightest tones across the snow cover show good agreement with areas of lower elevation snow, more likely in a melting condition, while the medium gray-tones and dark tones occur across the higher elevation snow cover.

Comparison of the apparent snow cover boundary in Figure 7-18 with the boundary observed in the 5 April visible image shows excellent agreement. The brighter tones in the ATI image outlining the snow cover along the entire western slope, may actually define the extent of wet melting snow cover at the lower elevations. The medium gray-tones and darker levels likely represent drier, colder snow at the higher elevations.

8. DISCUSSION OF RESULTS

8.1 Comparison Between HCMM and Other Satellite Imagery

The HCMM imagery acquired for analysis in this investigation was the standard data product provided by the NASA GSFC Data Processing Facility. As is the case with any standard-processed data, variations in the quality of the images did exist, with some images being processed in a darker tone than others. Nevertheless, the overall quality of the HCMM imagery, both the visible and the thermal IR, was considered to be excellent. The images appeared to be essentially noise-free and were of a quality equal to or better than that of other current satellite data. HCMM images processed for a specific purpose, such as for snow cover mapping or for detecting oceanic thermal patterns, would have even greater utility than the standard-processed products.

The relative resolution utility of HCMM, NOAA VHRR, and Landsat was determined for each study area. Comparative maps of the snow line mapped from HCMM and Landsat visible imagery and from HCMM and VHRR thermal IR imagery are shown in Section 7. These maps indicate that the resolution of the HCMM visible imagery (500 m) is adequate for mapping the areal extent of the snow cover; although small variations in the snow line can be mapped in greater detail from the 80 m Landsat imagery, it appears that the overall snow extent can be mapped from HCMM as accurately as from Landsat. Moreover, because the HCMM areal coverage is much more extensive than that of Landsat, HCMM may actually have greater utility than Landsat for monitoring snow extent.

In the thermal IR imagery (600 m resolution), HCMM provides greater detail in the thermal patterns associated with snow cover than is provided by the 1 km resolution NOAA VHRR data or the 1.1 km Advanced VHRR data. It appears that for useful mapping of snow surface temperature, a spatial resolution at least as good as that of HCMM is desirable.

Another important factor with regard to the quality of the HCMM thermal IR imagery as compared to NOAA VHRR and Landsat is the improved thermal sensitivity of the sensor (NEΔT of 0.4°K). As is the case with spatial resolution, the analysis of HCMM data indicates that a thermal

sensitivity at least as good as that of HCMM is necessary for useful mapping of snow surface temperature. For example, it is doubtful that the Landsat-3 thermal band (even if it had not had severe noise problems) would have been as useful as HCMM, despite having a better spatial resolution, because of its relatively poor thermal sensitivity. It should be noted in this regard that the NOAA AVHRR has a significantly improved sensitivity over the VHRR, so does provide improved thermal data.

As mentioned above, the orbital characteristics of HCMM provide adequate spatial coverage. If a HCMM-type system were to be used to provide operationally useful data, however, the repeat cycle would not be adequate. For monitoring snow cover, a daily or every-other-day repeat cycle would be necessary, primarily because of cloudiness.

8.2 Calibration of HCMM Radiometer

Although the snow cover extent and some thermal variations within the snow-covered area could be mapped from the HCMM imagery, it was necessary to analyze the digital data (CCT's) to determine actual snow surface temperatures and threshold temperatures at the snow line. Analysis of the digital data product, of course, eliminates the problems associated with variations in photo-processing of imagery products.

Except in some nighttime passes, the limited range of the radiometer (lower cutoff of 260°K) was not a problem. In those instances, some snow-covered areas could not be mapped because the temperatures were below 260°K. The snow surface temperatures are of greatest interest to the hydrologist, however, during the snowmelt season, when the temperatures are near 273°K (0°C). Nevertheless, HCMM could have potential for arctic studies, but the limited lower range of the sensor would make the data only marginally useful.

The results of comparisons between HCMM and other data sources, including U-2 data, station temperature reports, and a limited amount of special snow surface temperature measurements, indicate that the HCMM thermal IR temperatures are consistently lower than the correlative measurements. In each case where a comparative analysis was possible, the HCMM temperatures were 3-5°C lower. It should be noted, however, that the differences were very consistent for the entire data sample analyzed; there was no indication of greater differences for the 1979

cases than the May and July 1978 cases. It appears, therefore, that perhaps the temperature offset (-5°C) based on the White Sands calibration should not have been applied to the HCMM data.

8.3 Automated Data Analysis Methods

The digital data product is essential for monitoring snow surface temperature because the problems with photo-processing of imagery could be significant if HCMM-type data were to be used on an operational basis. The analysis of digital printouts, however, is a tedious and time-consuming process. The automated contour plotting program developed for use with HCMM data greatly simplifies the analysis procedure and is a step toward an automated analysis method.

The contour plotting program, described in Section 5, allows any temperature contour to be plotted at any desired scale. The program is considered to be a unique development in that it plots a temperature contour directly through a raster-to-vector conversion process, and does not require a sophisticated image processing device. Although in this investigation the temperature contours were overlaid onto the visible images, it would be possible to automate the analysis of both channels of data. Threshold brightness values could be established to delineate the snow line in the visible data; several temperature contours could then be plotted at the same scale enabling the temperature at the snow line and the temperatures of the snow cover surface to be derived immediately.

8.4 Usefulness of Day/Night Registered Data

The availability of day/night registered data was unique to the HCMM program. It has not been possible to acquire day/night data sets from other satellite systems, such as the NOAA VHRR or AVHRR. The day/night temperature difference (ΔT) data were analyzed in imagery and digital format for the three Sierras cases; a cursory analysis of the apparent thermal inertia (ATI) imagery was also carried out.

Snow cover extent is clearly delineated in the ΔT imagery because the ΔT values over snow are distinctly smaller than over the surrounding non-snow-covered terrain. In some instances, it is also easier to

detect clouds over snow in the ΔT images than in either the visible or IR images. However, it is not possible to detect much variation in ΔT across the snowpack in the ΔT imagery. Therefore, because snow extent can also be mapped readily from both the visible and daytime IR imagery, the results of the analysis indicate that the ΔT images do not provide significant additional information that cannot be derived from the daytime and nighttime HCMM imagery.

In the digitized data, some variation in the ΔT values is observed across the snowpack. In all three cases analyzed, the ΔT values were somewhat smaller over the higher elevation snow than at lower elevations, apparently the result of less warming during the day. These data could, therefore, provide some additional information on the behavior of the snowpack. To be of use operationally, it would be necessary to apply some method of automated analysis, such as that described in the previous section.

The ATI images for the May 1978 and April 1979 cases were also examined. Whereas the patterns depicted in the May images (12-hour and 36-hour) were not of high contrast, the ATI patterns over the Sierras in the April case were very well defined. The tonal patterns in the April ATI image define the Sierras snow cover and show good agreement with the snow extent as mapped from the visible image. Moreover, there is some indication that the areas of higher thermal inertia (brighter tones) are associated with the lower elevation snow cover, where melting is more likely to be occurring; the areas of lower thermal inertia (darker tones) occur in the higher elevations, where the colder snow surfaces exist. Considerable further study would be needed to determine whether these data do actually provide information useful for snowmelt prediction.

8.5 Use of HCMM Thermal Data to Assist in Snowmelt Runoff Prediction

The results of the data analysis have shown that HCMM thermal IR data provide useful information on both snow extent and snow surface temperature. During daytime, when a greater temperature contrast exists between snow and the adjacent non-snow-covered terrain, the snow line can be mapped as accurately from thermal IR as from visible imagery. At

night, interpretation of the snow line in HCMM thermal imagery may be ambiguous primarily because of a lesser contrast in temperature between snow-covered and snow-free terrain.

For mapping snow extent alone, however, the HCMM thermal imagery does not provide any information additional to that which can be derived from visible imagery. With regard to cloud interference, in fact, the thermal data may be more severely affected than the visible data (snow can at times be mapped in the visible through a layer of thin cirrus cloud; the same layer may be completely opaque in the thermal IR).

The advantage of thermal IR data is to provide additional information on snow surface temperature, which cannot be derived from visible data alone. Using a system with the characteristics of HCMM, except with more frequent repeat coverage, it would be possible to monitor the snow surface temperature continually throughout the snowmelt period. As indicated by the lack of correlative data for this investigation, very little snow surface temperature data are currently collected. If accurately calibrated, HCMM can provide information on when the snow surface temperature reaches the freezing level during the daytime, and whether the temperature is dropping below freezing or remaining above freezing during the night. Although the day/night temperature difference data provide some useful information, the absolute temperature values during daytime and nighttime would be needed to monitor snowmelt conditions.

For HCMM data to be a useful source of information to assist in snowmelt runoff prediction, accurate sensor calibration will be essential. The availability of correlative surface truth measurements on a routine basis for verification of the satellite data may be necessary if these data are to be used to their optimal potential. If the user can be confident of the sensor calibration, then an automated analysis method can be used to integrate HCMM data directly into a snowmelt prediction scheme.

9. CONCLUSIONS

Aside from the very limited amount of useful data from the Landsat-3 thermal band, the Heat Capacity Mapping Mission has provided the highest resolution thermal infrared data yet acquired from a space platform. The results of this investigation have demonstrated the application of the excellent quality HCMM data to snow hydrology.

Comparison of the resolution of the HCMM visible and thermal imagery with that of other satellites suggests that the HCMM resolution may have the greatest utility for snow mapping. Operational satellite systems, with poorer resolution than that of HCMM, may not provide the necessary detail in snow extent maps. Landsat, on the other hand, provides greater detail than HCMM, but does not provide areal coverage adequate to map larger river basins. A system with the spatial resolution and areal coverage of HCMM may, therefore, be the most useful system in the future for operational snow mapping purposes.

Analysis of HCMM data for two study areas, the Salt-Verde Watershed in Arizona and the southern Sierra Nevada in California, has shown that snow extent can be mapped and snow surface temperature determined from the thermal IR data. Snow extent can be mapped more reliably from the daytime thermal imagery, when the temperature contrast between snow and adjacent snow-free terrain is greater; interpretation of the snow line in nighttime imagery may be ambiguous because of the cooling of the surrounding land. Although the snow line can be mapped as accurately from the thermal imagery as from the visible imagery, the use of thermal data to determine snow extent does not offer any advantages over the use of visible data.

The advantage of thermal data with the sensitivity and resolution of the HCMM system is in determining snow surface temperature. With careful calibration, a sensor system like HCMM could provide snow surface temperature data of value for snowmelt runoff prediction. The calibration of the HCMM data was assessed through comparison with U-2 thermal data and other correlative data; the comparisons indicated that the HCMM measurements were consistently about 3-5°C too low. No apparent degradation in the HCMM calibration was observed in the 1979 data as compared to the 1978 data. These results suggest that the 5°C correction to the

HCMM data based on the White Sands calibration should not have been applied.

The analysis of HCMM digital data to derive snow surface temperature is a tedious and time-consuming process. An automated analysis method would be required, therefore, to use HCMM-type data operationally. An approach to an automated analysis method was developed as part of this investigation.

In addition to the daytime and nighttime data analysis, the day/night temperature difference was also derived from HCMM registered data sets. For snow hydrology applications, however, it does not appear that the day/night registered data sets provide any information that cannot be derived from the day and night data, separately. To assess snowmelt conditions, absolute snow surface temperatures are needed for both daytime and nighttime, rather than the temperature difference. Moreover, the application to snow hydrology of apparent thermal inertia, another product that can be derived from the day/night data sets, is also not readily apparent. The results of the analysis imply, therefore, that for snow hydrology purposes, alone, it would be difficult to justify the production of day/night registered data sets.

Remote sensing from satellites has now been used for some time on a routine basis to derive snow cover extent for hydrologic purposes. The data collected by HCMM have demonstrated that high quality thermal infrared measurements can provide additional information useful to the hydrologist. The results of the research carried out using HCMM data should be considered in the development of future satellite systems to monitor snowpacks. Unquestionably, remote sensing will continue to be a vital part of effective water management in the river basins of the western United States.

10. REFERENCES

Anderson, H.W., 1963: Managing California's Snow Zone Lands for Water, U.S. Forest Service Research Paper PSW-6, Pacific SW Forest and Range Experiment Station, Berkeley, California.

Barnes, J.C. and C.J. Bowley, 1972: Snow Studies Using Thermal Infrared Measurements from Earth Satellites, Final Report under Subcontract to ARA, Inc. (NOAA/NESS Contract No. 1-35350), Environmental Research & Technology, Inc. Concord, Massachusetts, 112 pp.

Barnes, J.C. and C.J. Bowley, 1974: Handbook of Techniques for Satellite Snow Mapping, Final Report under Contract No. NAS5-21803 to NASA/ Goddard Space Flight Center, Environmental Research & Technology, Inc., Concord, Mass., 95 pp.

Barnes, J.C., C.J. Bowley and J.L. Cogan, 1974: Snow Mapping Applications of Thermal Infrared Data from the NOAA Satellite Very High Resolution Radiometer, Final Report under Contract No. 3-35385 to National Environmental Satellite Service, Environmental Research & Technology, Inc., Concord, Mass.

Barnes, W.L. and J.C. Price, 1980: "Calibration of a Satellite Infrared Radiometer", Applied Optics, 19 (13), 2153-2161.

Bowley, C.J., J.C. Barnes and A. Rango, 1979: Satellite Snow Mapping and Runoff Prediction Handbook, Final Report under Contract No. NAS5-24410 to NASA/Goddard Space Flight Center, Environmental Research & Technology, Inc., Concord, Mass., 87 pp.

Burke, H.K., A.J. Bussey and K.R. Hardy, 1978: Thin Cirrus Cloud over the Tropical Pacific, Interim Report No. 3 under Contract No. F19628-76-C-0069 to Air Force Geophysics Laboratory, Hanscom AFB, Mass. (AFGL-TR-78-0259), Environmental Research & Technology, Inc., Concord, Mass., 39 pp.

Cogan, J.L. and J.H. Willand, 1976: "Measurement of Sea Surface Temperature by the NOAA-2 Satellite", Journal of Applied Meteorology, Vol. 15, No. 2, 173-180.

Court, A., 1963: "Snow Cover Relations in the Kings River Basin, California", J. of Geophysical Res., 68 (16), 4751-4761.

Dozier, J., 1980: "A Clear-Sky Spectral Solar Radiation Model for Snow-Covered Mountainous Terrain", Water Resources Research, Vol. 16, No. 4, 709-718.

Edgerton, A.T., et al., 1968: Passive Microwave Measurements of Snow, Soils and Snow-Ice-Water Systems, Technical Report No. 4 (SGD 8 29-6) Contract NOnr 4767 (oo) NR 387-033 to Office of Naval Research, Space Division, Aerojet-General Corporation, Azusa, California, 180 pp.

Frampton, M. and D. Marks, 1980: "Mapping Snow Surface Temperature from Thermal Satellite Data in the Southern Sierra Nevada", paper presented at the 1980 Western Snow Conference, Laramie, Wyoming, Computer Systems Laboratory, U. of California, Santa Barbara, Calif.

Geiger, R., 1965: The Climate Near the Ground, Harvard University Press, Cambridge, Mass., 611 pp.

Griggs, M., 1968: "Emissivities of Natural Surfaces in the 8- to 14-Micron Spectral Region", Journal of Geophysical Research, 73 (24), 7545-7551.

Murphy, C.J., W.L. Barnes and D. Escoe, 1978: The Heat Capacity Mapping Mission, NASA Publication X-940-77-212, NASA Goddard Space Flight Center, Greenbelt, Maryland.

NASA, 1980: Heat Capacity Mapping Mission Users Guide, prepared by NASA Goddard Space Flight Center, Greenbelt, Maryland, 120 pp.

Rangaswamy, S. and J. Subbarayudu, 1978: Program "RADTRA" to Computer Atmospheric Attenuation Correction, Final Report under Contract No. NAS5-24272 to NASA, Systems and Applied Sciences Corp.

Rango, A. (ed.), 1975: Proceedings of Workshop on Operational Applications of Satellite Snowcover Observations, NASA Publication SP-391, Washington, D.C., 430 pp.

Rango, A. and R. Peterson (ed.), 1980: Proceedings of Final Workshop on Operational Applications of Satellite Snowcover Observations, NASA Conference Publication 2116, Washington, D.C., 302 pp.

Rango, A., J.F. Hannaford, R.L. Hall, M. Rosenzweig and A.J. Brown, 1979: "Snow-Covered Area Utilization in Runoff Forecasts", Journal of the Hydraulics Division, ASCE, 105 (HY1), 53-66.

Shafer, B.A. and A.B. Super, 1971: Infrared Temperature Sensing of Snow-Covered Terrain, Final Report under Contract No. DAHC04-67-C-0058 to Dept. of Army (Durham), Montana State University, Bozeman, Montana, 95 pp.

Weisnet, D.R., 1979: Applications of Remote Sensing to Hydrology, WMO Operational Hydrology Report No. 12 (WMO No. 513), Geneva, 52 pp.